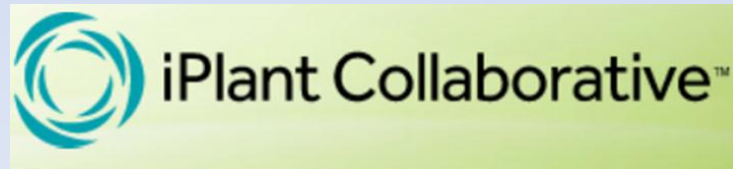


**METHODS COMPARISON
FOR THE PRODUCTION OF
INTERPOLATED CLIMATE LAYERS FOR USE IN SPECIES MODELING:
Interpolation of maximum temperature in Oregon.
10-18-2012**

**Report
Benoit Parmentier**



PRESENTATION - TABLE OF CONTENT

I. Introduction

1. Study area
2. Covariates and data inputs
3. Interpolation methods
4. Workflow for method comparison
5. Model runs and sampling scheme

II. Prediction results

1. Methods (GWR, Kriging, GAM, CAI, fusion) with covariates
2. Interpolated surfaces: Daily tmax prediction for 5 methods

III. Method Accuracy assessment

1. Accuracy metrics and boxplots (MAE & RMSE)
2. Multisampling: variation in proportions and samples
3. Spatial distance: Accuracy in terms of closest training station
4. Station density and accuracy (MAE)
5. Visualization of results for CAI and Fusion: a first comparison
6. Accuracy at specific meteorological stations

IV. Preliminary conclusions

1. General conclusions about method comparison
2. Specific conclusions about the CAI and Fusion comparison

METHOD AND MODEL COMPARISONS FOR CLIMATE INTERPOLATION

- **GOAL:**

Select a method that performs well for interpolation at the global level across multiple seasons and years.

- **Compare systematically model results across different dimensions:**

→ Across methods: variation among statistical procedures

→ Across time : variation among day of years and seasons as well as across multiyears

→ Across samples: variation in training and testing samples

→ Across covariates: variation among combinations of covariates

- **Main conclusion at this stage:**

1. Comparison over a full year, **2010**, shows that on average methods give similar results in terms of RMSE and MAE. Results conform to conclusions found in the literature.
2. Indirect-multiple steps methods (CAI and Fusion) perform better with lower average MAE and RMSE. This is in line with the conclusions found in the literature.
3. MAE and RMSE metrics are not sufficient to evaluate the model outputs i.e. some predictions are overly smooth and do not include expected topographical features.

The inclusion of covariates such as elevation or LST add some of the missing spatial variability.

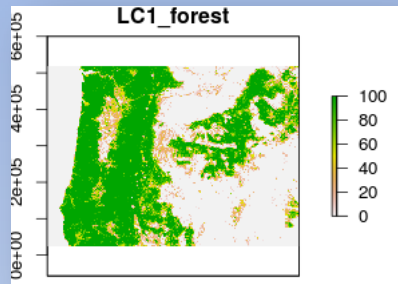
I. INTRODUCTION

1. Study area
2. Covariates and data input
3. Interpolation methods
4. Workflow for method comparison
5. Model runs and sampling scheme

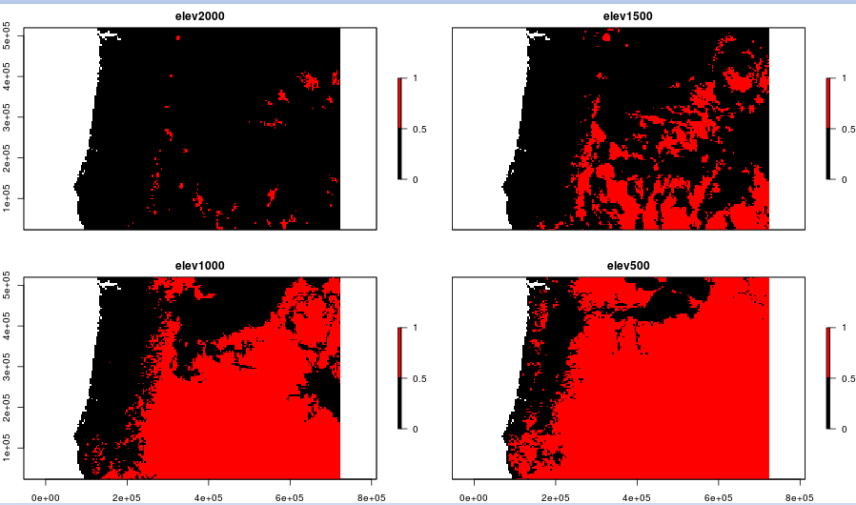
1. STUDY AREA: OREGON



Mask created by reclassifying all values with water=100



Forest land cover in %



Areas: (in pixels~1km²)

- Total area covered by image: 399,320
- Total land area: 357,363 (category 1)
- Total water area: 41,957 (category 0)
- Total area in Oregon: 296,732

Topography:

- land < 500m: 19.2%
- land >1000m: 51.2%
- land > 2000m: 1.6%
- Water: 10.6%

Landscape:

- Forest: 34% of the landmass have 100 % forest
- Grass and shrubs: also covers extensively the state but with less %.
- Agriculture in the Willamette valley and North in the Washington State.

Stations period	GHCND Station Count in OR
Average per day in 2010	~160
Year 2010	186
2001-2010	193
1980-2010	1093

2. COVARIATES AND DATA INPUT

Coding name	Variable	Source	Explanation
ELEV_SRTM	elevation	SRTM	Aggregated from 90m to 1km using NASA Space Shuttle Radar Topography Mission (SRTM).
Lat	Geog. coordinate	GHCND	Stations latitude from the GHCND database (NCDC)
Lon	Geog. coordinate	GHCND	Stations longitude from the GHCND database (NCDC)
Eastness	Aspect	SRTM	Transformed aspect variable derived from SRTM (NASA)
Northness	Aspect	SRTM	Transformed aspect variable derived from SRTM (NASA)
DISTOC	Maritime effect	LCC	Distance from the coast
LC1	forest	LCC	From Land Cover Consensus product derived in Jetz Lab
LC3	grass	LCC	From Land Cover Consensus product derived in Jetz Lab
LC4	Crop	LCC	From Land Cover Consensus product derived in Jetz Lab
LC6	Urban	LCC	From Land Cover Consensus product derived in Jetz Lab
CANHEIGHT	canopy height	GLAS	Derived from Geoscience Laser Altimeter System on Icesat
LST	Day surface temperature	MODIS	Monthly average Land Surface temperature derived over the 2001-2010 time period using MOD11A1.
tmax	Daily maximum air temperature	GHCND	Air temperature measurement from the GHCND database

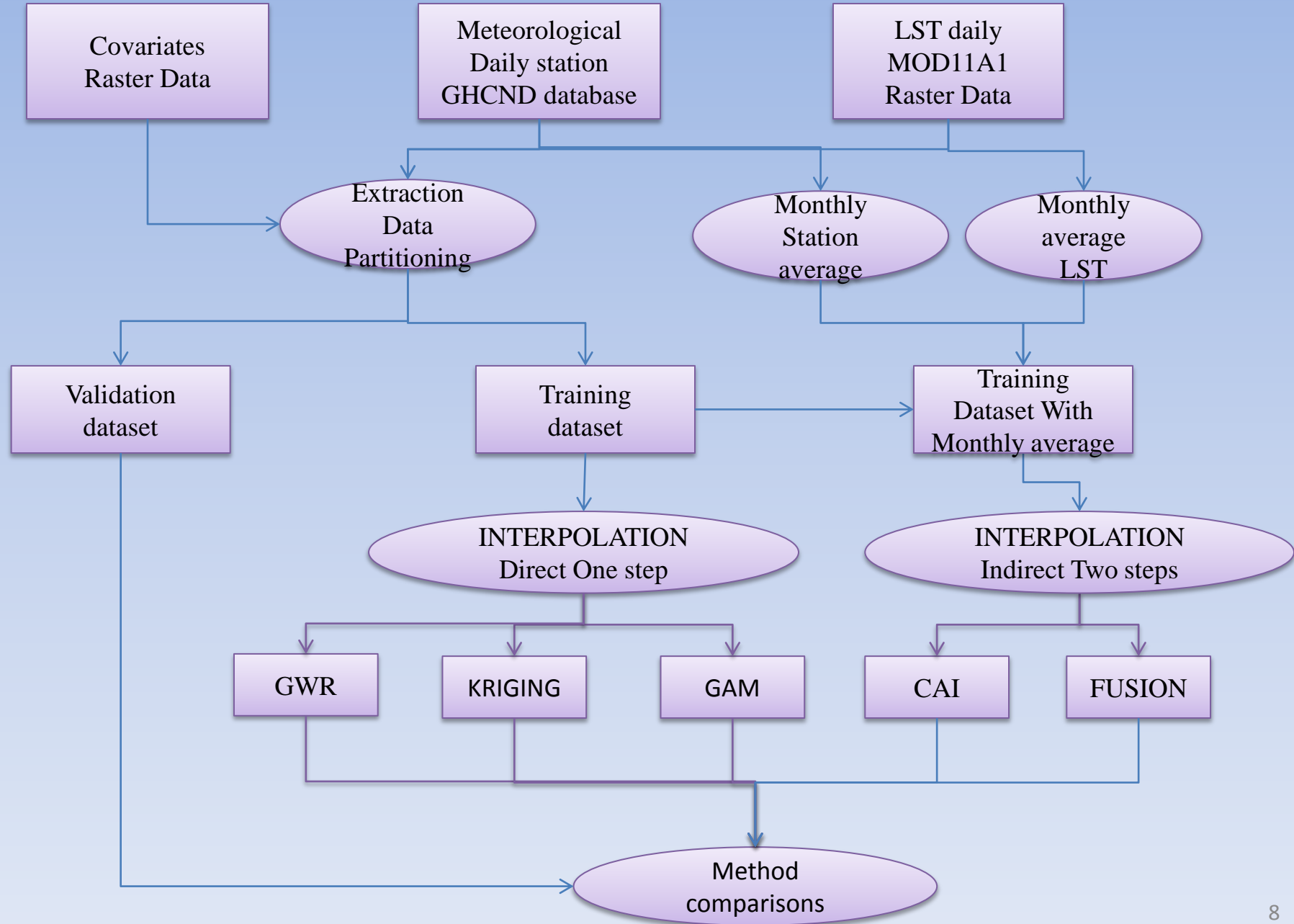
Note that all raster datasets are processed at 1km resolution which is the spatial resolution of the interpolated surfaces.

3. INTERPOLATION METHODS

Methods	General form	Examples	Used in the method comparison
Environmental correlation/gradients	$Y = a_0 + a_1x_1 + a_2x_2 + \dots + a_n \cdot x_n$	Multiple linear regression with environmental covariates	Yes: most models include covariates except simple kriging
Geostatistical/moving averages	$y_0 = \sum a_i \cdot y_i$ with a_i being the weights	IDW, Simple Kriging, Ordinary Kriging	Yes: Kriging and GWR
Hybrid methods	$Y = a_0 + a_1x_1 + a_2x_2 + \dots + a_n \cdot x_n$ $Y = a_0 + a_1x_1 + a_2x_2 + \dots + \sum a_i \cdot y_i$ a_i dependent on distance and /or covariates	Universal Kriging, PRISM, GAM-TPS.	Yes: GAM and GWR
Climatology Aided Interpolation (CAI)	$Y = Y_{av} + Y_{dev}$ $Y_{dev} = a_0 + a_1x_1 + a_2x_2 + \dots + a_n \cdot x_n$	Two stages regression with monthly average/modeled surface and daily anomalies/deviations.	Yes: CAI and Fusion with kriging and GAM
Machine Learning	$y = \text{pattern}(x_1, x_2, \dots, x_n)$	MultiLayer Perceptron (MLP), Regression Tree	Not used in this research

Methods in the literature may be divided in five broad categories: environmental correlation Gradient, geostatistical moving averages, hybrid methods, Climatology Aided Interpolation, And Machine Learning. In this research, we have tested five methods: Geographically Weighted Regression (GWR), Kriging, General Additive Models (GAM), Climatology Aided Interpolation (CAI), Fusion.

4. GENERAL WORKFLOW METHOD COMPARISON



METHODS USED TO COMPARE AND ASSESS INTERPOLATION RESULTS

Procedures	Studies
1.Reporting fit metric	Everywhere: Jolly et al. 2005, Willmott and Matsuura 1995, New 2001, Attore et al. 2007, Daly et al. 2002 etc.
3.Cross-validation	Jolly et al. 2005, Willmott and Matsuura 1995, New 1999 etc.
3.Data partitioning/hold out	Price et al. 2000, Vicente-Serrano et al. 2003, Hijmans et al. 2005, Attore et al. 2007, McKenney et al. 2006.
4.Grid aggregation	Hijmans et al. 2005, Hosfra et al. 2008, Haylock et al. 2008
5.Error uncertainty	Hijmans et al. 2005, Daly et al. 2002,
6.Error regression study	Thorthton et al. 1997, Price et al. 2000, Stahl et al. 2006.
7.Visualization /mapping of errors/residuals	Hijmans et al. 2005, Jarvis and Stuart 2001
8. Product comparison	Hijmans et al. 2005, Daly et al. 2002, New et al. 2002,...
9. Temporal aggregation	Hijmans et al. 2005

Following the interpolation review, we settled on methods highlighted in bold and added two novel procedures: multi sampling and error in terms of distance to closest fitting station,⁹

5. SUMMARY TABLE OF MODELS RUN AND INPUT

Method Model	Constant sampling	365 dates	Multi sampling	Run Time for 365dates	Covariates
GAM1	X	X	X	24h	lat, long, ELEV_SRTM, slope, Eastness, Northness, DISTOC, LST LC1, LC3
GAM2		X		24h	lat, long, ELEV_SRTM, slope, Eastness, Northness, DISTOC, LSTLC1, LC3, CANHEIGHT
GAM3		X		6h	lat, long, ELEV, slope, Eastness, Northness, DISTOC, LST, LC1, LC3, LC4, LC6
FUS1 (kr)	X	X	X	3-4h	dailyTmax, Tmax monthly, LST
FUS1 (GAM)	X	X		24h	lat, long, ELEV, slope, Eastness, Northness, DISTOC, LST, LC1, LC3
CAI1 (Kr)		X	X	3-4h	dailyTmax, Tmax monthly, LST
CAI1 (GAM)		X	X	28hh	lat, long, ELEV, slope, Eastness, Northness, DISTOC, LST, LC1, LC3
CAI2 (GAM)				24h	lat, long, ELEV_SRTM, slope, Eastness, Northness, DISTOC, LST, LC1, LC3, CANHEIGHT
GWR		X		132	lat, long, ELEV, slope, Eastness, Northness, DISTOC, LC1, LC3
Kriging		X	X	48h	lat, long, ELEV, slope, Eastness, Northness, DISTOC, LC1, LC3

We tested interpolation results by accounting for five parameters:

- **Constant sampling:** using constant training and testing in a series of model runs.
- **Multi sampling:** variation in the proportion of hold out and in the training and testing.
- **365 dates:** run over the year 2010 (365 dates) using 30% hold out and random sampling.
- **Covariates:** variation in the covariates, interactions and/or smooth terms.
- **Method model:** variation in the modeling technique used.

This required a number of “runs” or predictions with a combination of various parameters.

II. PREDICTION RESULTS

1. Methods (Kriging, GWR, GAM, CAI, fusion) with covariates
2. Interpolated surface: Daily tmax prediction for 5 methods.

KRIGING METHOD

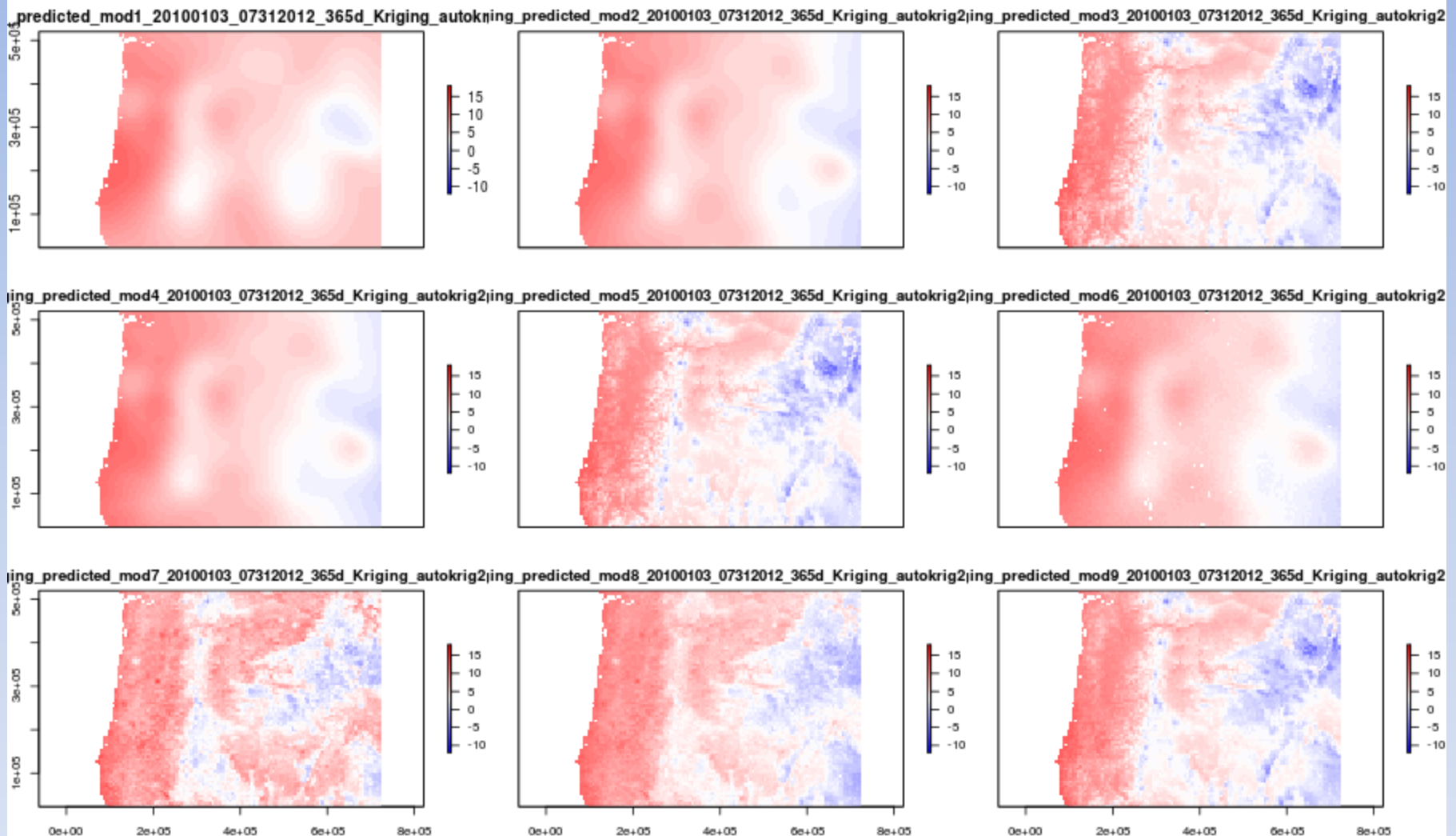
- There are nine models:

Model	Functional form
Mod1	$t_{max} \sim t_{max}$
Mod2	$t_{max} \sim x_{OR83M} + y_{OR83M}$
Mod3	$t_{max} \sim x_{OR83M} + y_{OR83M} + ELEV_SRTM$
Mod4	$t_{max} \sim x_{OR83M} + y_{OR83M} + DISTOC$
Mod5	$t_{max} \sim x_{OR83M} + y_{OR83M} + ELEV_SRTM + DISTOC$
Mod6	$t_{max} \sim x_{OR83M} + y_{OR83M} + Northness + Eastness$
Mod7	$t_{max} \sim LST$
Mod8	$t_{max} \sim x_{OR83M} + y_{OR83M} + LST$
Mod9	$t_{max} \sim x_{OR83M} + y_{OR83M} + ELEV_SRTM + LST$

Kriging was run over 365 dates:

- A different variogram is fitted automatically for every day of the year following the method described in Hiemstra et al. 2008.
- The variogram is fitted based on the training information and applied to the entire prediction grid.

KRIGING METHOD



Predictions using Kriging method for 8 different models on January 3, 2010. Note that without elevation and LST variables (mod1, mod2, mod4, mod6), prediction are very smooth.

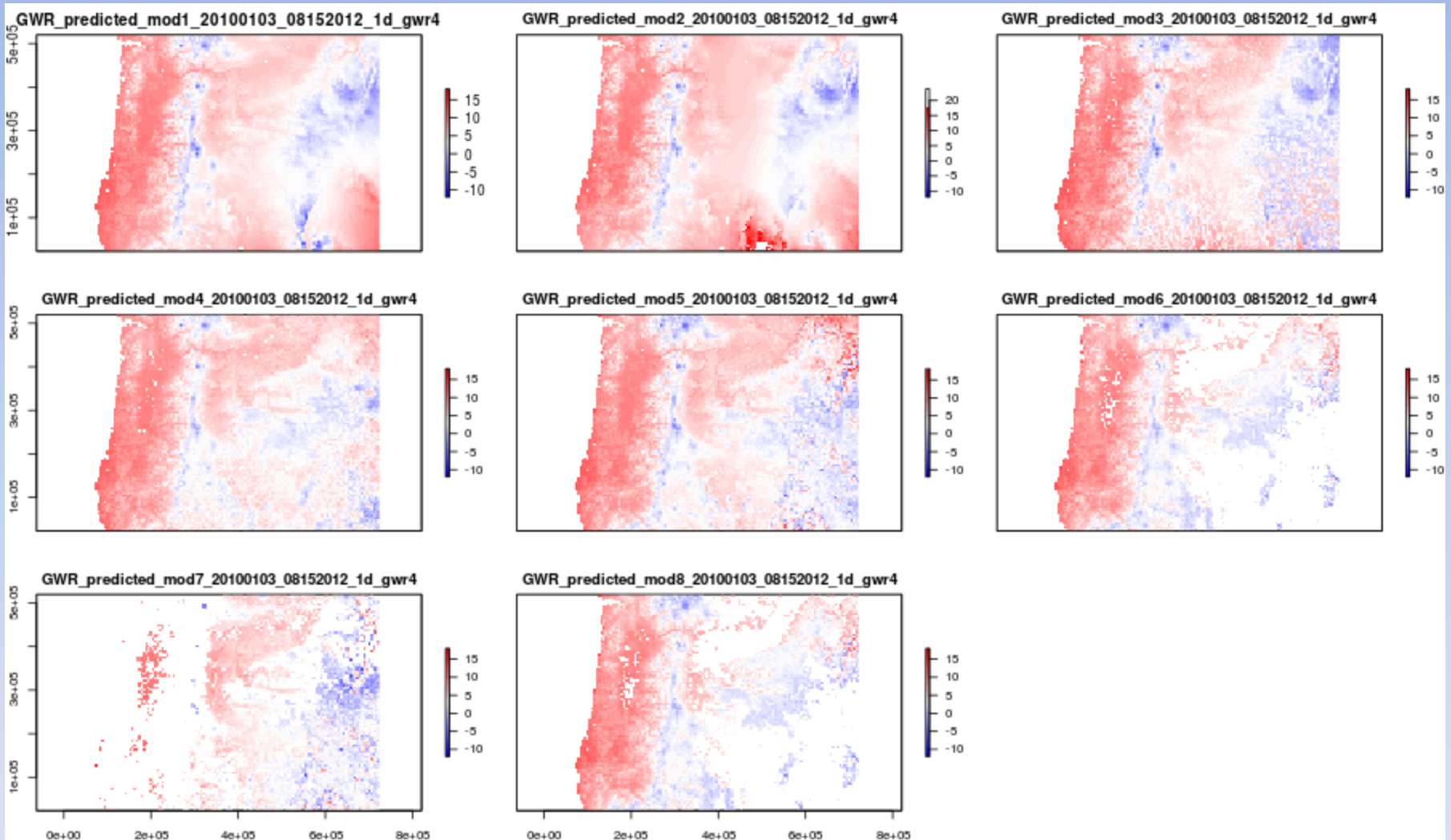
GWR METHOD

- Eight models were tested for the GWR method:

Model	Functional form
Mod1	$t_{\max} \sim \text{lat} + \text{lon} + \text{ELEV_SRTM}$
Mod2	$t_{\max} \sim \text{lat} * \text{lon} + \text{ELEV_SRTM}$
Mod3	$t_{\max} \sim \text{lat} + \text{lon} + \text{ELEV_SRTM} + \text{Northness} + \text{Eastness} + \text{DISTOC}$
Mod4	$t_{\max} \sim \text{lat} * \text{lon} + \text{ELEV_SRTM} + \text{Northness} * \text{Eastness} + \text{DISTOC} + \text{LST}$
Mod5	$t_{\max} \sim \text{lat} + \text{lon} + \text{ELEV_SRTM} + \text{Northness_w} + \text{Eastness_w} + \text{DISTOC} + \text{LST}$
Mod6	$t_{\max} \sim \text{lat} + \text{lon} + \text{ELEV_SRTM} + \text{Northness_w} + \text{Eastness_w} + \text{DISTOC} + \text{LST} + \text{LC1}$
Mod7	$t_{\max} \sim \text{lat} + \text{lon} + \text{ELEV_SRTM} + \text{Northness_w} + \text{Eastness_w} + \text{DISTOC} + \text{LST} + \text{LC3}$
Mod8	$t_{\max} \sim \text{lat} + \text{lon} + \text{ELEV_SRTM} + \text{Northness_w} + \text{Eastness_w} + \text{DISTOC} + \text{LST} + \text{LST} * \text{LC1}$

- The GWR method requires that there are no missing values in the inputs so it was necessary to remove some grid points.
- The Gaussian model was used as the distance function.
- The bandwidth is determined by using the training dataset. Models are then fitted using the training samples and applied to the entire prediction grid. Validation is done through testing samples.

GWR METHOD



Predictions using GWR method for 8 different models on January 3, 2010. Note that inclusions of LC1 and LC3 variables removes information and does not improve predictions (last three models).

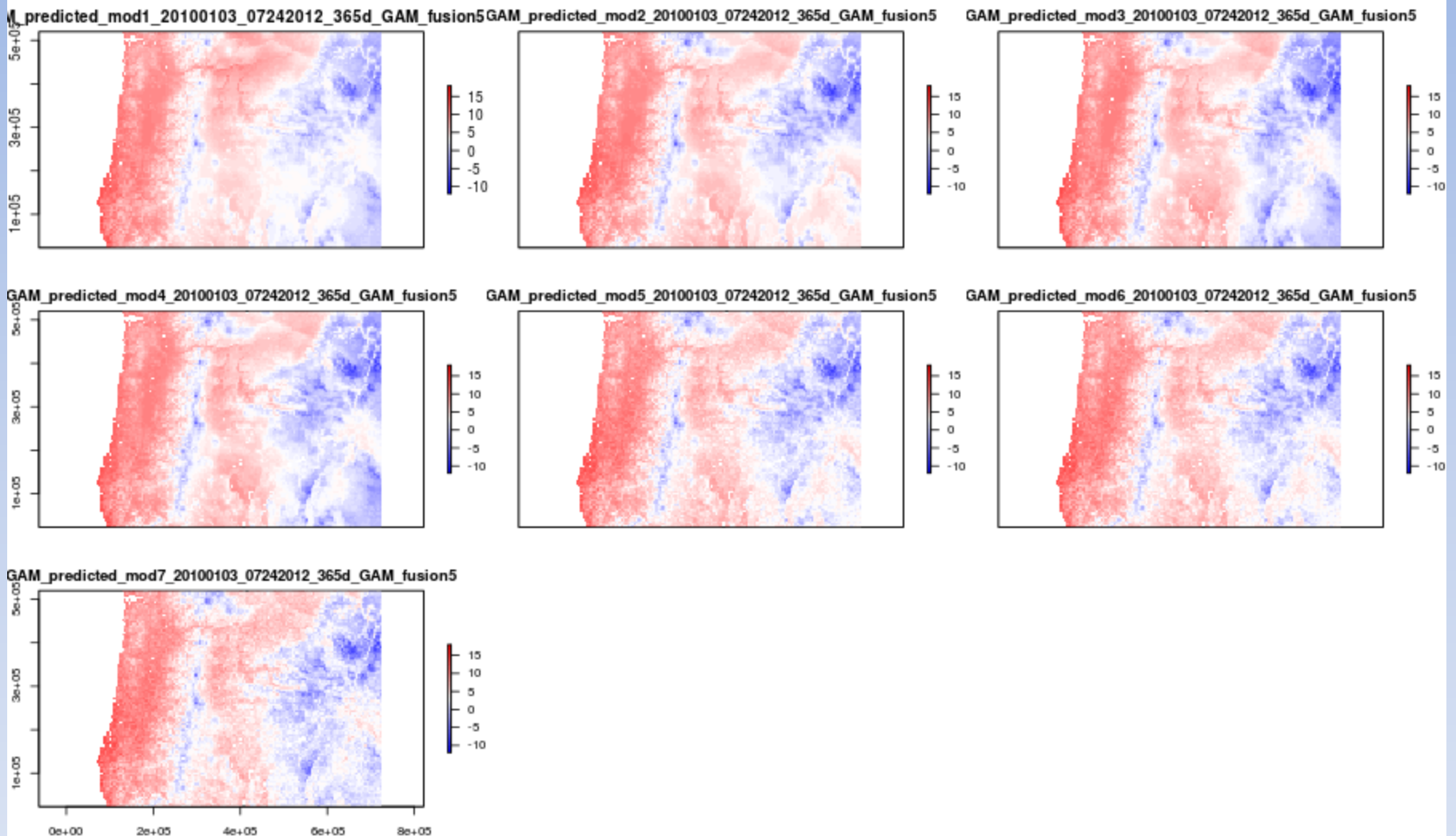
GAM METHOD: GAM1

There are eight models:

Model	Functional Form
Mod1	$t_{max} \sim f(\text{lat}) + f(\text{lon}) + f(\text{ELEV_SRTM})$
Mod2	$t_{max} \sim f(\text{lat}, \text{lon}) + f(\text{ELEV_SRTM})$
Mod3	$t_{max} \sim f(\text{lat}) + s(\text{lon}) + s(\text{ELEV_SRTM}) + s(\text{Northness}) + s(\text{Eastness}) + f(\text{DISTOC})$
Mod4	$t_{max} \sim f(\text{lat}) + s(\text{lon}) + f(\text{ELEV_SRTM}) + f(\text{Northness}) + s(\text{Eastness}) + f(\text{DISTOC}) + f(\text{LST})$
Mod5	$t_{max} \sim f(\text{lat}, \text{lon}) + f(\text{ELEV_SRTM}) + f(\text{Northness}, \text{Eastness}) + f(\text{DISTOC}) + f(\text{LST})$
Mod6	$t_{max} \sim f(\text{lat}, \text{lon}) + f(\text{ELEV_SRTM}) + f(\text{Northness}, \text{Eastness}) + f(\text{DISTOC}) + f(\text{LST}) + f(\text{LC1})$
Mod7	$t_{max} \sim f(\text{lat}, \text{lon}) + f(\text{ELEV_SRTM}) + f(\text{Northness}, \text{Eastness}) + f(\text{DISTOC}) + f(\text{LST}) + f(\text{LC3})$
Mod8	$t_{max} \sim f(\text{lat}, \text{lon}) + f(\text{ELEV_SRTM}) + f(\text{Northness}, \text{Eastness}) + f(\text{DISTOC}) + f(\text{LST}) + f(\text{LC1}, \text{LC3})$

- GAM uses function bases to model the relationship between covariates and the response variable (t_{max}). Terms with function bases are called “smooth terms” and symbolized by $f(\dots)$.
- GAM smooth terms allow for flexible representation of relationships (Woods 2008).
- Terms are added linearly but can be nested to include interactions among covariates such as in $f(\text{lat}, \text{long})$ (Woods 2008).

GAM METHOD: GAM1



Predictions using GAM method for 8 different models on January 3, 2010.

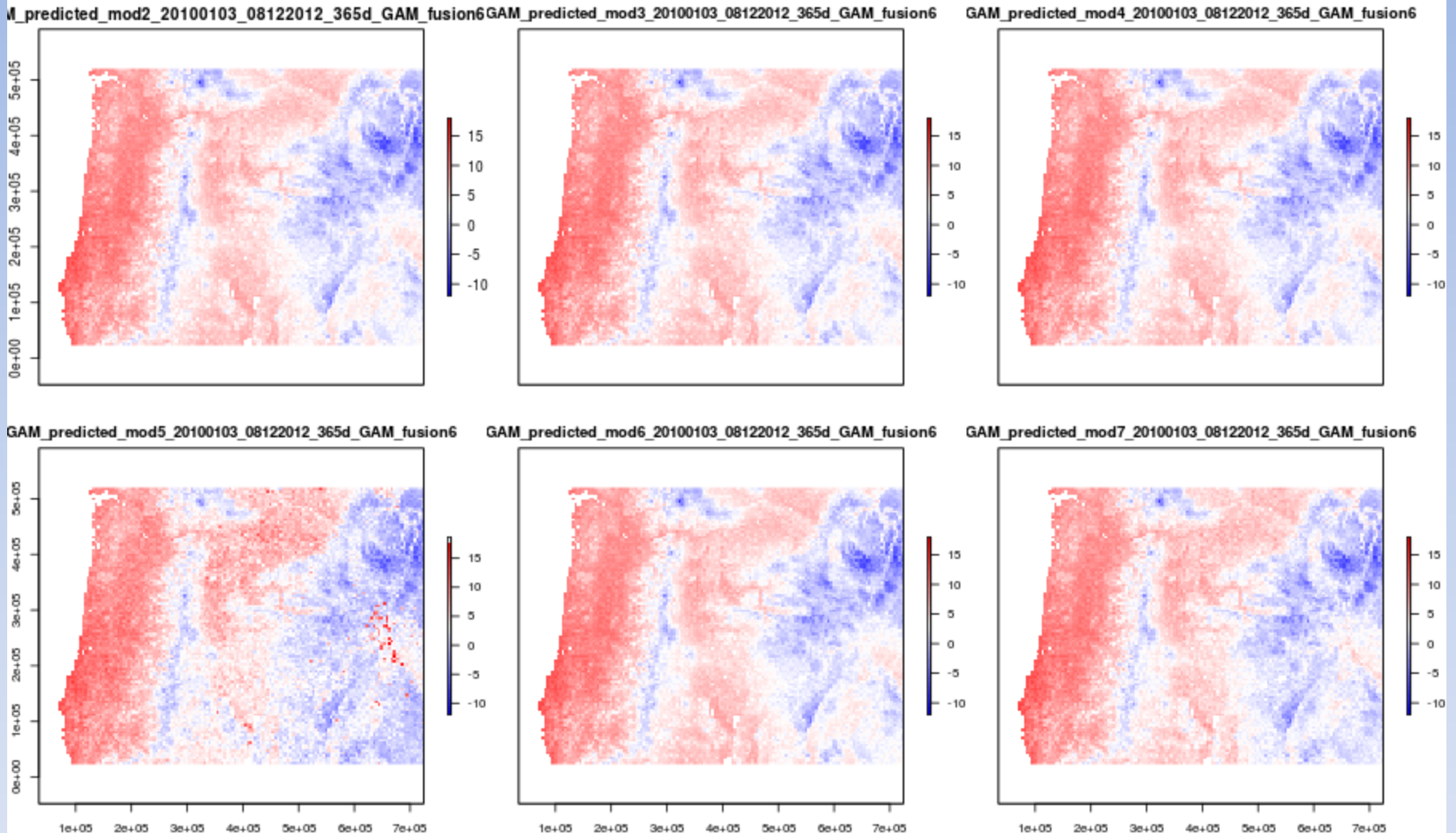
GAM METHOD: GAM2

- There are eight models:

Model	Formula
Mod1	$t_{max} \sim f(\text{lat}, \text{lon}, \text{ELEV_SRTM})$
Mod2	$t_{max} \sim f(\text{lat}, \text{lon}) + f(\text{ELEV_SRTM}) + f(\text{Northness}, \text{Eastness}) + f(\text{DISTOC}) + f(\text{LST}) + f(\text{CANHEIGHT})$
Mod3	$t_{max} \sim f(\text{lat}, \text{lon}) + f(\text{ELEV_SRTM}) + f(\text{Northness}, \text{Eastness}) + f(\text{DISTOC}) + f(\text{LST}, \text{CANHEIGHT})$
Mod4	$t_{max} \sim f(\text{lat}, \text{lon}) + f(\text{ELEV_SRTM}) + f(\text{Northness}, \text{Eastness}) + f(\text{DISTOC}) + f(\text{LST}, \text{LC1})$
Mod5	$t_{max} \sim f(\text{lat}, \text{lon}) + f(\text{ELEV_SRTM}) + f(\text{Northness}, \text{Eastness}) + f(\text{DISTOC}) + f(\text{LST}, \text{LC3})$
Mod6	$t_{max} \sim f(\text{lat}, \text{lon}) + f(\text{ELEV_SRTM}) + f(\text{Northness}, \text{Eastness}) + f(\text{DISTOC}) + f(\text{LST}) + f(\text{LC1})$
Mod7	$t_{max} \sim f(\text{lat}, \text{lon}) + f(\text{ELEV_SRTM}) + f(\text{Northness}, \text{Eastness}) + f(\text{DISTOC}) + f(\text{LST}) + f(\text{LC3})$
Mod8	$t_{max} \sim f(\text{lat}, \text{lon}) + f(\text{ELEV_SRTM}) + f(\text{Northness}, \text{Eastness}) + f(\text{DISTOC}) + f(\text{LST}, \text{LC1}) + f(\text{LST}, \text{LC3})$

- GAM fitting requires a larger number of samples to estimate model parameters in particular for nested terms (Woods 2008).
- Mod1 has a functional form that corresponds to the one used in the WORLDCLIM product (Hijmans et al. 2005).
- We included land cover covariates (LC1, LC3 and CANHEIGHT) in the series of GAM model (“RUN2”). LC1, LC3 and CANHEIGHT correspond to “forest”, “grass” and “canopy height” respectively.

GAM METHOD: GAM2



Predictions using GAM method for 8 different models on January 3, 2010.

GAM METHOD: GAM2

Model	Number of dates predicted
Mod1	There were 115 dates predicted and no prediction for January 3.
Mod2	There were 262 dates predicted.
Mod3	There were 262 dates predicted.
Mod4	There were 262 images predicted
Mod5	There were 364 dates predicted.
Mod6	There were 364 dates predicted.
Mod7	There were 364 dates predicted.
Mod8	There were 0 dates predicted.

General comments:

- We found that models with more than two interactive terms (e.g. mod1) have a low number
- Of date predicted because the number fitting parameters in GAM increases.
- Land cover in Oregon is dominated by 2 categories: forest (LC1) and LC3 (grass). These two
- Land cover appear to be the opposite of each other i.e. when forest cover is high grass is low and therefore cancel each other out. The prevalence of zero values also render the fitting of model arduous.

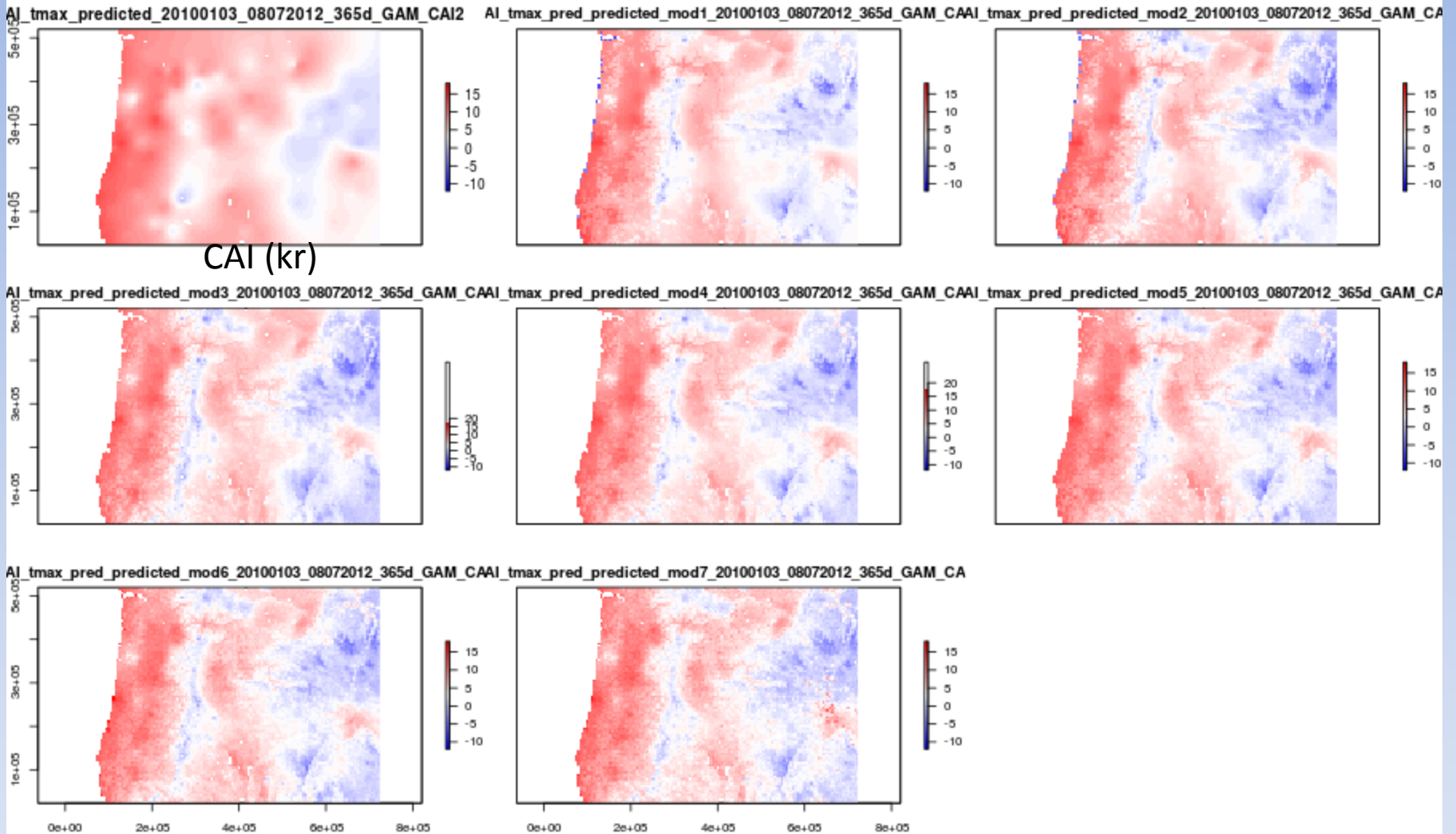
CAI METHOD: CAI1

We produced 9 predictions using 9 models

Model	Functional form
Mod1	$T_{Max} \sim f(\text{lat}) + f(\text{lon}) + f(\text{ELEV_SRTM})$
Mod2	$T_{Max} \sim f(\text{lat}, \text{lon}) + f(\text{ELEV_SRTM})$
Mod3	$T_{Max} \sim f(\text{lat}) + s(\text{lon}) + s(\text{ELEV_SRTM}) + s(\text{Northness}) + s(\text{Eastness}) + f(\text{DISTOC})$
Mod4	$T_{Max} \sim f(\text{lat}) + s(\text{lon}) + f(\text{ELEV_SRTM}) + f(\text{Northness}) + s(\text{Eastness}) + f(\text{DISTOC}) + f(\text{LST})$
Mod5	$T_{Max} \sim f(\text{lat}, \text{lon}) + f(\text{ELEV_SRTM}) + f(\text{Northness}, \text{Eastness}) + f(\text{DISTOC}) + f(\text{LST})$
Mod6	$T_{Max} \sim f(\text{lat}, \text{lon}) + f(\text{ELEV_SRTM}) + f(\text{Northness}, \text{Eastness}) + f(\text{DISTOC}) + f(\text{LST}) + f(\text{LC1})$
Mod7	$T_{Max} \sim f(\text{lat}, \text{lon}) + f(\text{ELEV_SRTM}) + f(\text{Northness}, \text{Eastness}) + f(\text{DISTOC}) + f(\text{LST}) + f(\text{LC3})$
Mod8	$T_{Max} \sim f(\text{lat}, \text{lon}) + f(\text{ELEV_SRTM}) + f(\text{Northness}, \text{Eastness}) + f(\text{DISTOC}) + f(\text{LST}) + f(\text{LC1}, \text{LC3})$
Mod9	CAI with simple kriging

- The CAI methods requires the computation of long terms averages from meteorological stations over some period. For this study, we used a 10 year monthly average for every station.
- The long term average or “climatology” is kriged or modeled using GAM with covariates for every month to create a monthly climatology surface (model 1 through 8).
- The short term daily deviation is kriged to create a daily deviation surface.
- In Mod9, both the climatology and the deviations are kriged and then added together.

CAI METHOD: CAI1



dates	ns	metric	mod1	mod2	mod3	mod4	mod5	mod6	mod7	mod8	mod9
20100103	106	RMSE	2.543293	2.580984	2.467877	2.35899	2.313956	2.297404	2.405234	NA	2.110421

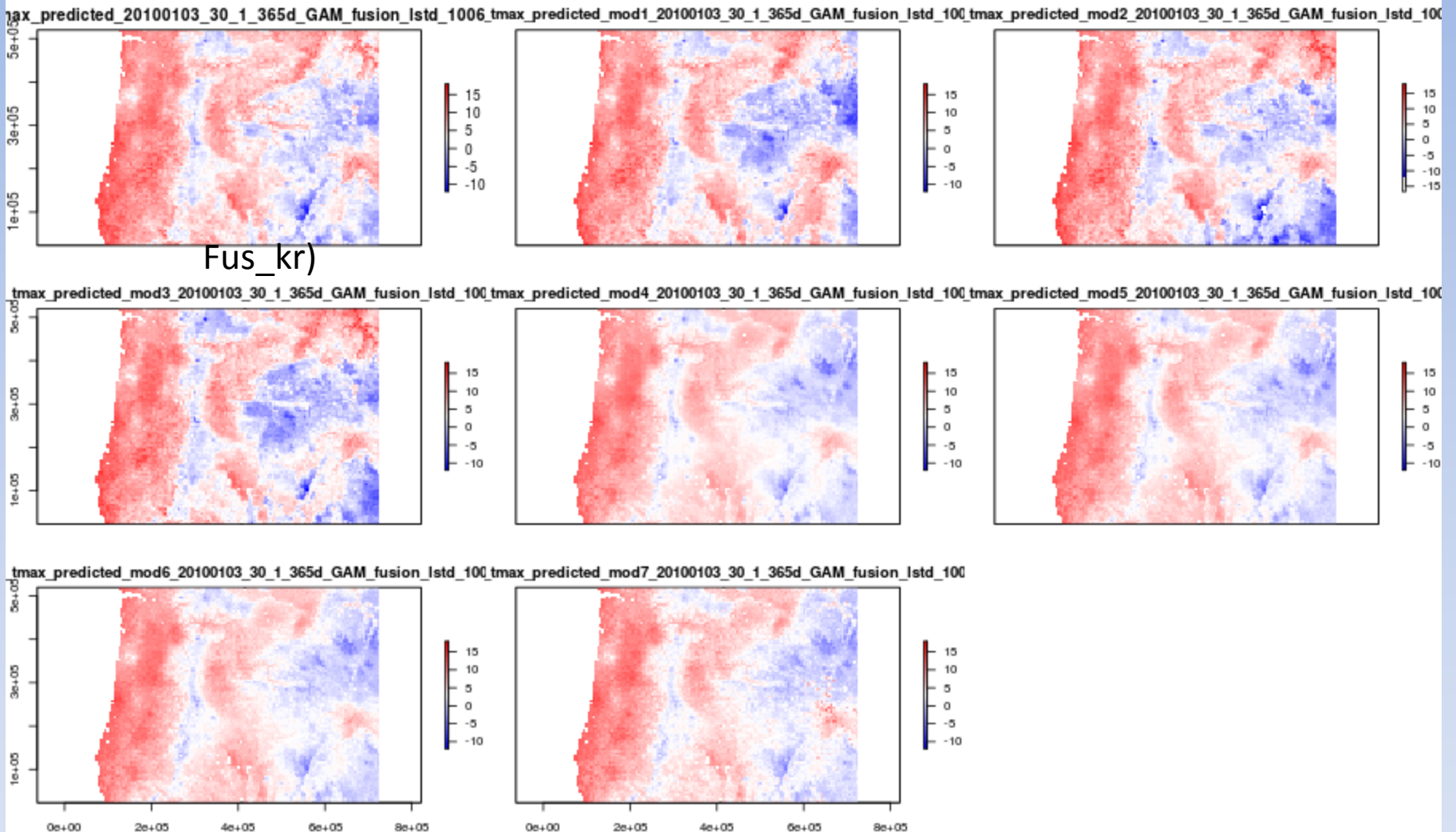
FUSION METHOD: FUS1

There are eight models:

Model	Functional form
Fus_kr	Fusion with simple kriging
Mod1	$LST_bias \sim f(lat) + f(lon) + f(ELEV_SRTM)$
Mod2	$LST_bias \sim f(lat,lon) + f(ELEV_SRTM)$
Mod3	$LST_bias \sim f(lat) + s(lon) + s(ELEV_SRTM) + s(Northness) + s(Eastness) + f(DISTOC)$
Mod4	$LST_bias \sim f(lat) + s(lon) + f(ELEV_SRTM) + f(Northness) + s(Eastness) + f(DISTOC) + f(LST)$
Mod5	$LST_bias \sim f(lat,lon) + f(ELEV_SRTM) + f(Northness,Eastness) + f(DISTOC) + f(LST)$
Mod6	$LST_bias \sim f(lat,lon) + f(ELEV_SRTM) + f(Northness,Eastness) + f(DISTOC) + f(LST) + f(LC1)$
Mod7	$LST_bias \sim f(lat,lon) + f(ELEV_SRTM) + f(Northness,Eastness) + f(DISTOC) + f(LST) + f(LC3)$
Mod8	$LST_bias \sim f(lat,lon) + f(ELEV_SRTM) + f(Northness,Eastness) + f(DISTOC) + f(LST) + f(LC1,LC3)$

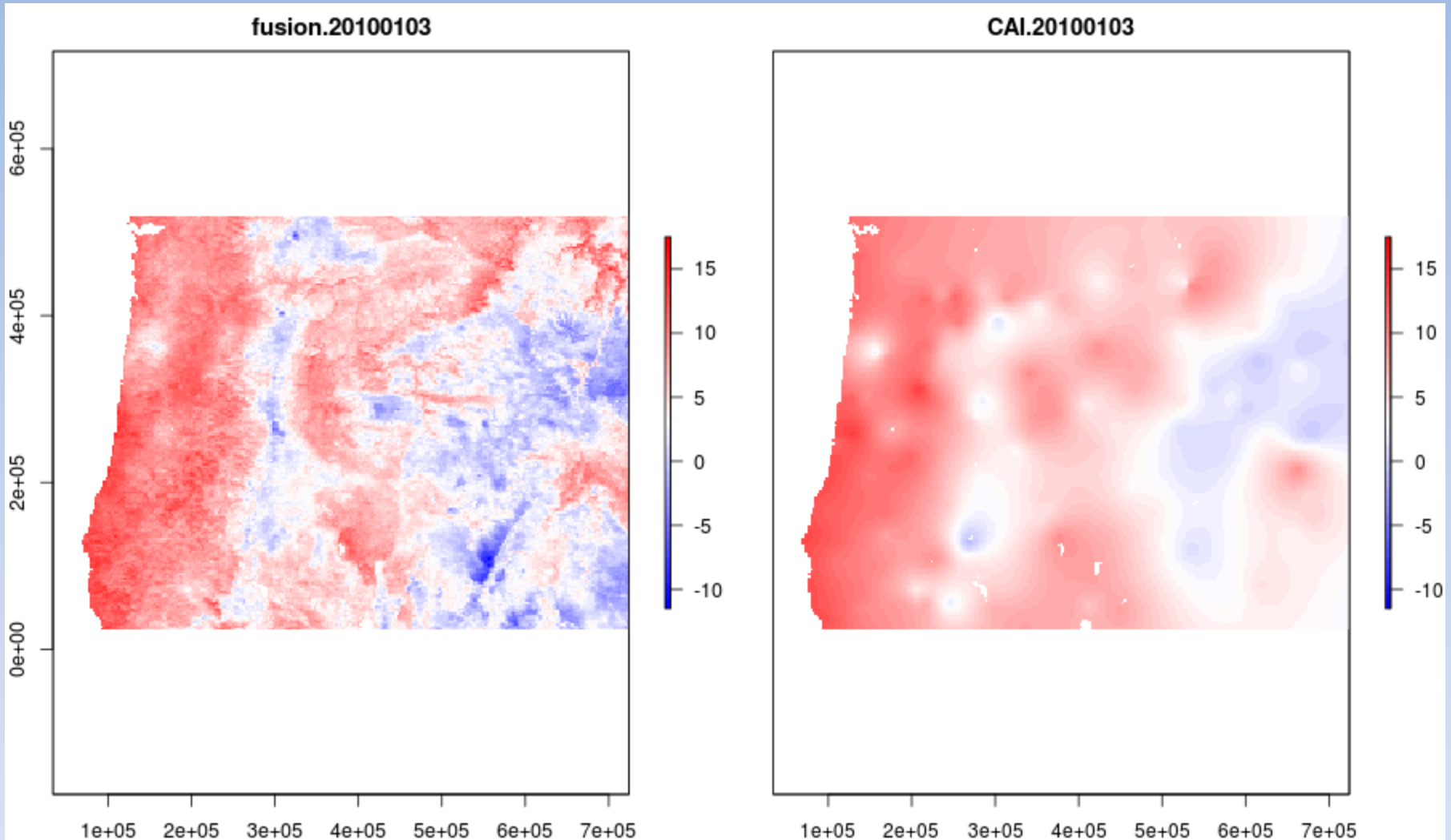
- The long term average or “satellite climatology” is computed from daily LST from MODIS. for every month to create a monthly climatology surface.
- The fusion methods requires the computation of monthly averages tmax over a 10 year period for meteorological stations. A biased surface is derived from the difference between monthly LST and monthly tmax. The bias surface is either modeled through GAM or though kriging.
- The short term daily deviation is kriged to create a daily deviation surface.

FUSION METHOD: FUS1



Predictions using GAM method for 8 different models on January 3, 2010.

FUSION (Kr) AND CAI (Kr)



Maximum temperature predictions for Fusion using Kriging (Fus_kr) and CAI (CAI_kr) using Kriging on January 3, 2010.

III. ASSESSMENT OF TMAX PREDICTION RESULTS

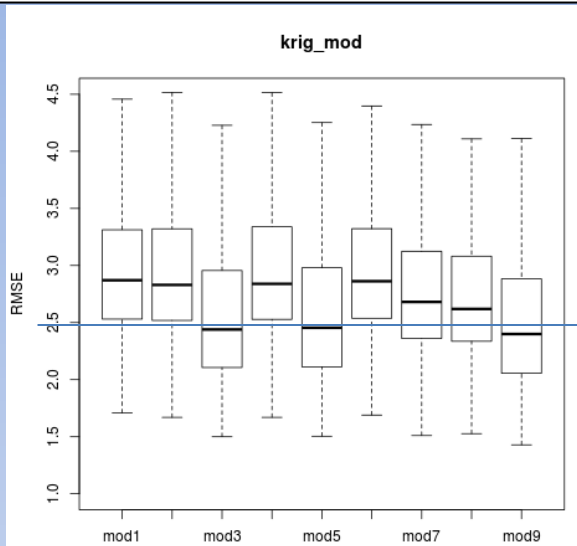
1. Accuracy metrics and boxplots (MAE & RMSE)
2. Multisampling: variation in proportions and samples
3. Spatial distance: Accuracy in terms of closest training station
4. Station density and accuracy (MAE)
5. Visualization of results for CAI and Fusion: a first comparison
6. Accuracy at specific meteorological stations

III. ASSESSMENT OF TMAX PREDICTION RESULTS

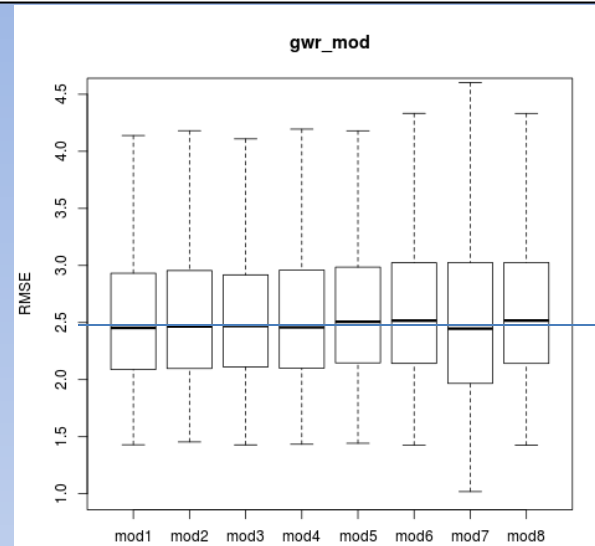
Accuracy procedure	Assessment explanation
Accuracy metric	Average MAE-RMSE and statistical distribution (boxplot) <i>Monthly average MAE-RMSE plots</i>
Sampling	Multisampling: variation of proportions of hold out and random sampling
Spatial distance	MAE in terms of distance to closest fitting station
Map visualization	Visual Spatial pattern and spatial variability (Moran'I and standard dev.), Map differencing
Density - Grid average	Spatial Density of station and MAE MAE grid averaging
Station accuracy	Predictions at ground station: time series and transect Scatterplot residuals and outliers analysis

Based on the literature review, we use 6 procedures to assess the interpolated surfaces.

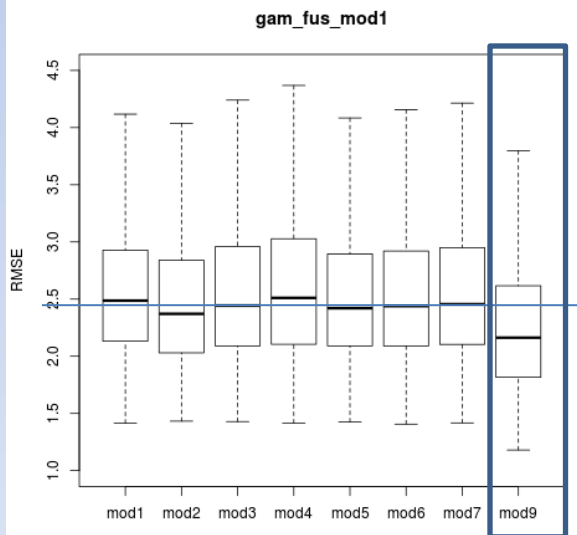
1. METHODS COMPARISON: ACCURACY METRIC - RMSE BOXPLOTS



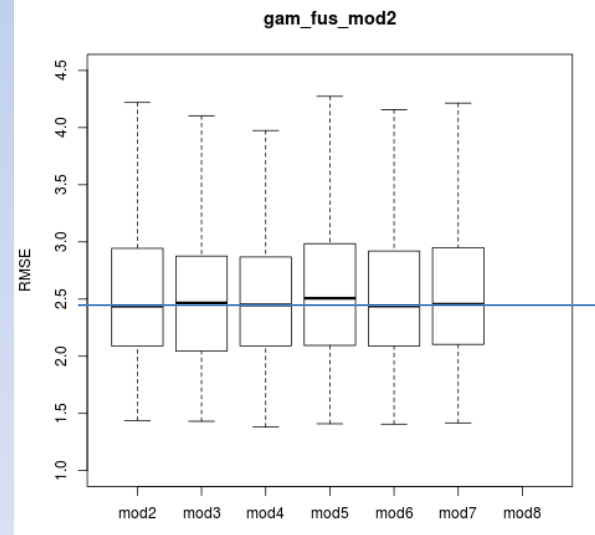
See model functional form on slide 12



See model functional form on slide 14



See model functional form on slide 16

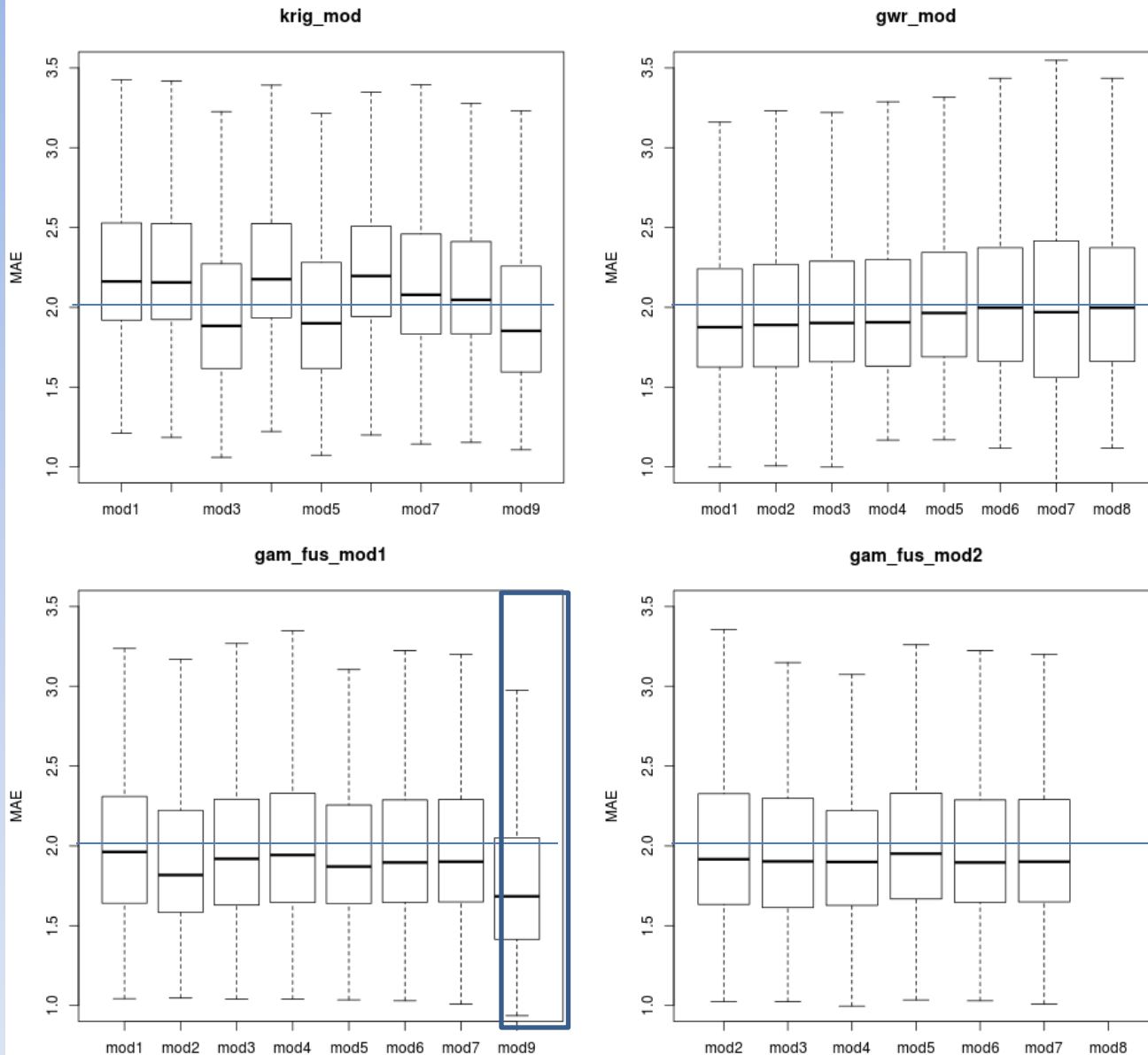


See model functional form on slide 18

**Blue lines at
RMSE= 2.5 C**

These boxplots are based on runs over 365 days with models described in earlier slides. Mod9 in the blue box corresponds to the fusion (kr) method. Gam_fus_mod2 corresponds₂₈ to RUN2 of GAM. Note that average RMSE (middle bar in the box) is the lowest for fusion (kr).

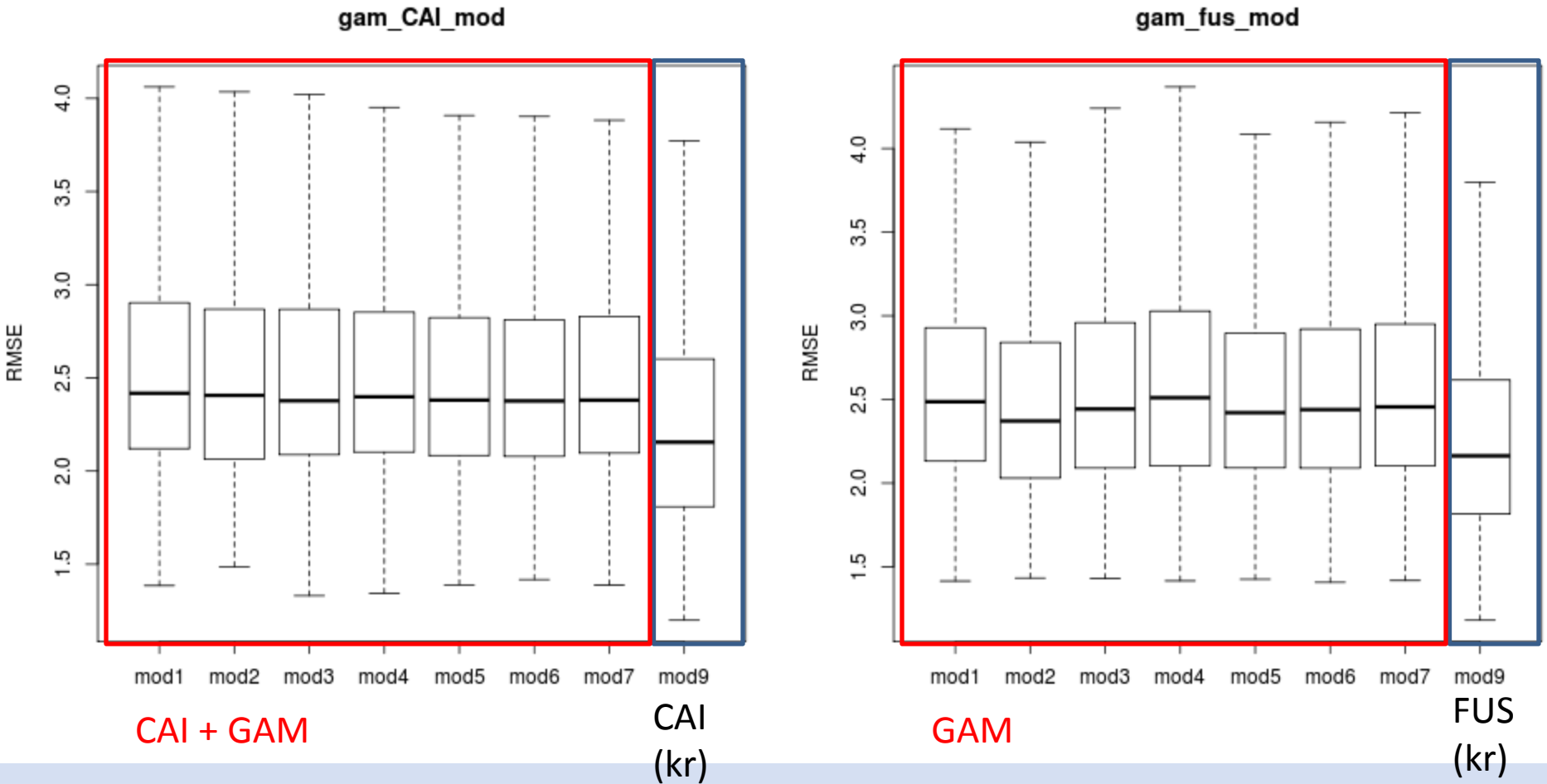
1. METHODS COMPARISON: ACCURACY METRIC - MAE BOXPLOTS



Blue line
at MAE=
2.0 C

Model 9 corresponds to the fusion (kr) method. Gam_fus_mod2 corresponds to RUN2 of GAM.

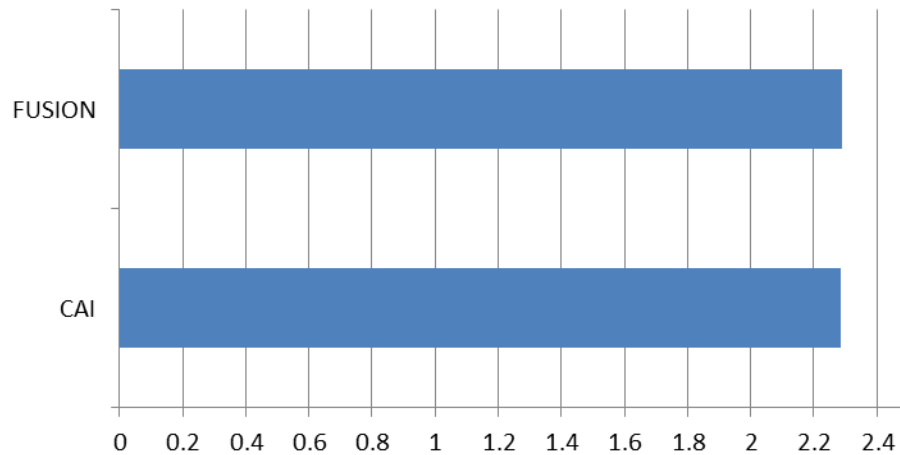
1. METHODS COMPARISON: ACCURACY METRIC - RMSE BOXPLOTS



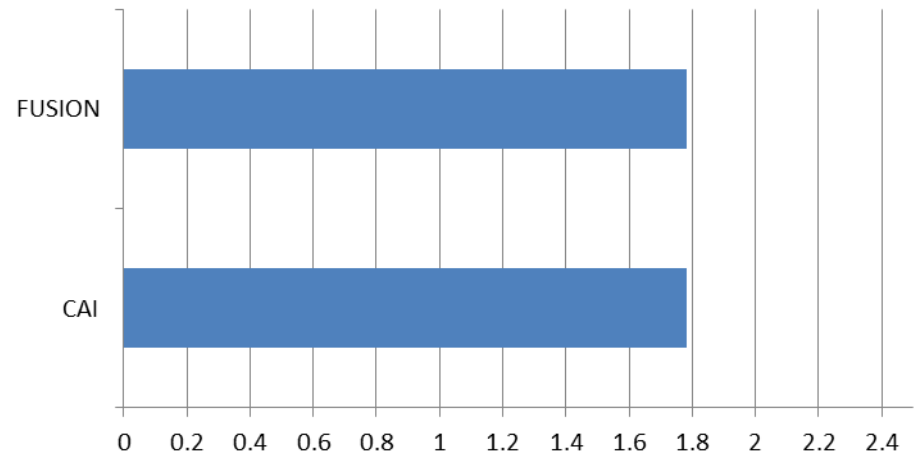
- CAI and Fusion boxplots indicate similar performance in the predictions of tmax.

1. METHODS COMPARISON: ACCURACY METRIC

MEAN RMSE FOR 365 DATES



MEAN MAE FOR 365 DATES



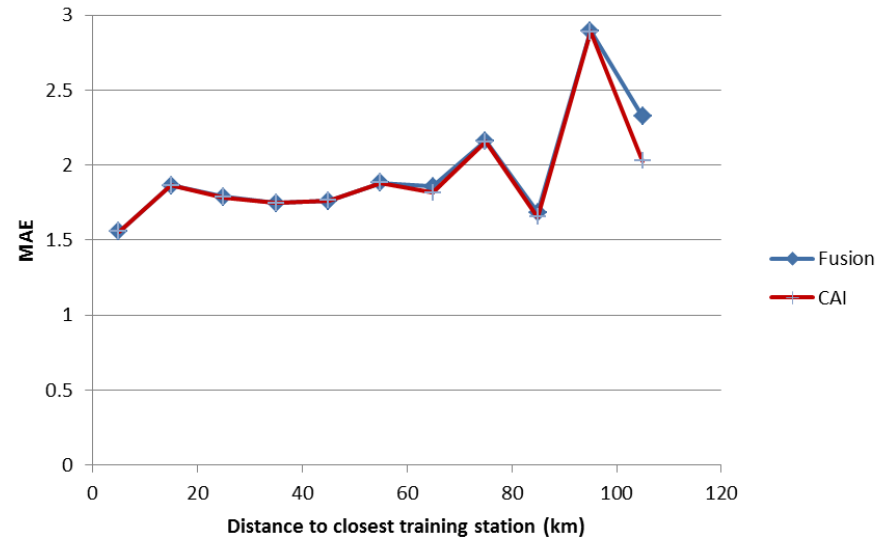
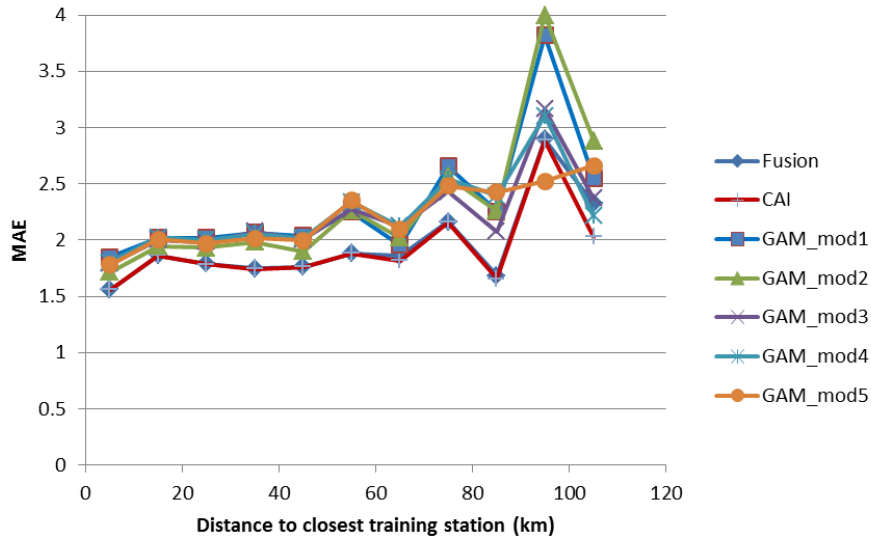
- The average RMSE AND MAE over 365 dates was computed for the two best method of predictions (CAI-Kr and Fusion-Kr). We found that:
 - Very slight differences in average with RMSEs around 2.29C and MAE around 1.78C
 - The standard deviations are also similar:
 - 0.65C (RMSE) and 0.51 C (MAE) for fusion
 - 0.65C (RMSE) and 0.52 C (MAE) for CAI

2. METHOD COMPARISON: MAE IN TERMS OF DISTANCE TO CLOSEST STATION

→ **General Idea:**

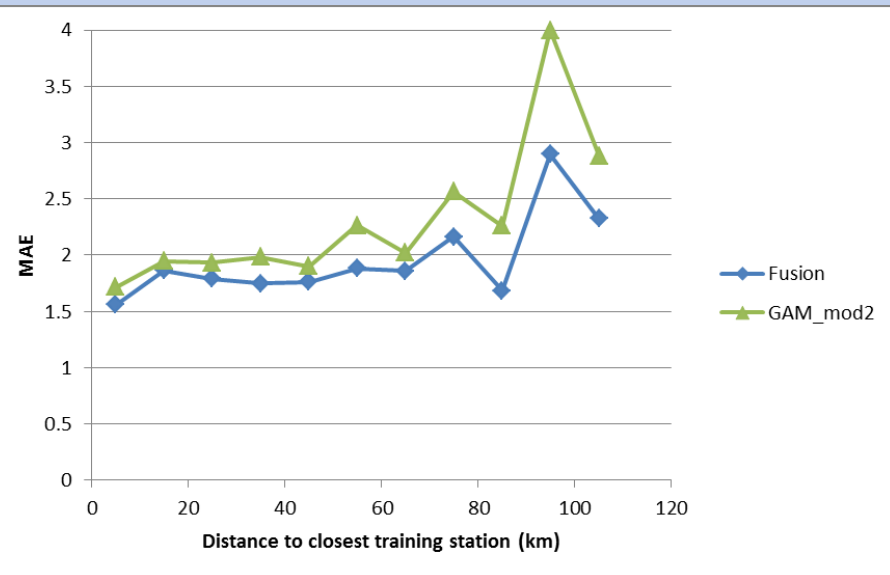
There is an expectation that predictions of t_{max} values at specific locations will be less accurate when there are no meteorological stations close by. This procedure captures this idea by plotting the MAE in terms of the distance to the closest neighboring station.

2. METHOD COMPARISON: MAE IN TERMS OF DISTANCE TO CLOSEST STATION



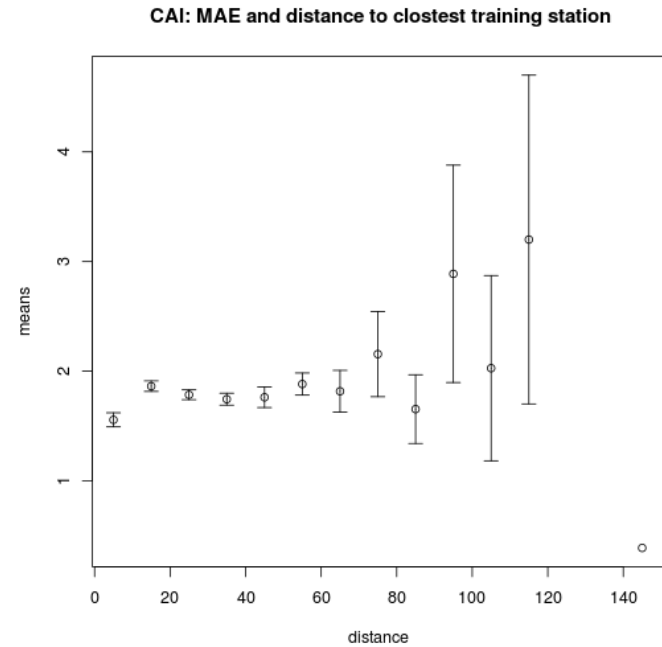
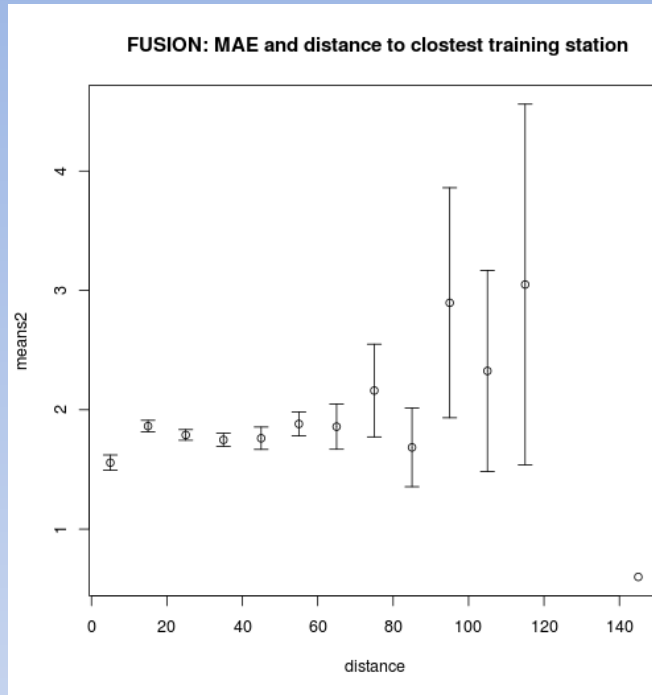
MAE are calculated:

- Using residuals over 365 dates
- Residuals (for each date) are binned in distance classes of 10km.
- *Distance classes are centered on a sequence from 5 to 115 by 10km steps.*
- Within each bin the MAE is calculated.



As expected, MAE increases when the distance to closest fitting station increases. **We note that Fusion (kr) and CAI (kr) have the lowest increases in MAE compared to the GAM models** described earlier. 33

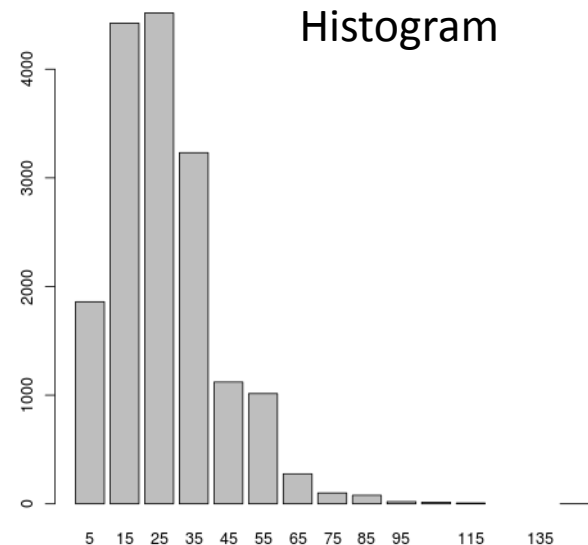
2. METHOD COMPARISON: MAE IN TERMS OF DISTANCE TO CLOSEST STATION



95% Confidence interval for MAE calculated:

- Using residuals over 365 dates
- Residuals binned per distance classes centered on the sequence from 5 to 115 by 10 steps.

The CI shows high uncertainty in high distance bin classes. This is due in part to the low frequency of station at distance greater than 65km (see histogram).

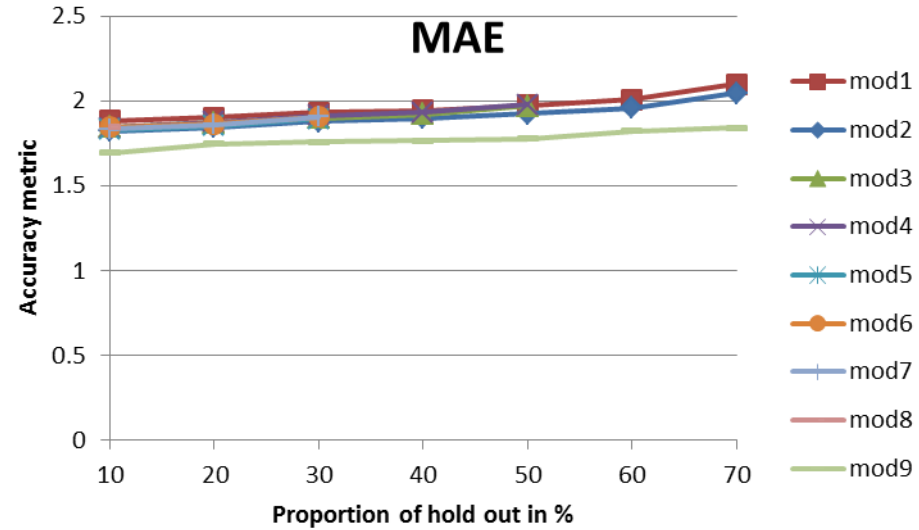
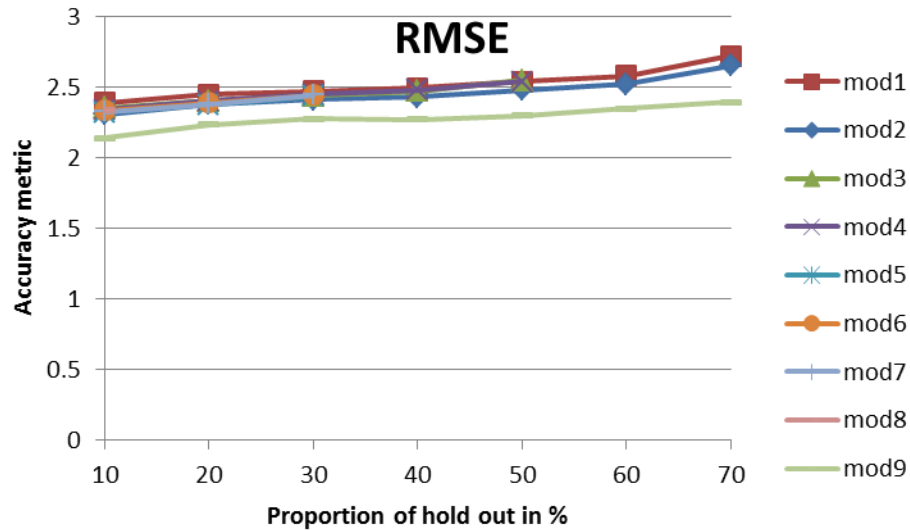


3. METHODS COMPARISON USING MULTISAMPLING PREDICTIONS

→ General Idea:

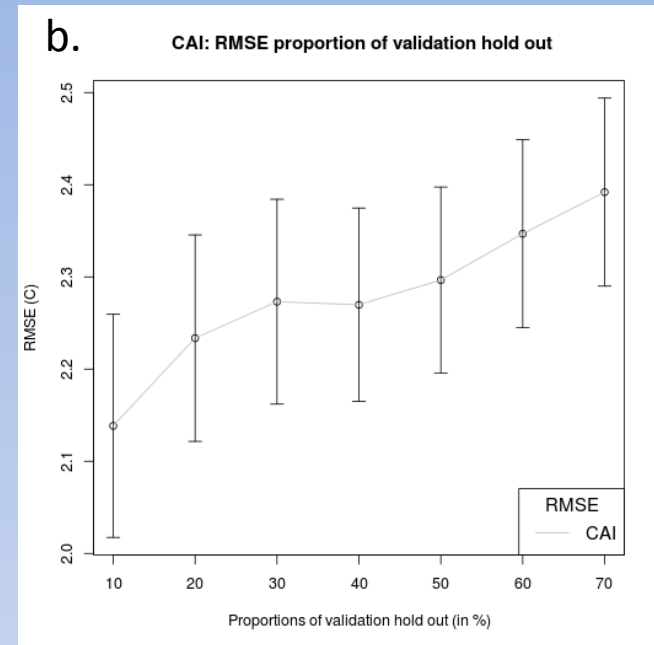
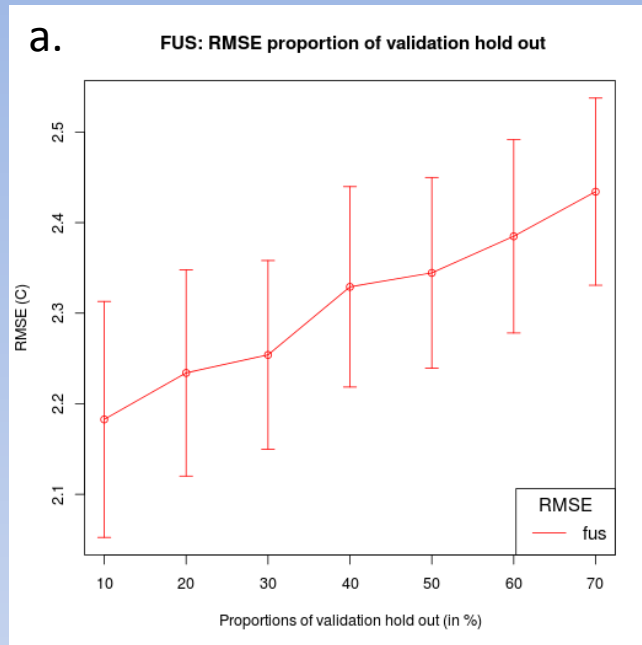
There is an expectation that predicted t_{max} values will be less accurate when the number of training stations used is low. The “multisampling” procedure captures this idea by plotting the MAE and RMSE in terms of the proportion of hold out. In order to account for the effect of selected samples in the accuracy metrics, we randomly sample stations 15 times for every proportion of hold out. Graphs presented are therefore MAE and RMSE averages with confidence intervals.

MULTISAMPLING AND PROPORTION OF VALIDATION HOLD OUT CAI MODELS



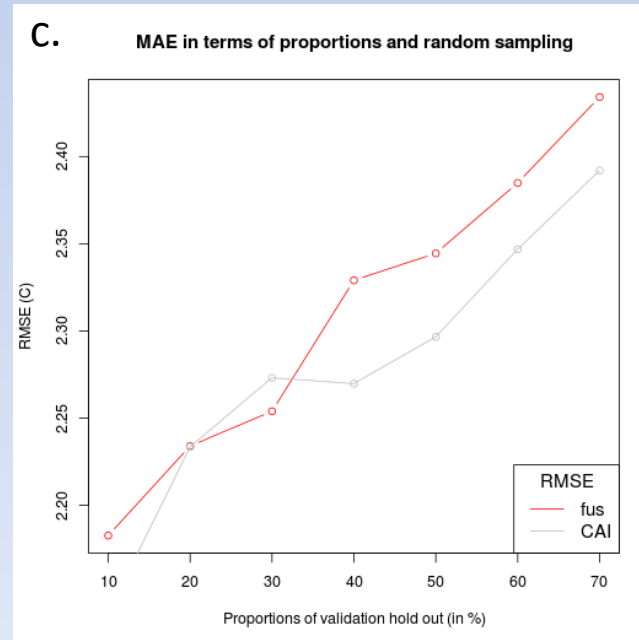
- This plot is based on averages over 10 dates, with 15 samples per run. Proportions were varied from 10 to 70% hold out. Models were described in slide 14 and 23.
- Total number of runs: $7 \times 15 \times 10 = 1050$ or raster predictions/images.
- Note that model 9 corresponds to CAI with Kriging and performs the best (lower green curve) compared to CAI with GAM.

3. MULTISAMPLING COMPARISON



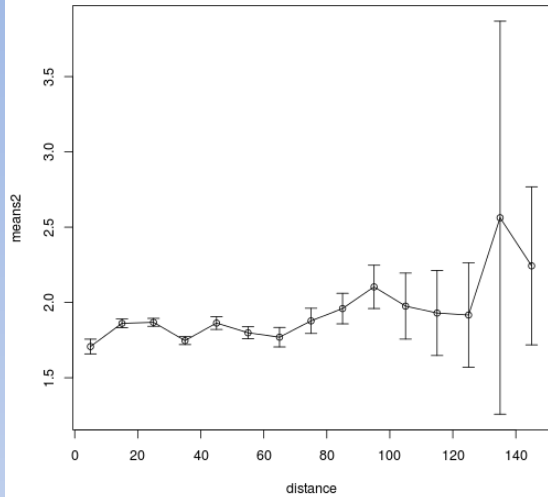
→ These plots compares CAI (kr) with Fusion (kr) using the multisampling procedure:

- We used CI plots to estimate uncertainty in the average RMSE values (plot a and plot b).
- Mean in MAE with proportion of hold out and random samples do not differentiate between CAI and fusion (plot c).

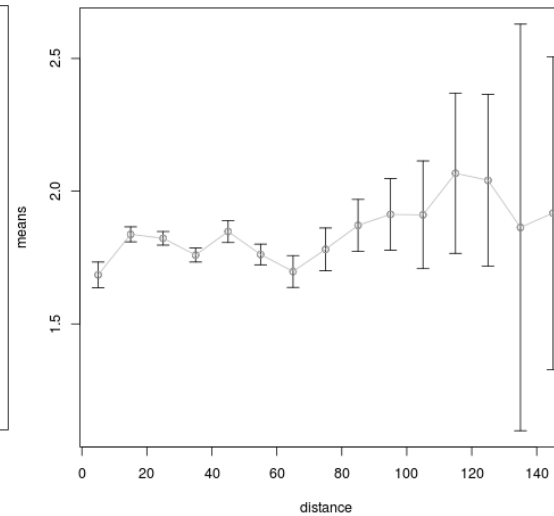


MAE IN TERMS OF DISTANCE TO CLOSEST STATION

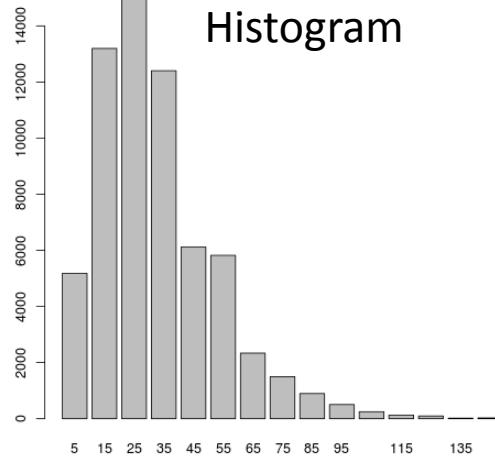
FUSION: MAE and distance to closest training station



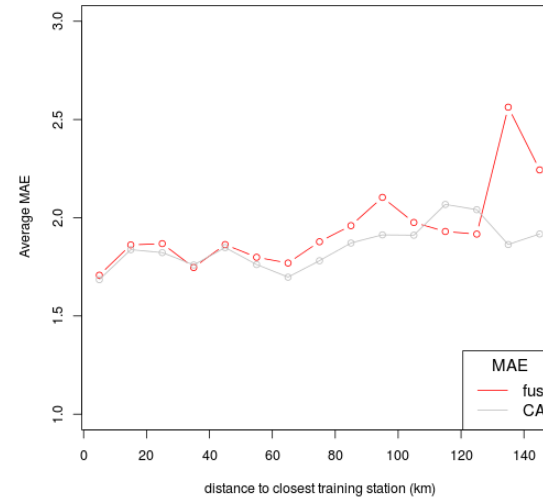
CAI: MAE and distance to closest training station



Histogram



MAE in terms of distance to closest station GAM and FUSION



We plotted the distance to MAE plot for the multisampling predictions. Residuals at validation stations were binned in distance classes for the 1050 predictions and the MAE was calculated for both CAI and Fusion methods. Results indicate that CAI and Fusion method perform similarly with MAE values increasing when distance to closest fitting station increases.

4. VISUALIZATION

COMPARISON OF SPATIAL PATTERNS OF PREDICTION

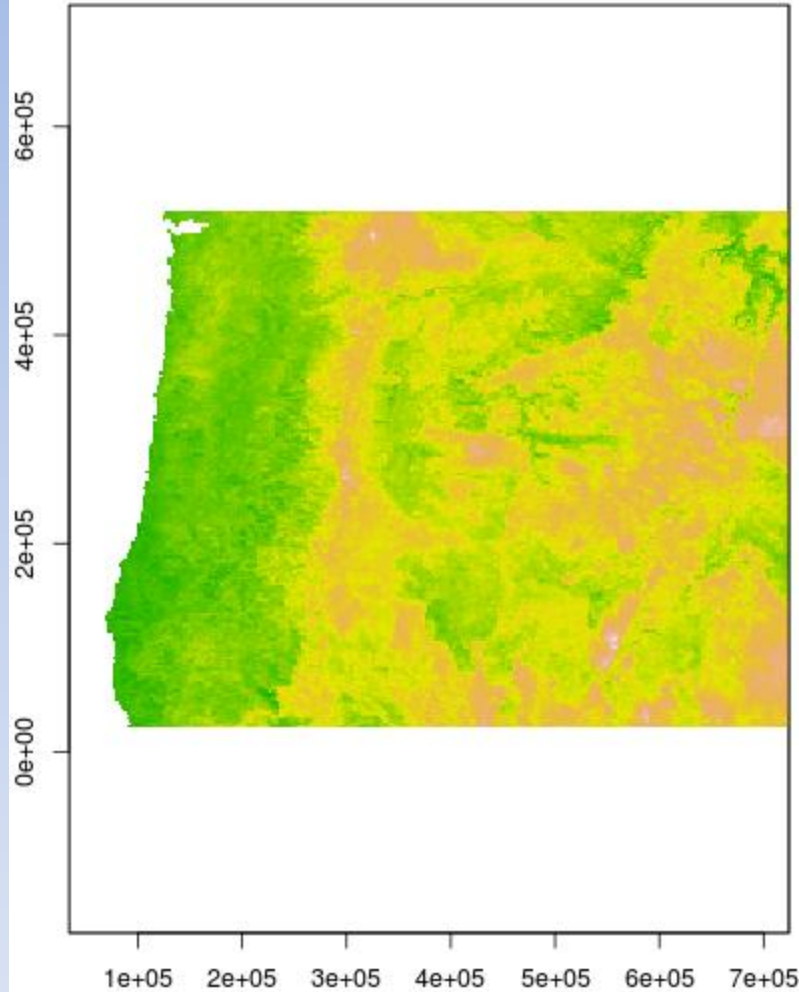
→ **General Idea:**

-The literature review highlights the importance of visualization of the results to assess model outputs and compare products.

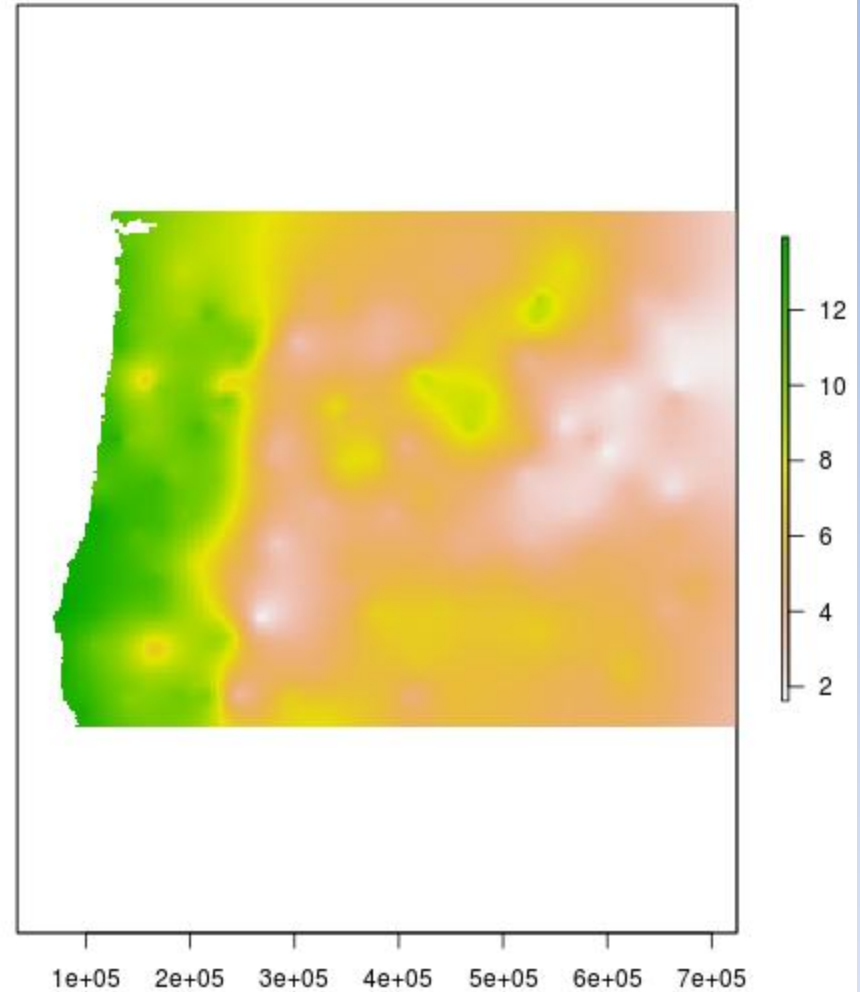
-Spatial patterns of tmax predictions should conform to expectation i.e. topographical patterns and landscape features should appear on prediction maps.

COMPARISON BETWEEN PREDICTIONS FOR FUSION AND CAI

sion_tmax_predicted_20100101_07242012_365d_GAM_fusion5



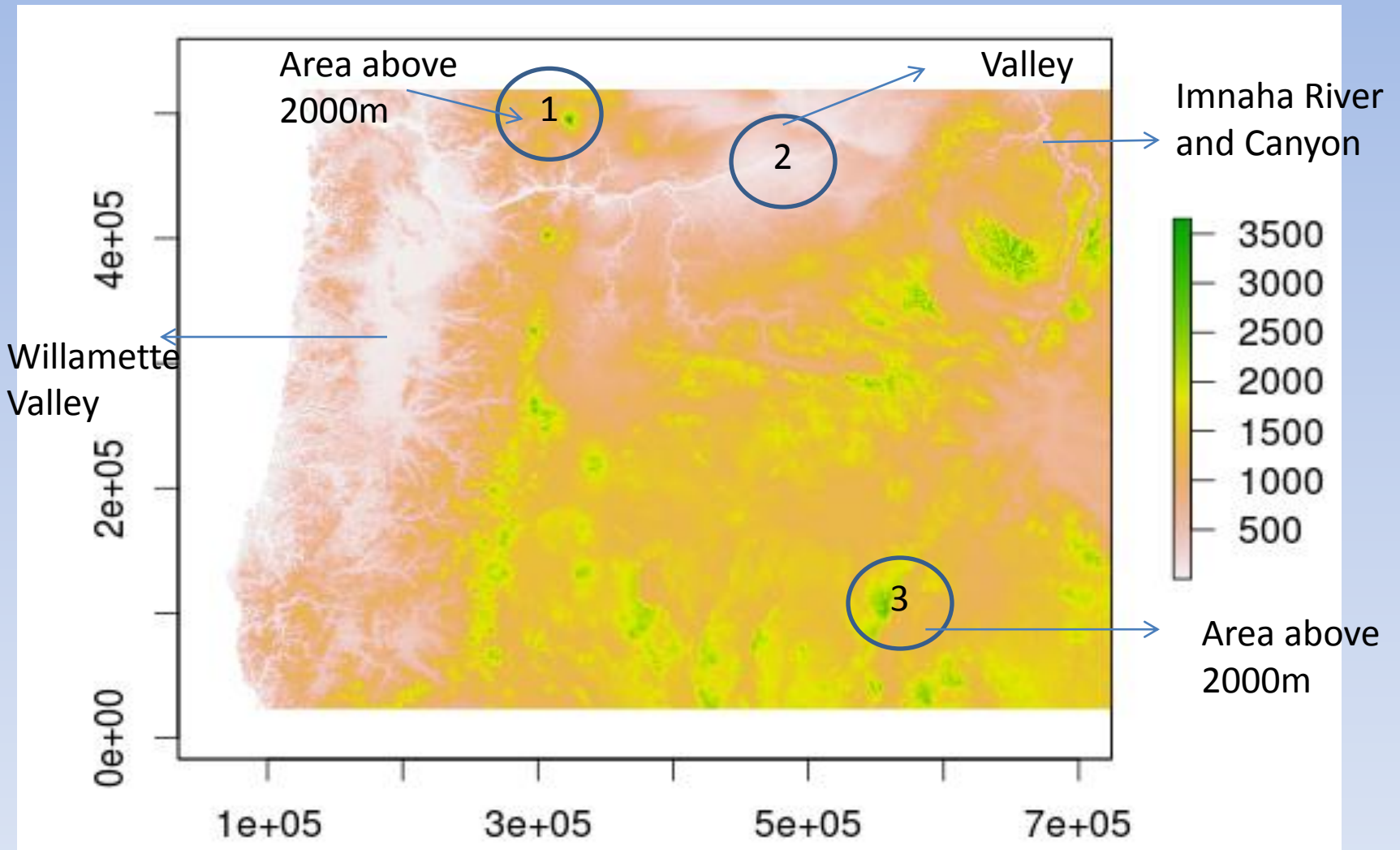
CAI_tmax_predicted_20100101_08072012_365d_GAM_CAI2



Date: January 1, 2012

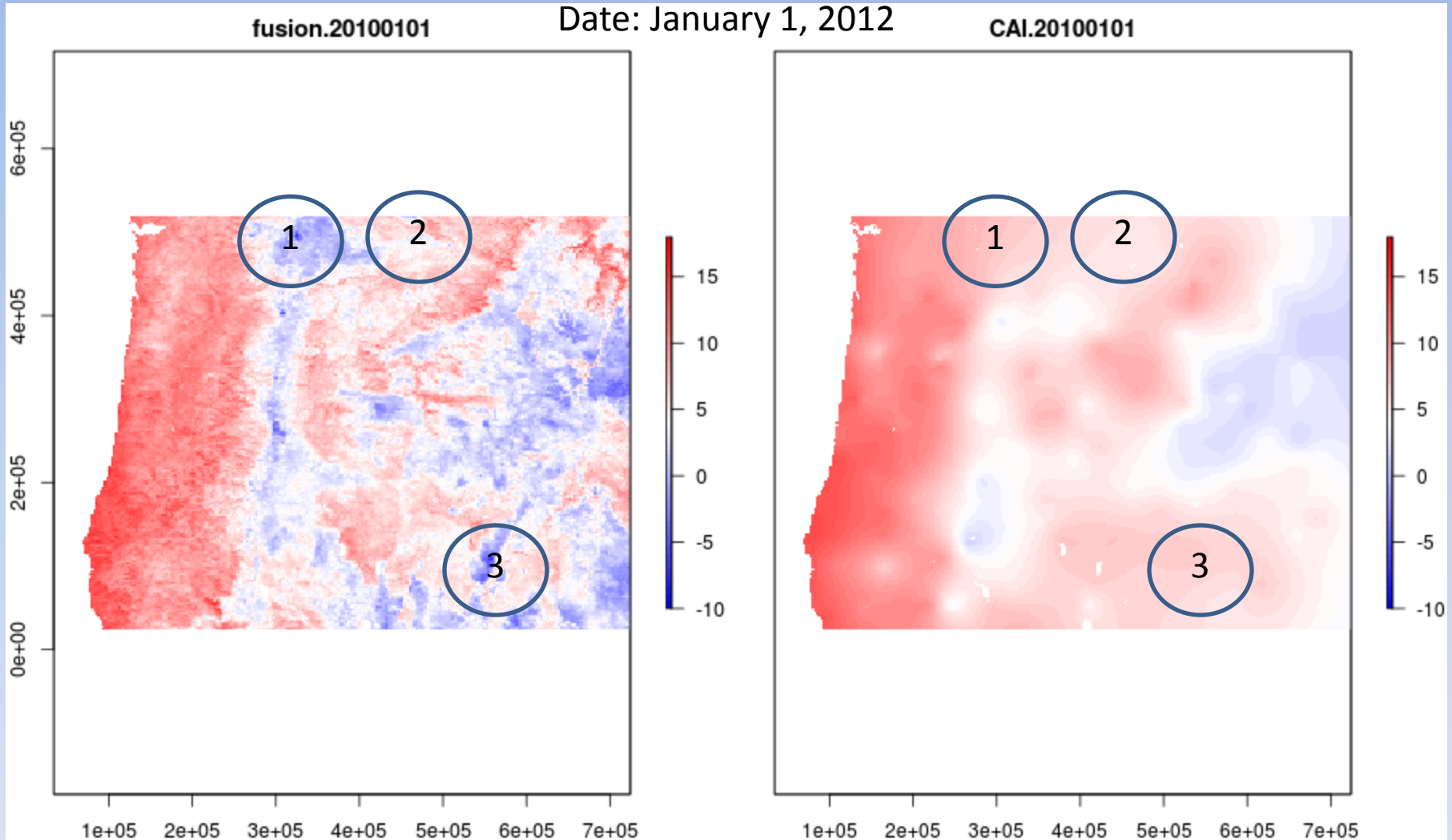
Note the difference in the range of tmax values for the two maps on the same day. This is visible in the palette range.

ELEVATION SRTM



The elevation is reported in meters.

COMPARISON BETWEEN PREDICTIONS FOR FUSION AND CAI

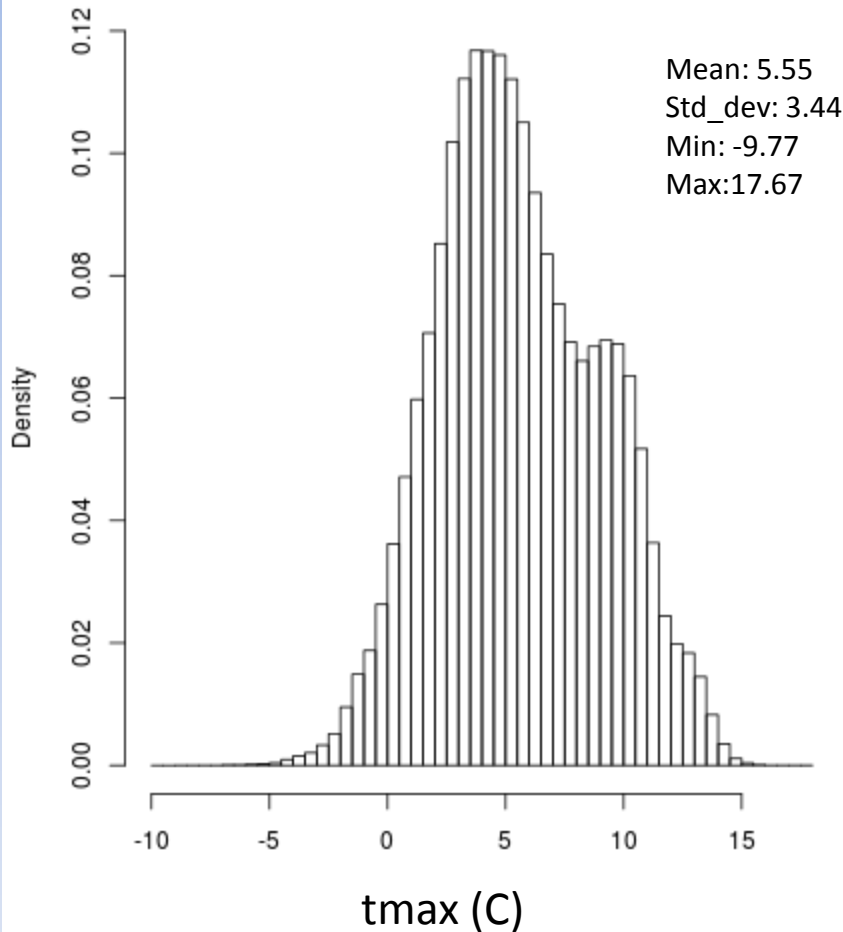


Areas to focus on are highlighted by circles and labeled by numbers. Area 1 and Area 3 correspond to high mountainous areas while area 2 is a low lying cultivated area.

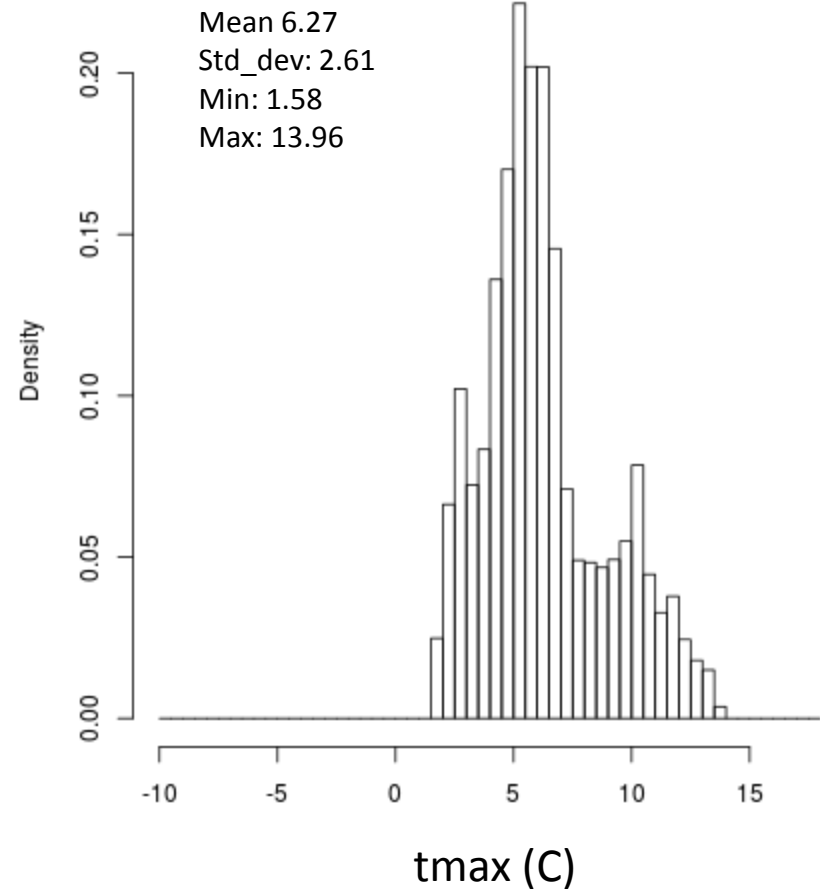
HISTOGRAM COMPARISON BETWEEN PREDICTIONS FOR FUSION AND CAI

Date: January 1, 2012

fusion.20100101

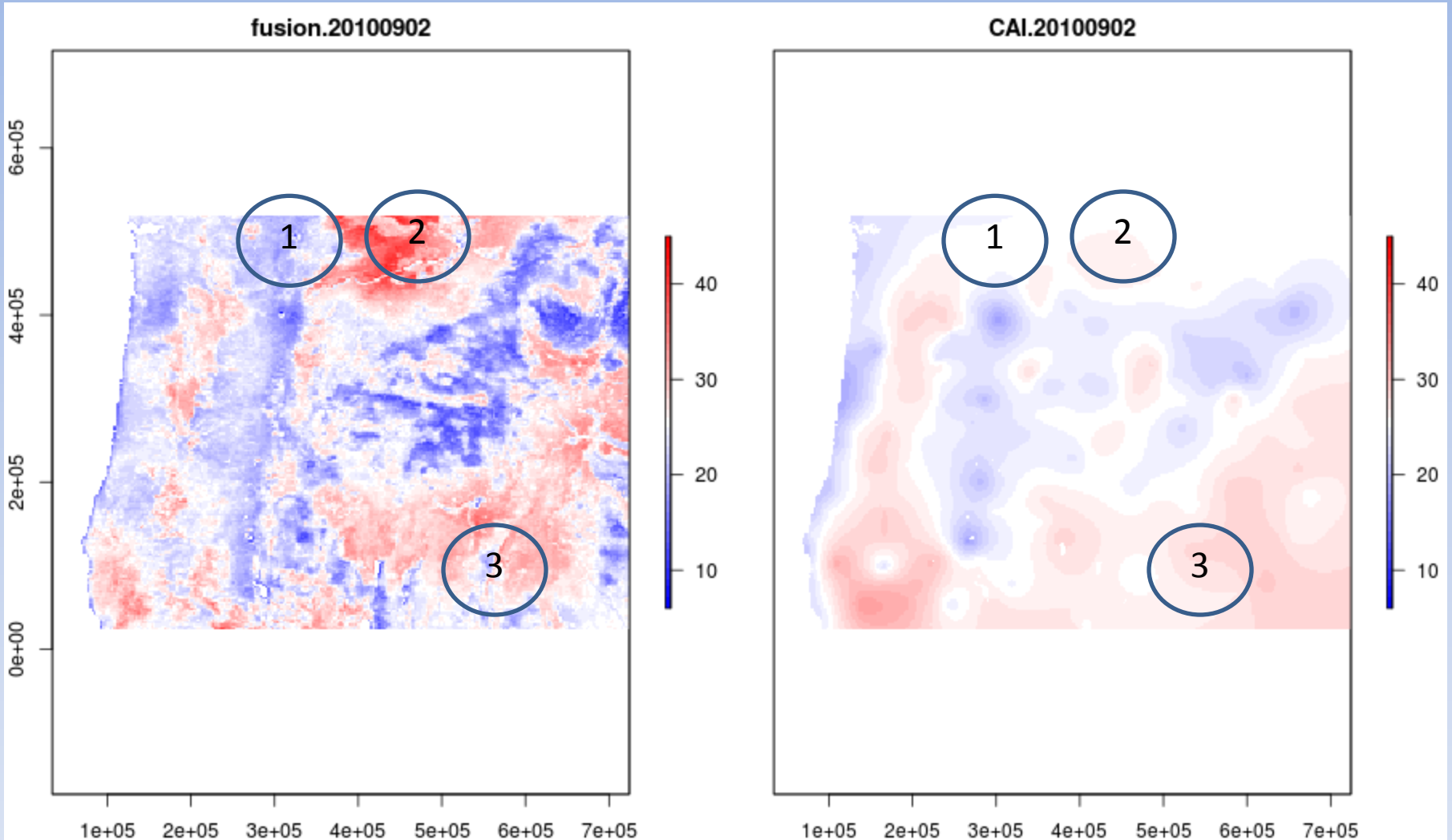


CAI.20100101



Note the difference in the range of tmax values for the two maps on the same day. The CAI histogram on the right indicate that there are not values below zero and that but both maps Have values are assembled around

COMPARE CAI AND FUSION PREDICTION MAPS OVER THE YEAR

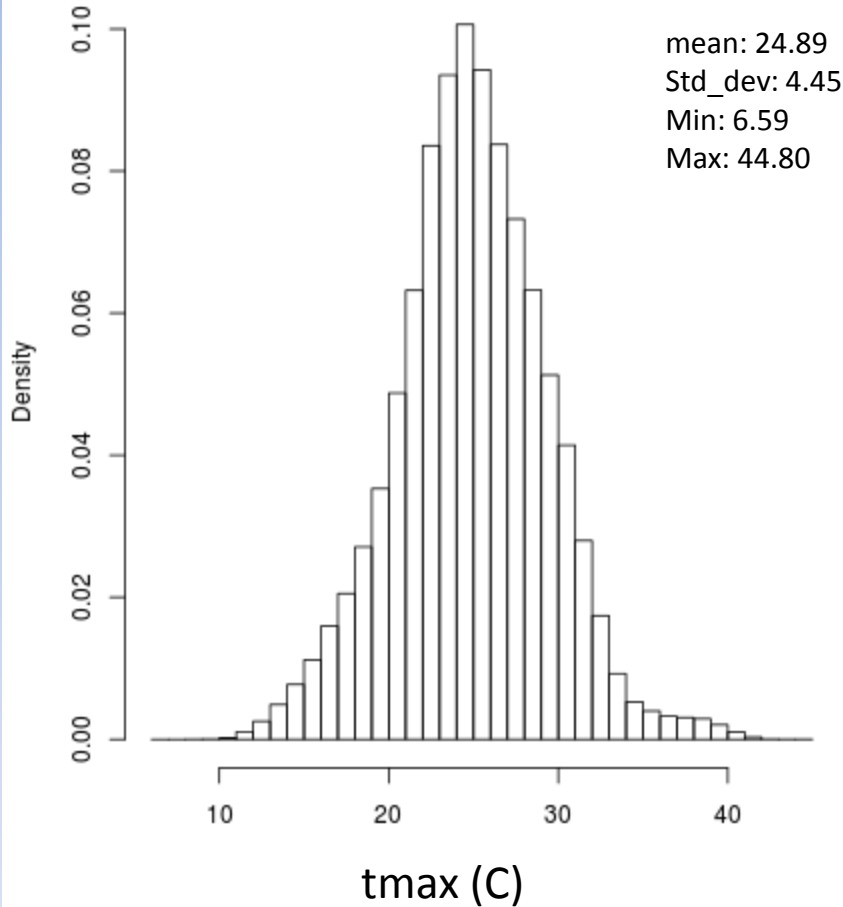


Predictions on September 2 2010 are similar but with a smoother surface for CAI.

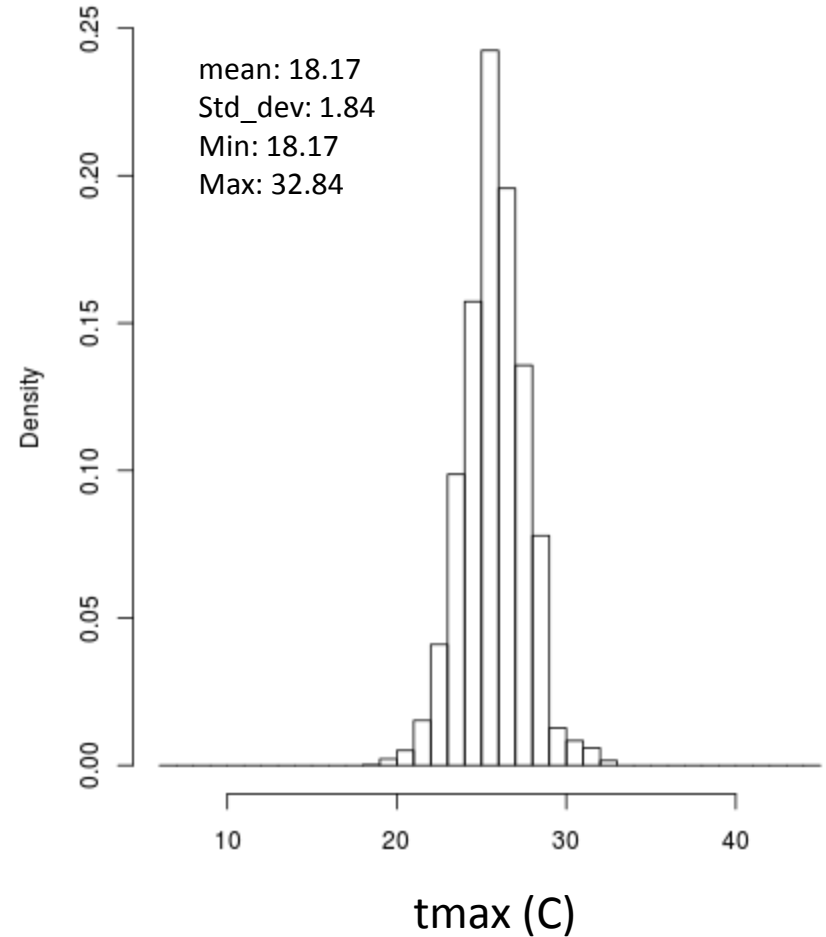
HISTOGRAM COMPARISON BETWEEN PREDICTIONS FOR FUSION AND CAI

Date: September 9, 2012

fusion.20100902

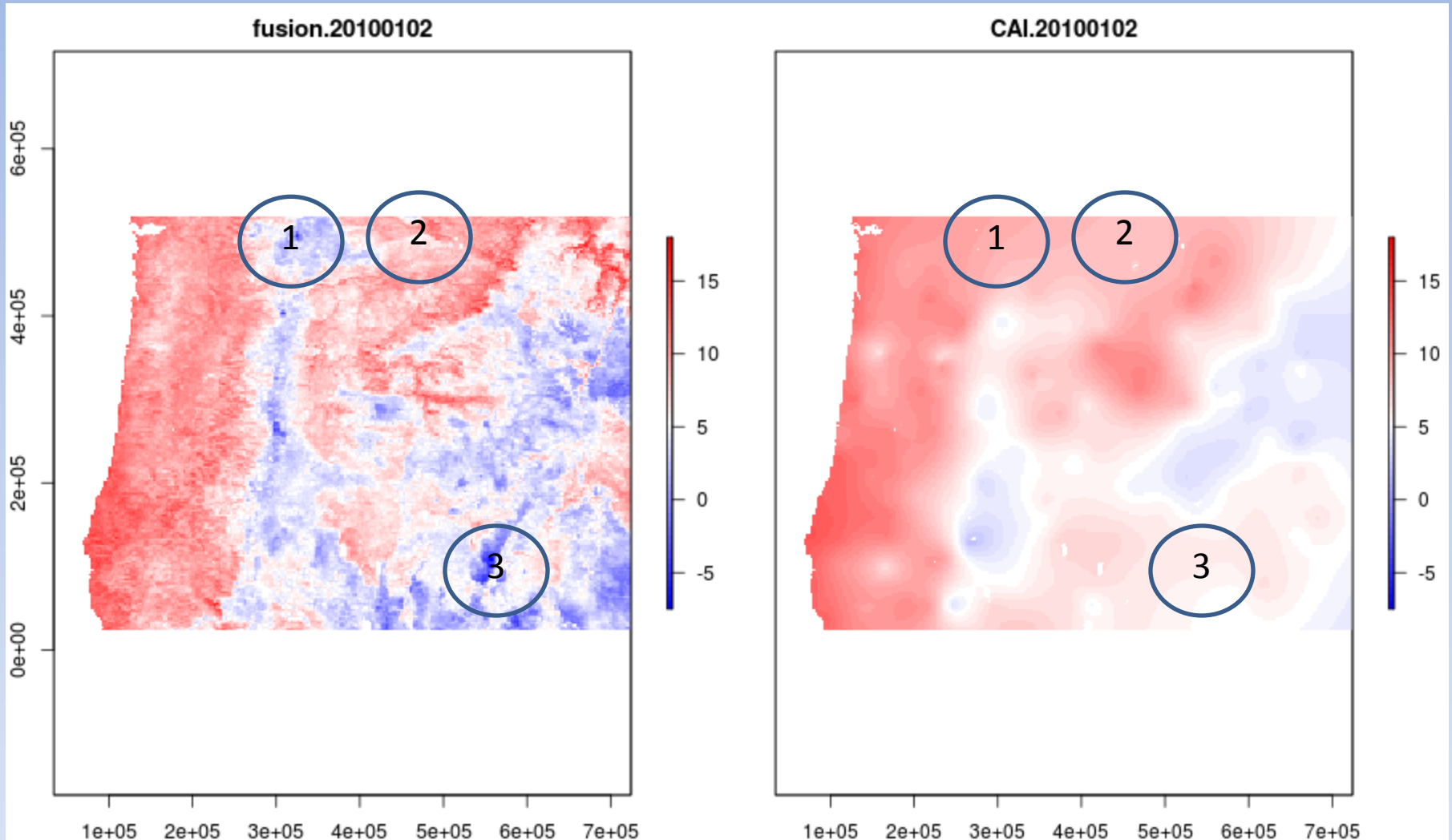


CAI.20100902



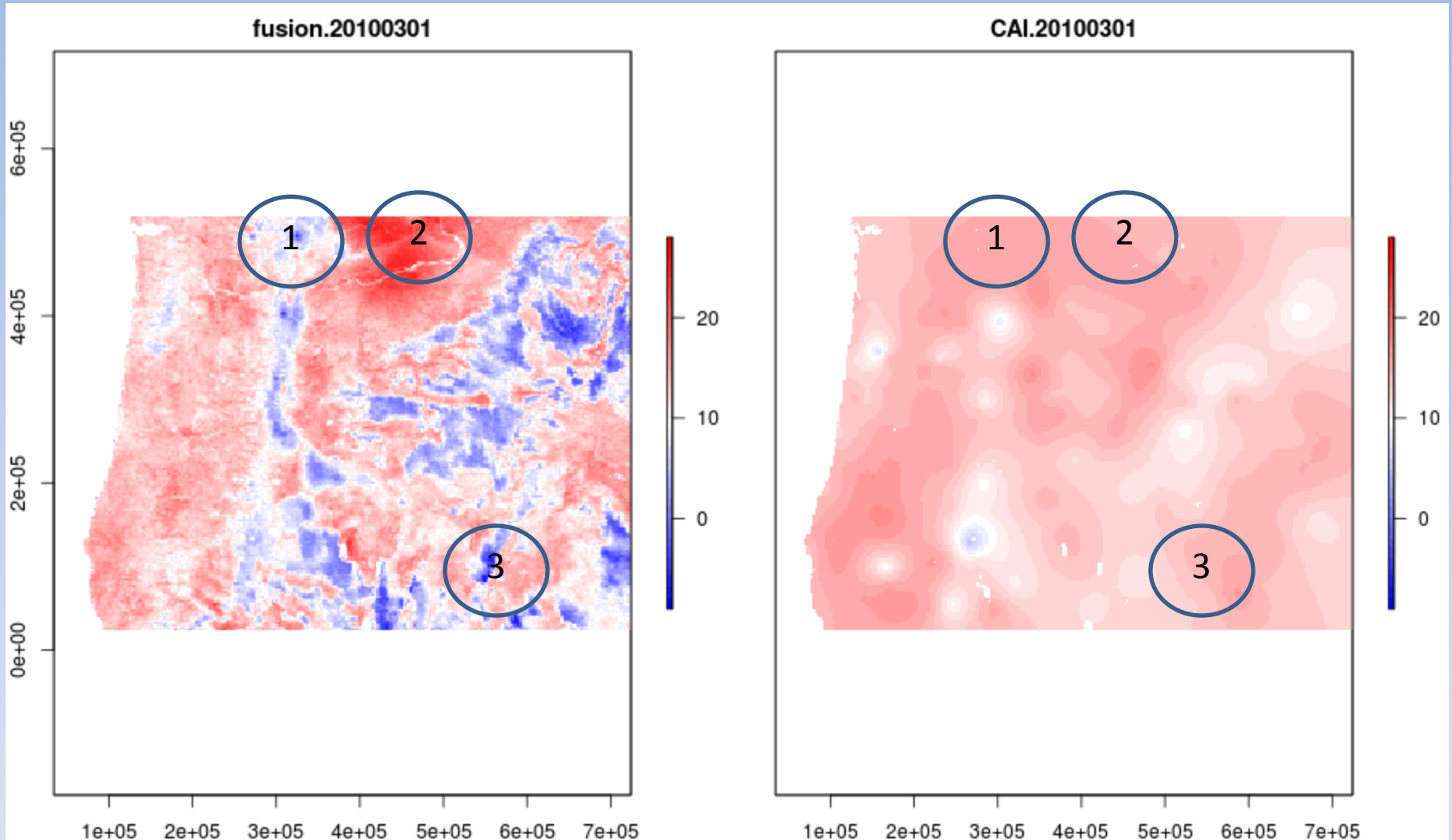
Note the difference in the range of tmax values for the two maps on the same day. The CAI histogram on the right indicate that there are not values below zero and that but both maps Have values are assembled around

COMPARE DIFFERENT CAI AND FUSION PREDICTION MAPS OVER THE YEAR



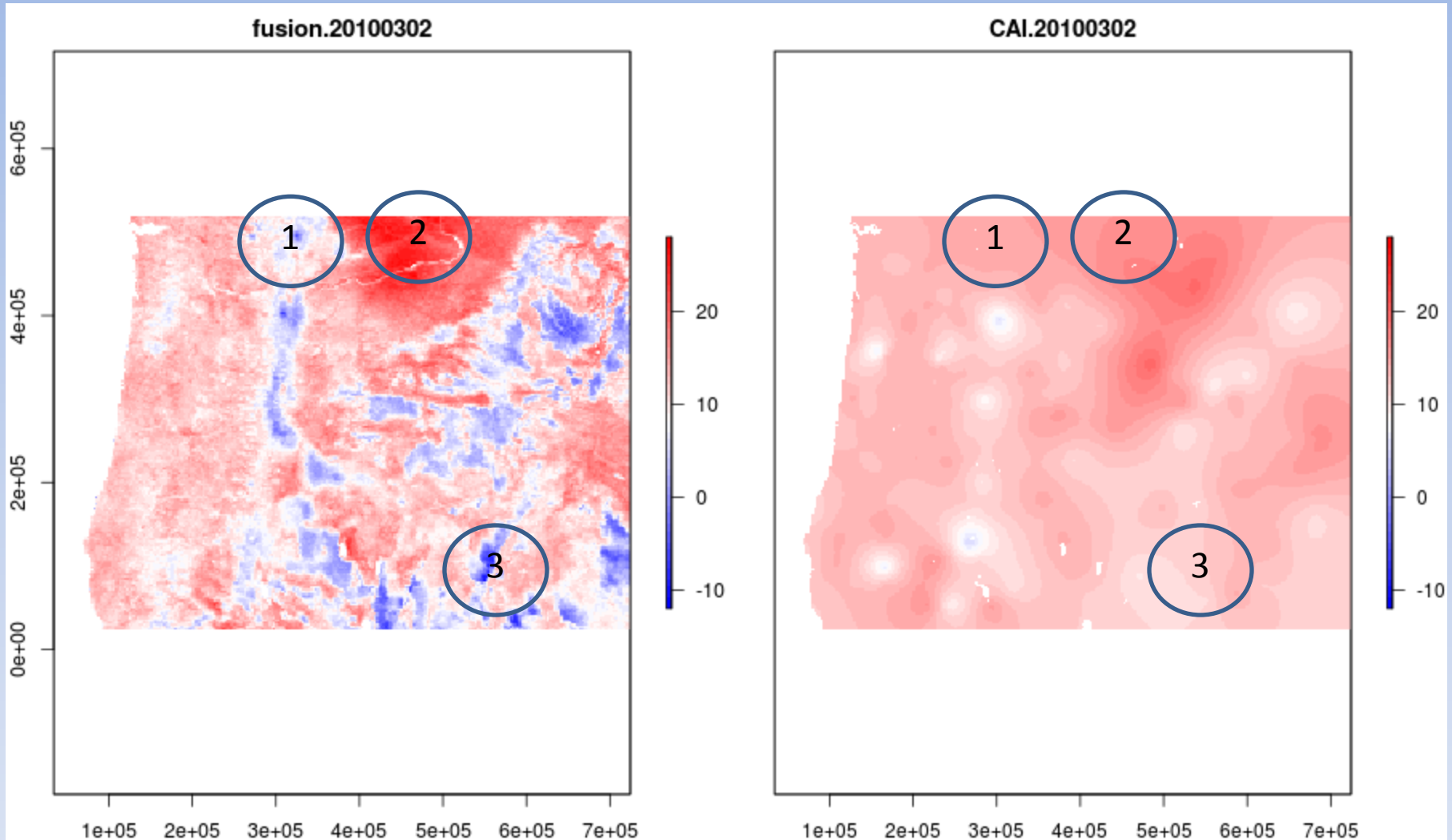
Note the differences in area 2 and area 3 in the two interpolated surfaces. Area 3 does not show the pattern of high elevation in CAI figure (on the left).

COMPARE DIFFERENT CAI AND FUSION PREDICTION MAPS OVER THE YEAR



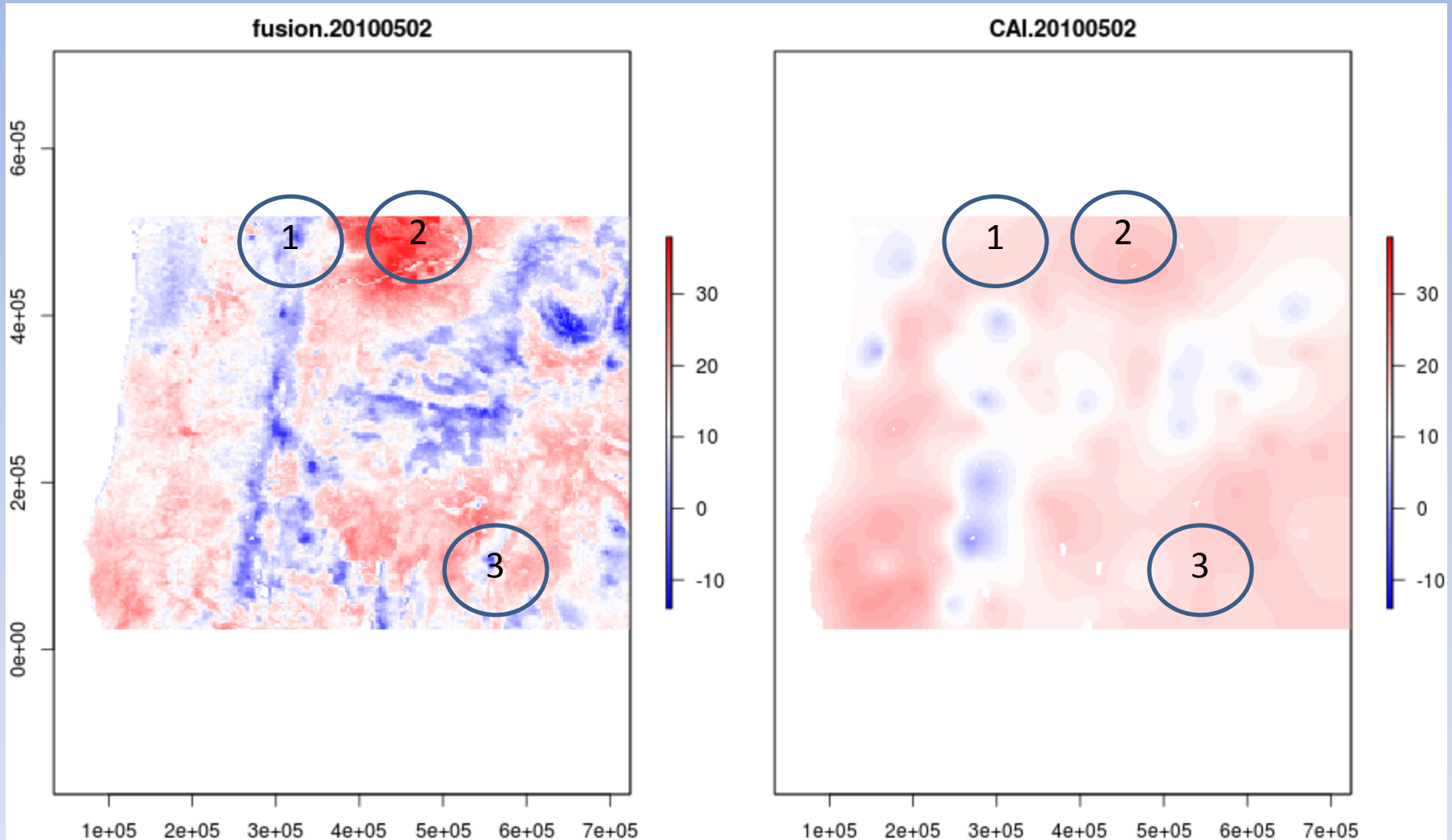
Note the differences in area 2 and area 3 in the two interpolated surfaces. Area 3 does not show the pattern of high elevation in CAI figure (on the left).

COMPARE DIFFERENT CAI AND FUSION PREDICTION MAPS OVER THE YEAR



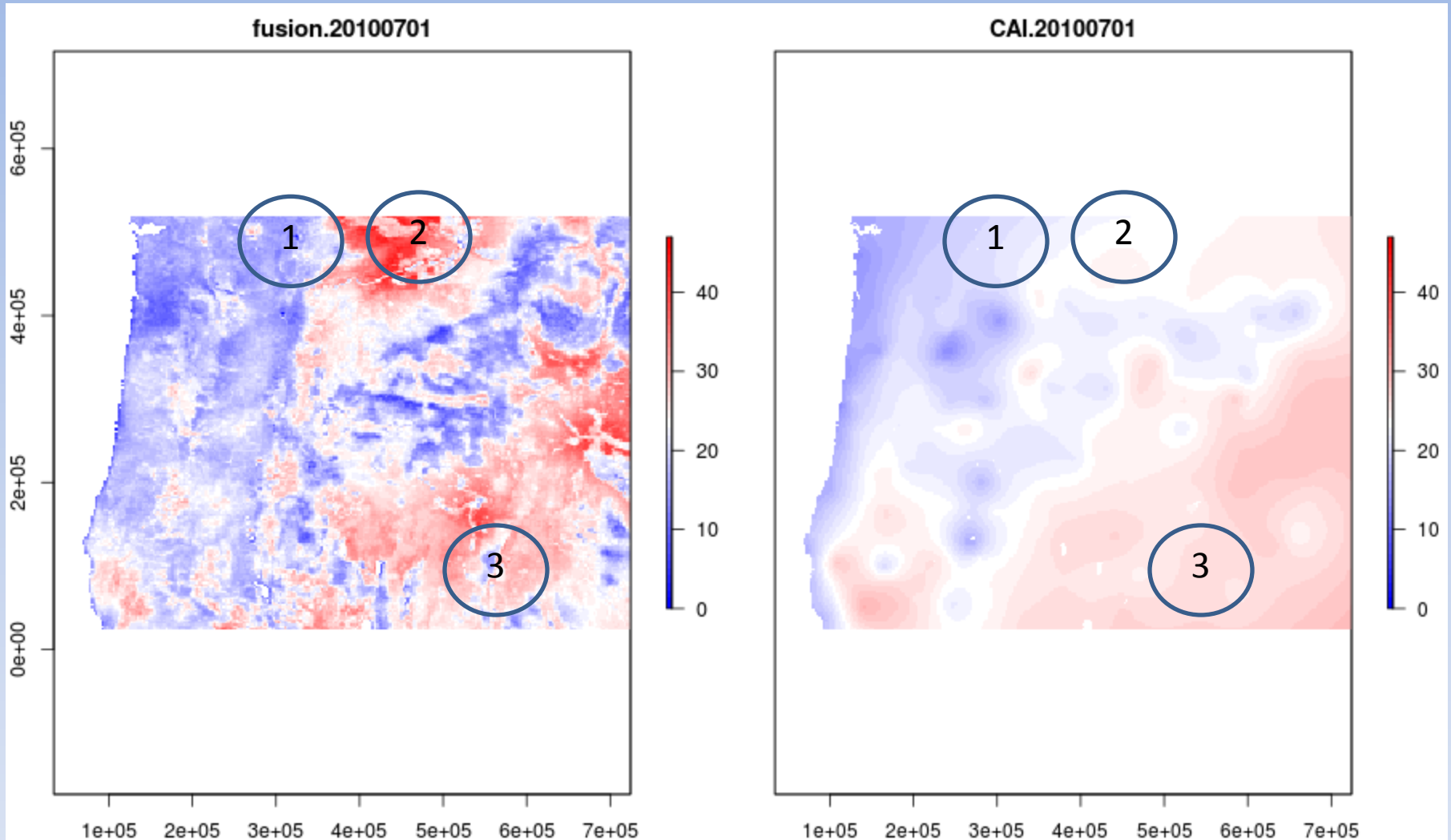
Note the differences in area 2 and area 3 in the two interpolated surfaces. Area 3 does not show the pattern of high elevation in CAI figure (on the left).

COMPARE DIFFERENT CAI AND FUSION PREDICTION MAPS OVER THE YEAR



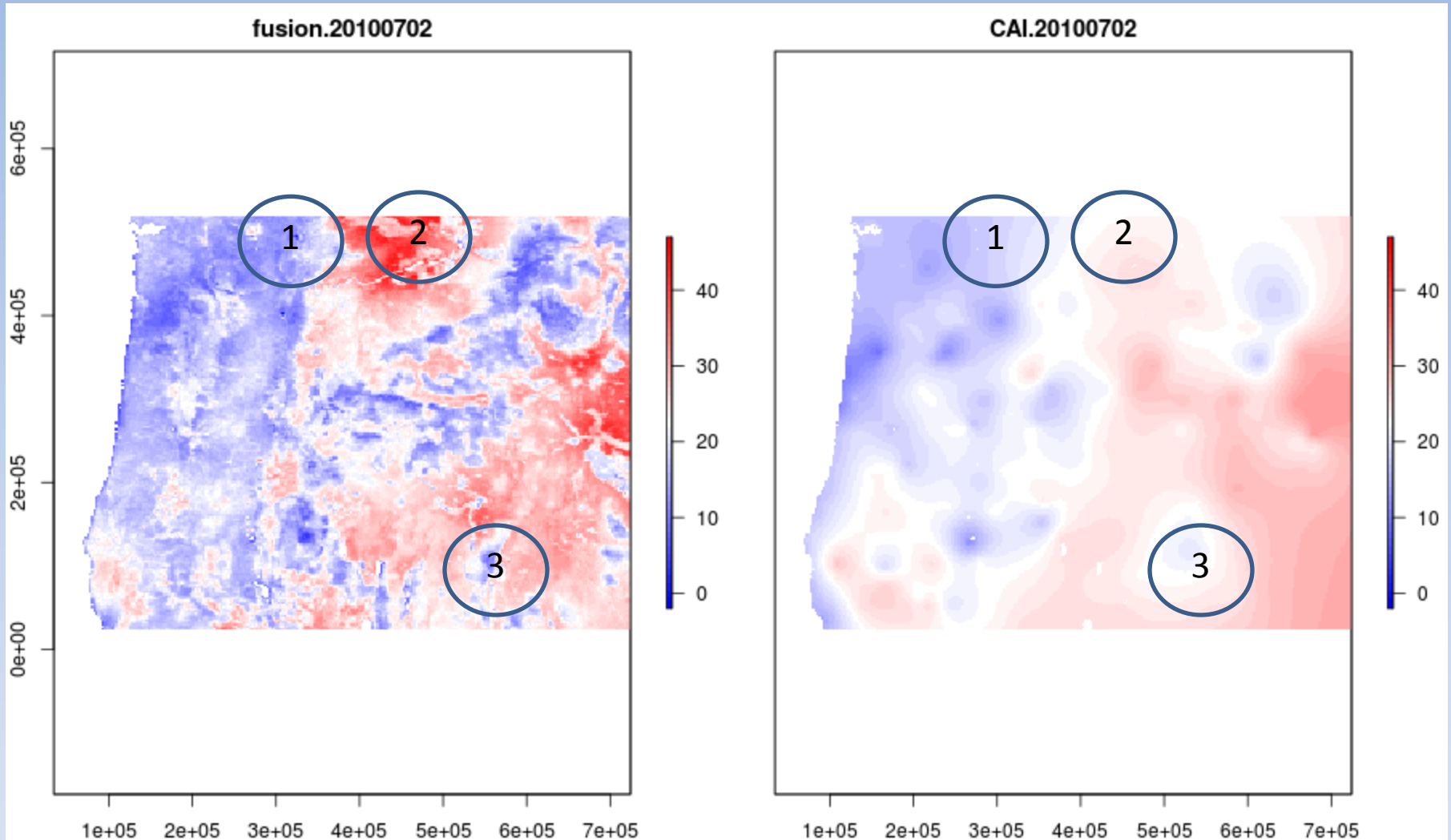
Note the cold temperatures in area 1 do not appear on the CAI map.

COMPARE DIFFERENT CAI AND FUSION PREDICTION MAPS OVER THE YEAR



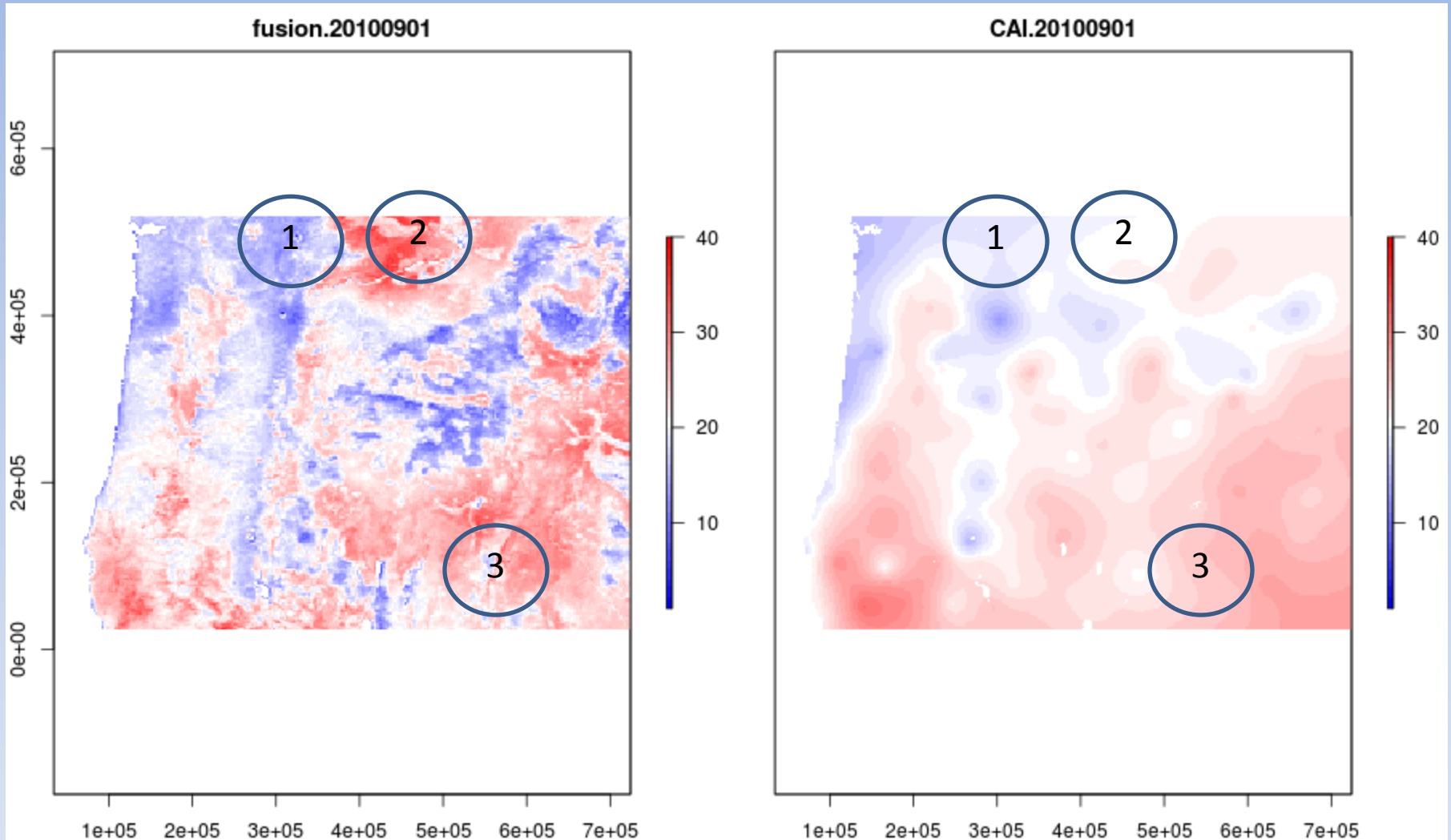
Note the differences in area 2 and area 3 in the two interpolated surfaces. Area 3 does not show the pattern of high elevation in CAI figure (on the left).

COMPARE DIFFERENT CAI AND FUSION PREDICTION MAPS OVER THE YEAR



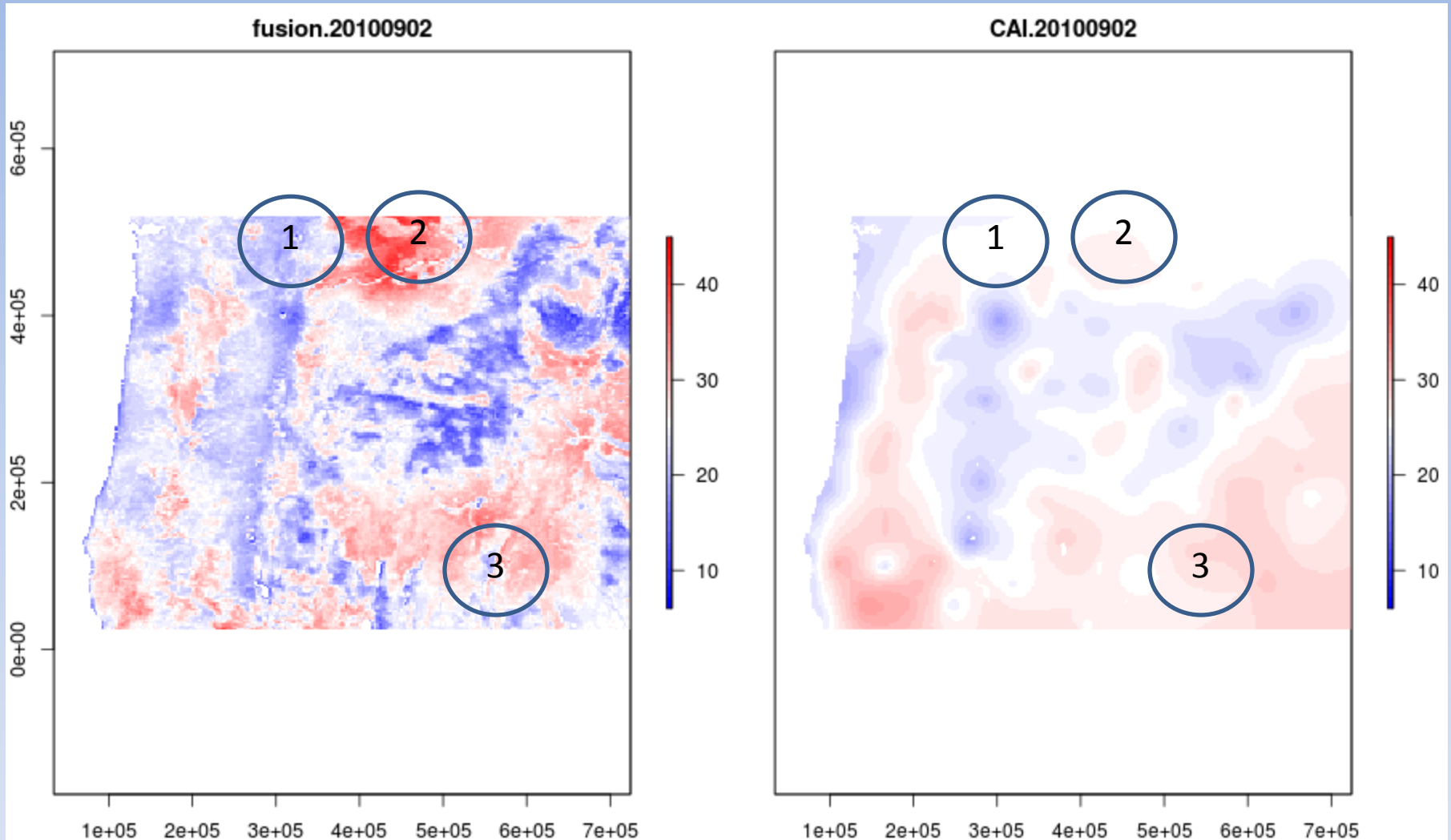
Note the differences in area 2 and area 3 in the two interpolated surfaces. Area 3 on CAI (figure on the left) does show the peak of elevation with lower temperature in the smooth manner.

COMPARE DIFFERENT CAI AND FUSION PREDICTION MAPS OVER THE YEAR



On September 1, 2010, there is a clear difference in the prediction in area 2. CAI predicts temperatures in the 10 to 20 C interval while Fusion predicts temperatures in the 20 to 40C₂ range.

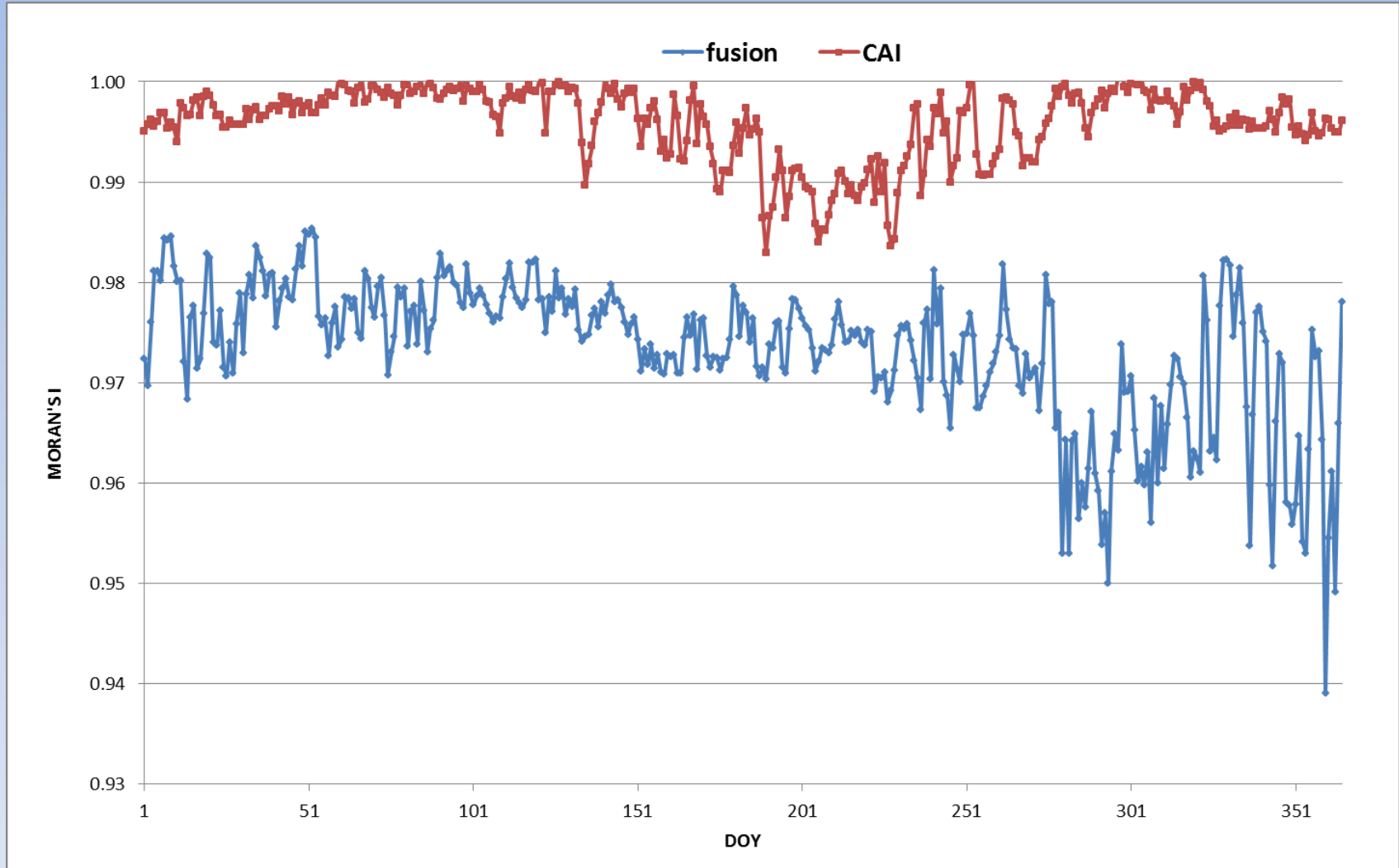
COMPARE DIFFERENT CAI AND FUSION PREDICTION MAPS OVER THE YEAR



While the general spatial pattern is similar on both maps, it is obvious that Fusion shows greater spatial details appearing to match Oregon topographical. This statement appears to hold for the 9 dates presented in the previous slides. Numerical evidence of the amount of spatial variability can be obtained by computing the standard deviation and Moran's I for every day over the full year 2010.

MORAN'S I FOR TMAX PREDICTIONS

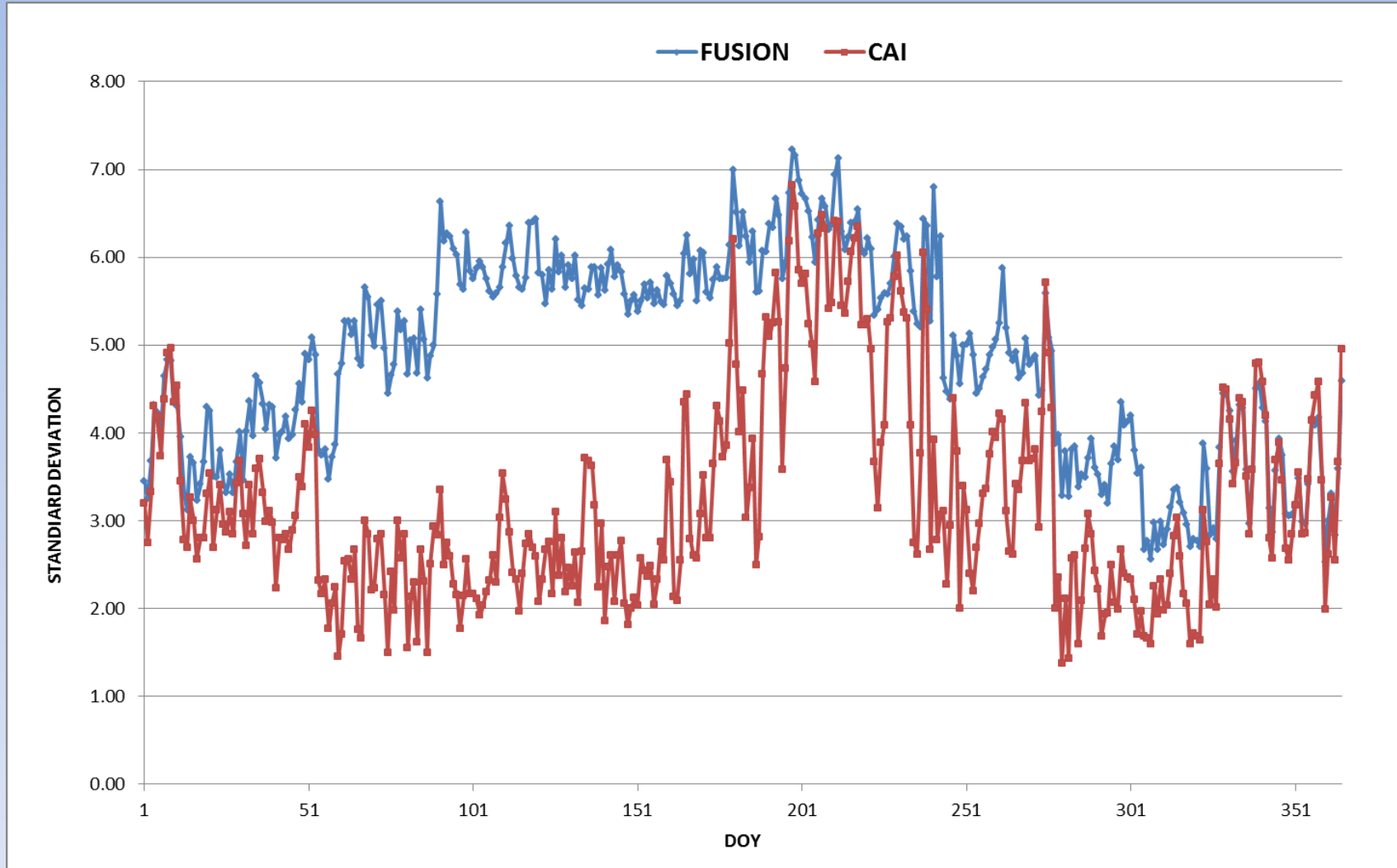
This figures was obtained by calculating the spatial autocorrelation (Moran's I) in each tmax prediction For every day of the year 2010. Note that DOY stands for Day Of Year.



There is less spatial autocorrelation in the fusion method → surface less smooth locally.
The fusion method must incorporate the spatial variability through the LST term.

STANDARD DEVIATION FOR TMAX PREDICTIONS

This figures was obtained by calculating the standard deviation in each tmax prediction For every day of the year 2010. Note that DOY stands for Day Of Year.

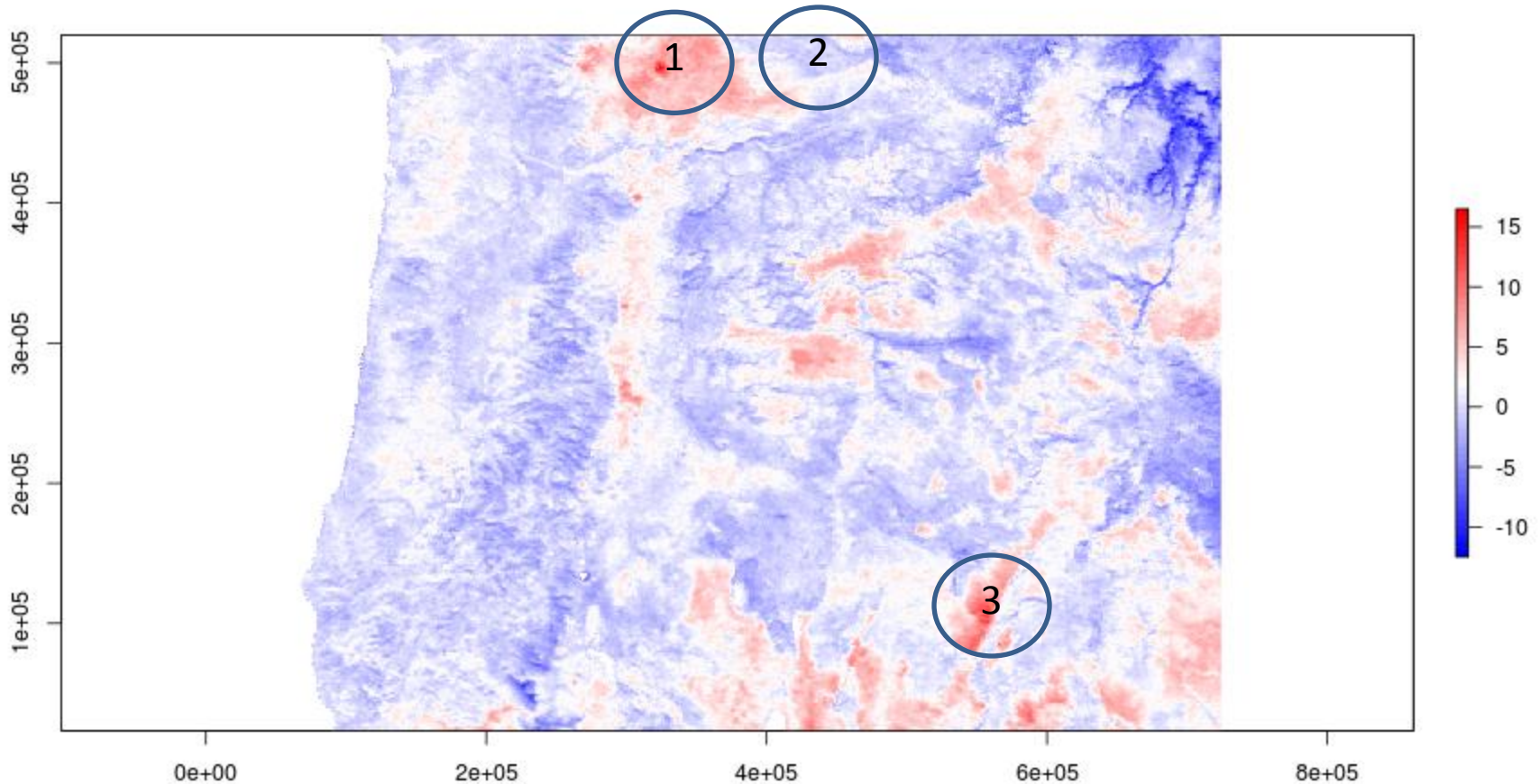


There is more variability in the Fusion prediction as indicated in the time series of standard deviation. Note however the spike in variability in CAI between DOY 200 and 240.

DIFFERENCE IMAGE BETWEEN CAI AND FUSION PREDICTIONS

$$\text{Difference} = \text{CAI_tmax_prediction} - \text{Fusion_tmax_prediction}$$

Difference between CAI and fusion for 20100101

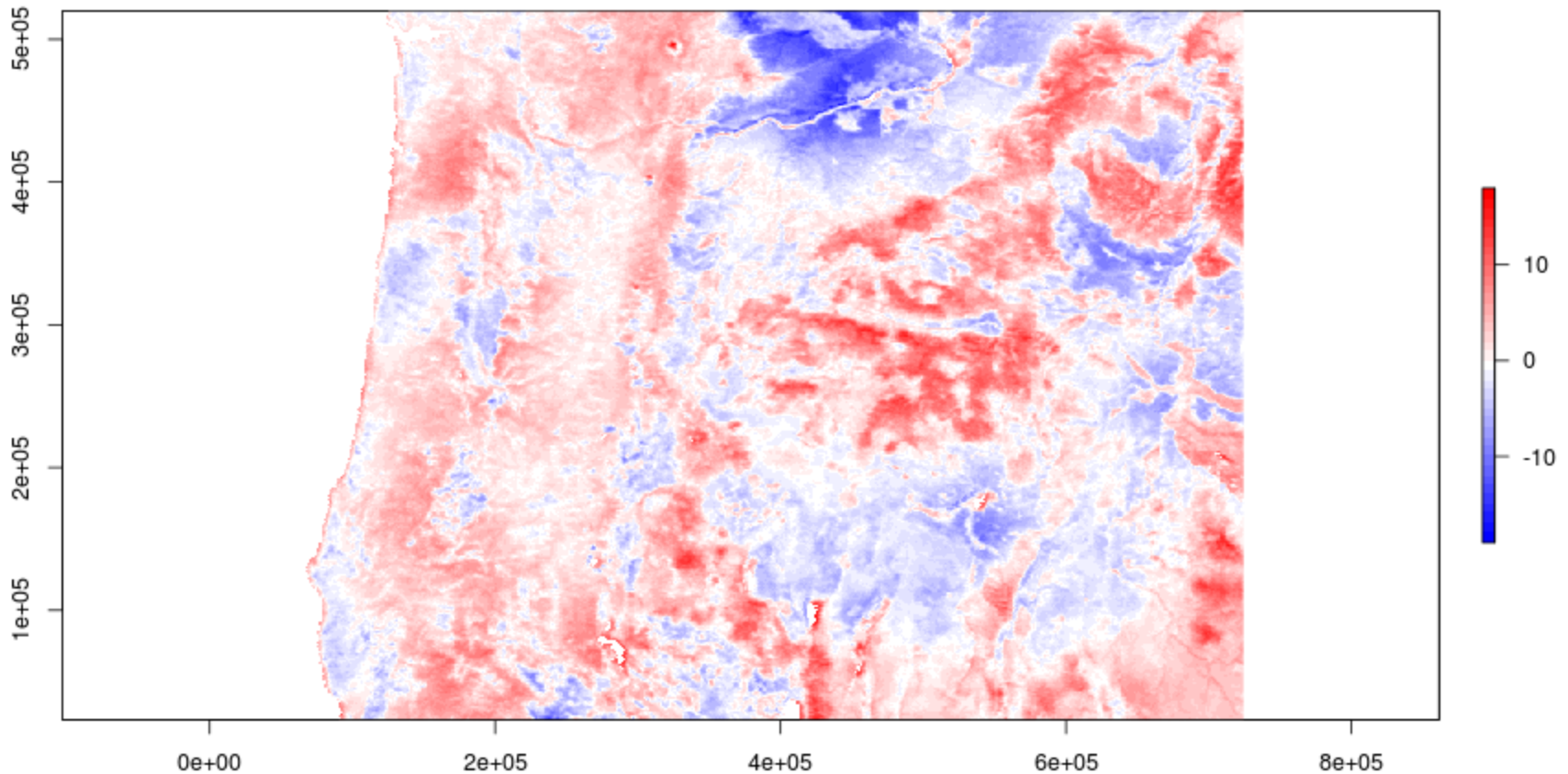


We note clear positive differences in the mountainous areas (areas 1 and 3). This indicates lower temperature predicted in the mountains by Fusion as compared to CAI. Note also the higher temperatures predicted by Fusion in the Northeast corner of the state clearly visible in the river course in blue.

DIFFERENCE IMAGE BETWEEN CAI AND FUSION PREDICTIONS

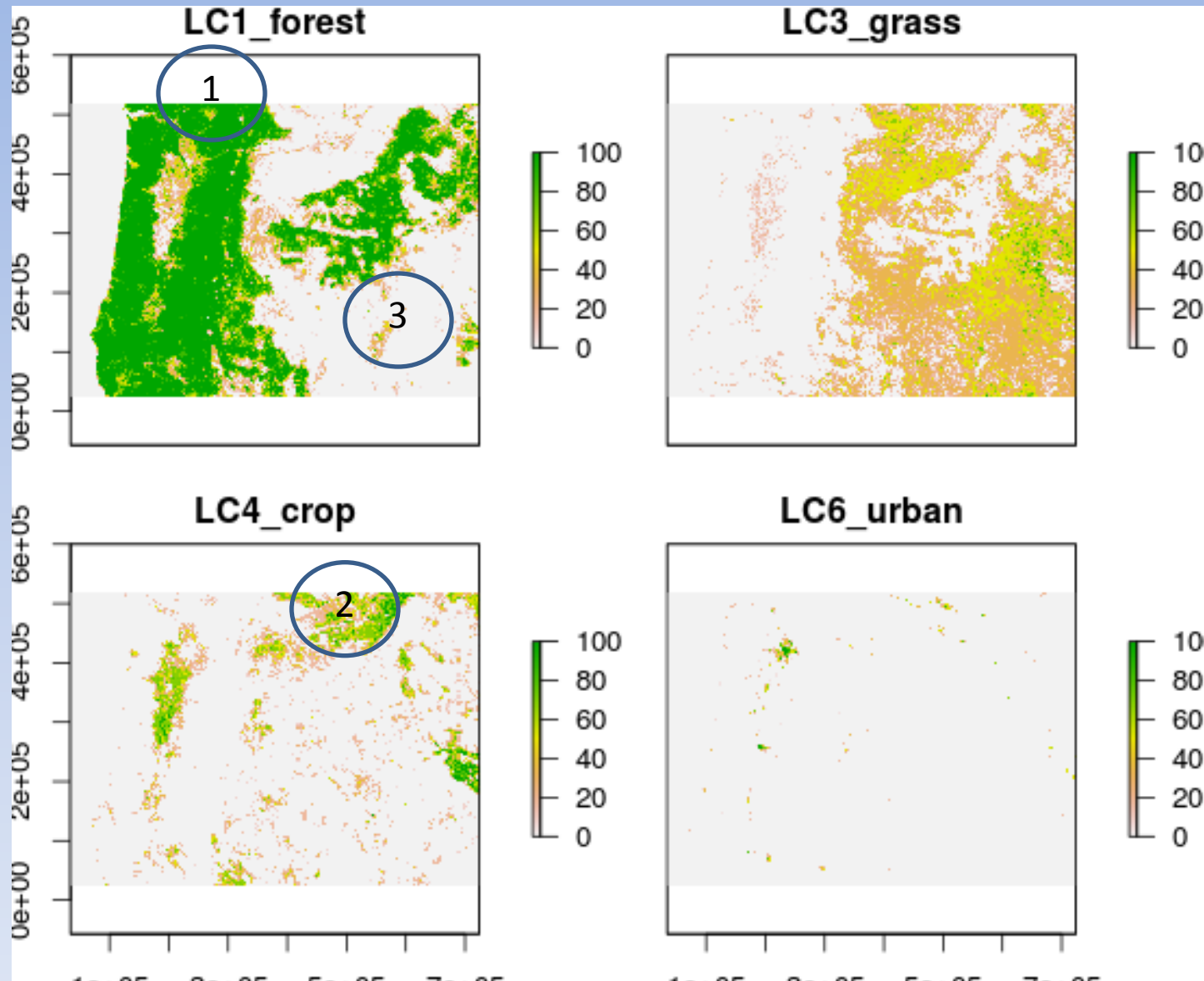
$$\text{Difference} = \text{CAI_tmax_prediction} - \text{Fusion_tmax_prediction}$$

Difference between CAI and fusion for 20100901



We note clear positive differences in the mountainous areas (areas 1 and 3). This indicates lower temperature predicted in the mountains by Fusion as compared to CAI. Note also the higher temperatures predicted by Fusion in the Northeast corner of the state clearly visible in the river course in blue.

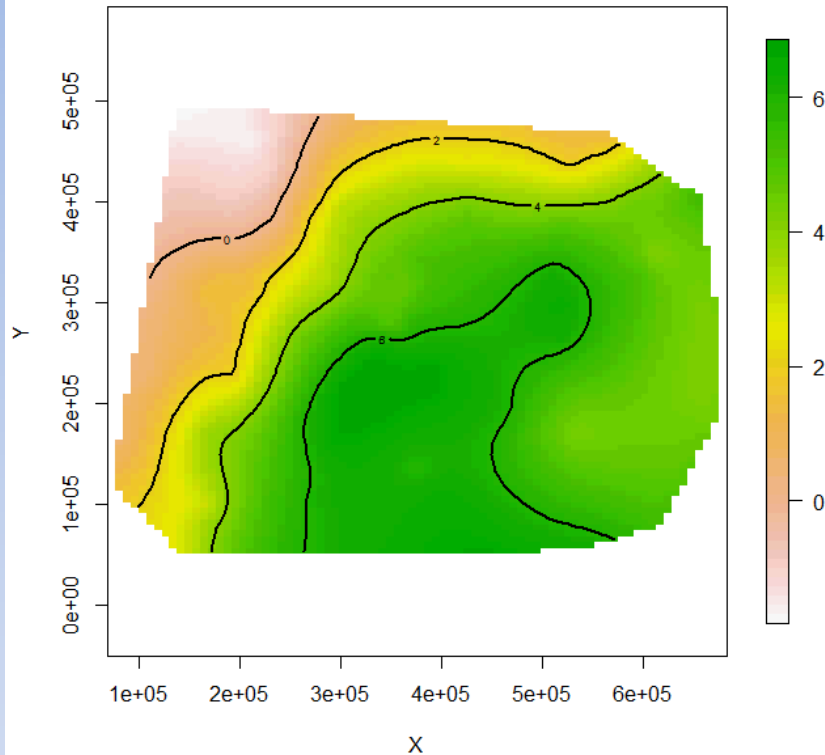
LAND COVER USED AS COVARIATES FOR THE MODELING



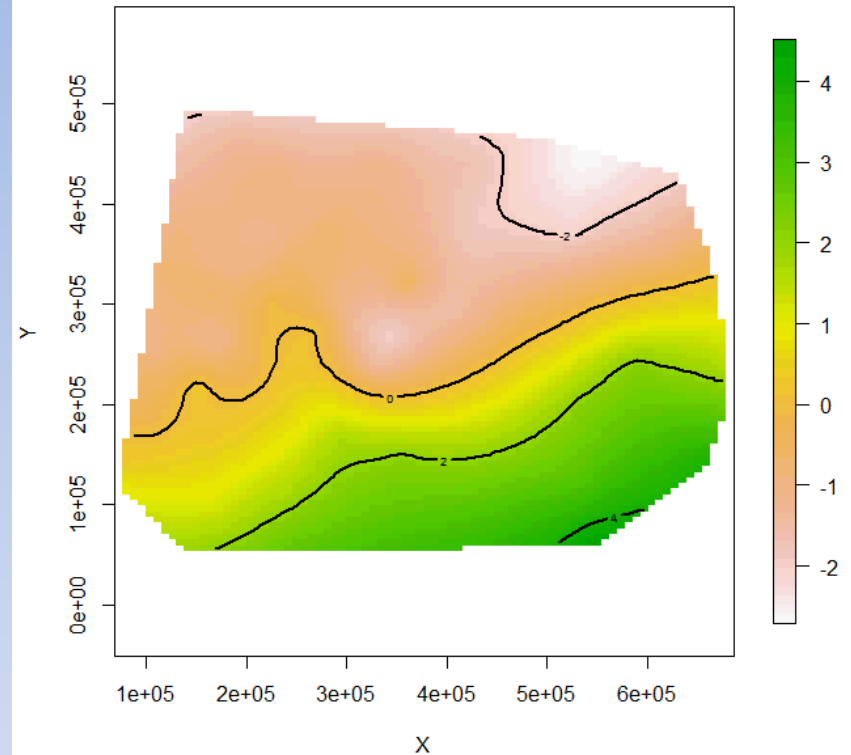
Note that area 1 and area 3 is covered by low concentration forest. Area 2 is covered by a high concentration of crop.

INDIRECT TWO STEPS METHODS: CAPTURING DAILY MOVEMENTS

Interpolated delta for Oct 15, 2010



Interpolated delta for Oct 16, 2010



It is also valuable to examine surfaces that were created during the interpolation procedure. Results indicate that the daily deviation surface on October 16 correspond to the arrival Of an air mass from the North West corner of the Oregon state. This suggests that the deviation Surface may capture air mass movements.

5. DENSITY OF STATION AND ACCURACY

General idea:

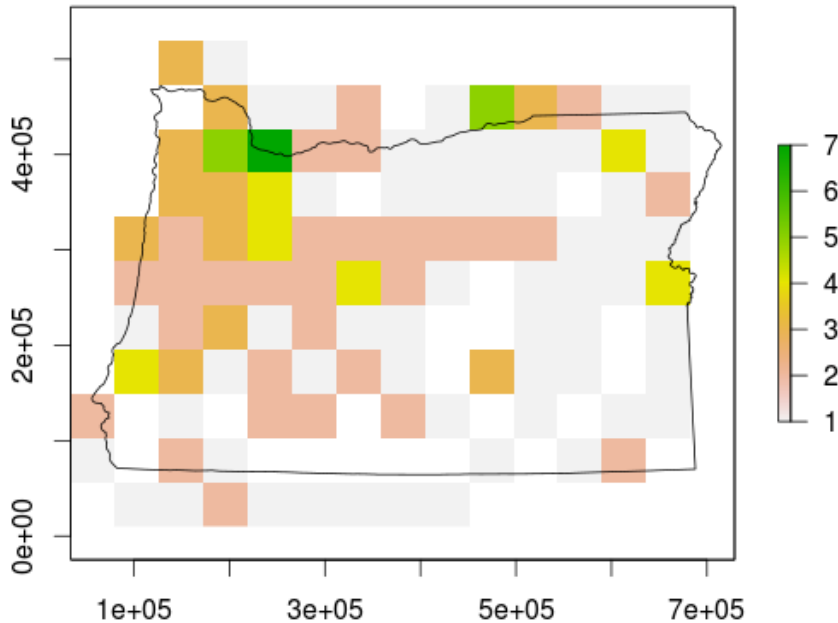
The interpolation literature indicate that accuracy is largely dependent on the network configuration and its density. We account for the station network configuration by plotting the MAE in terms of the number of stations in a 50x50km grid box.

Procedure:

1. Aggregation of original grid to a 50km spatial resolution i.e.~ 0.5 degree.
2. Count the number of station per 50 km grid boxes
3. Estimate the average accuracy per grid box using validation stations.
4. Plot of accuracy (MAE) vs number of stations

DENSITY OF STATION IN OREGON

Number of stations in coarsened 50km grid



Number of stations	count	percent
1	54	52.43
2	29	28.16
3	11	10.68
4	6	5.83
5	2	1.94
7	1	0.97

Total number of pixels: 165

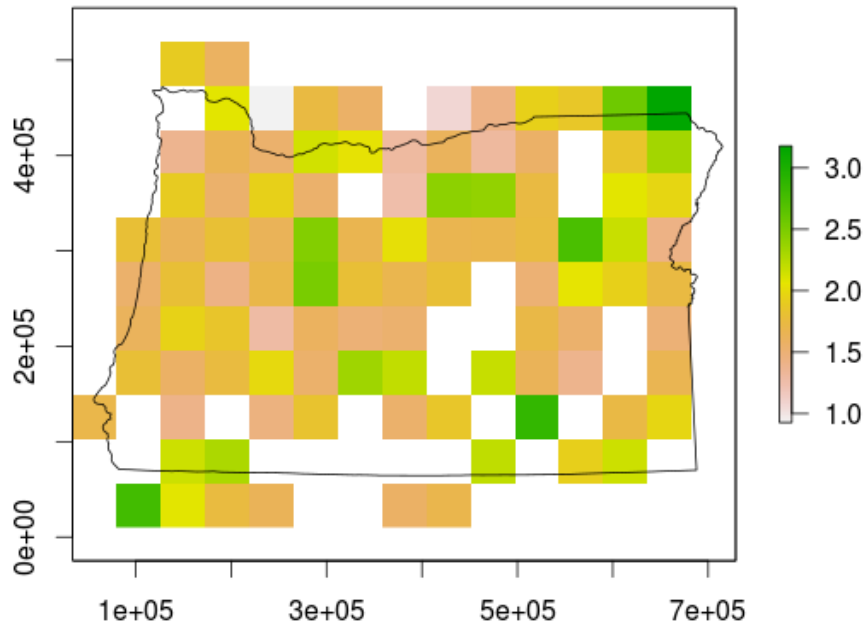
Total number of no data: 62

- The original 1km x 1km grid was coarsened to 50km x 50km cells and the number of station in each cell was calculated. We found that x number of cell contains only one station. The highest number of station are found near Portland and the lowest number in the Southeast basin.

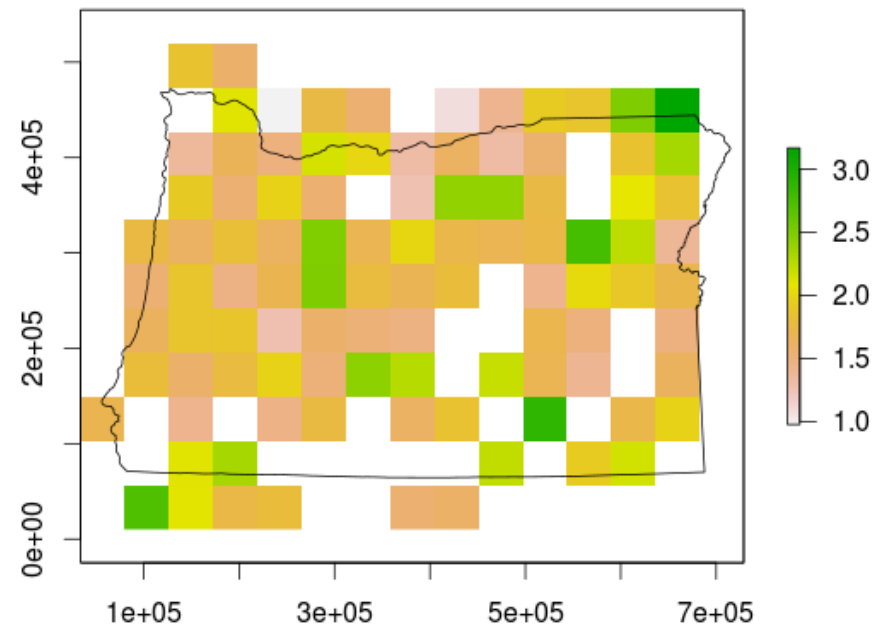
- Number of stations was based on all stations locations for year 2010. I am currently revising the algorithm to create a plot with the number of training station per box grid for each day.

DENSITY OF STATION IN OREGON

Fusion MAE in coarsened 50km grid

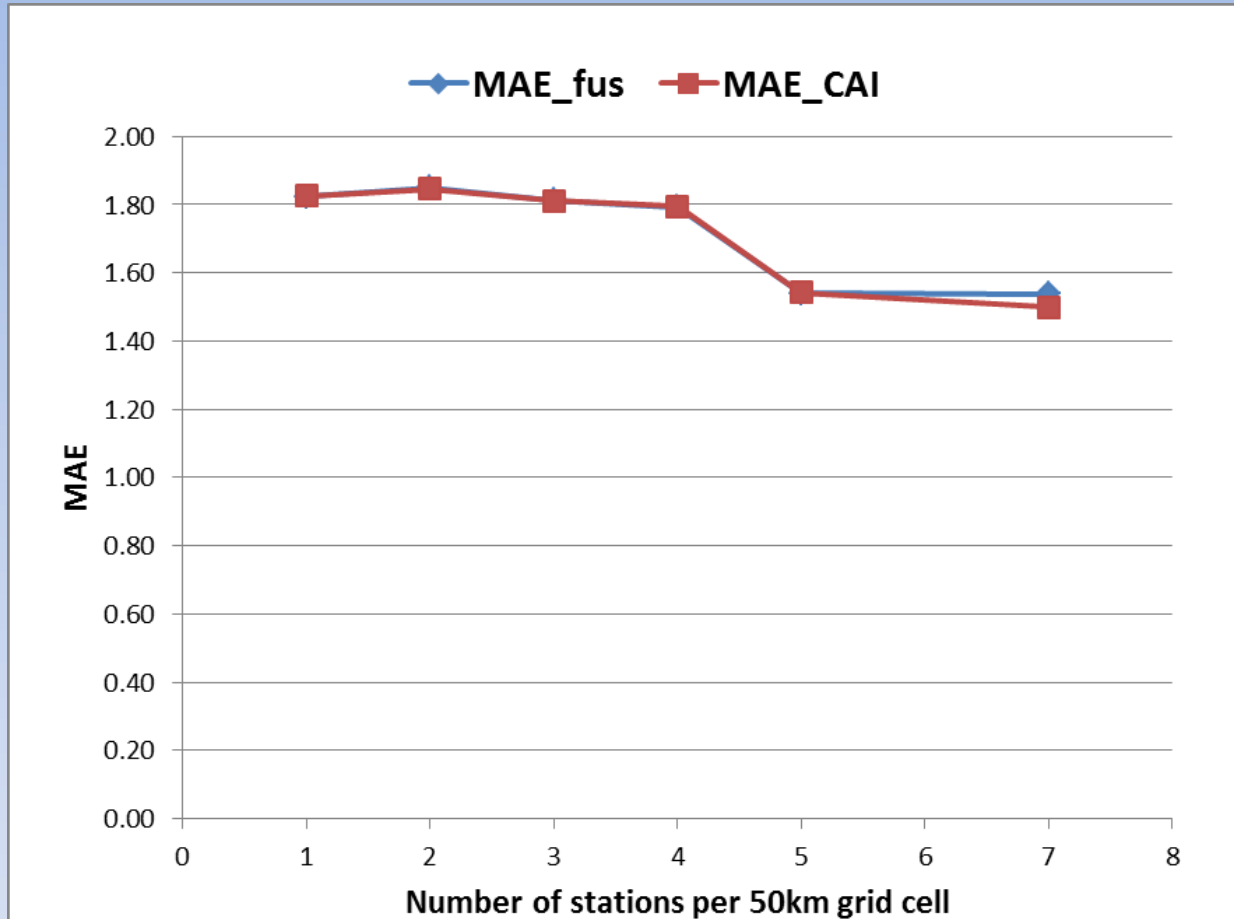


CAI MAE in coarsened 50km grid



CAI and Fusion show a similar pattern of averaged MAE. MAE values are the highest in the Northeast corner for both methods.

DENSITY OF STATION IN OREGON AND MAE



The plot conforms to the expectation i.e. MAE decreases as the number of station per grid box increases. Both methods show a similar pattern of decrease with little variation to separate CAI and Fusion methods.

6. METHOD COMPARISON

PREDICTIONS AND ACCURACY AT SPECIFIC METEOROLOGICAL STATIONS

General idea:

Aggregate measures such as MAE and RMSE hide the spatial variation within residuals, thus we should explore additional ways to recover the details by:

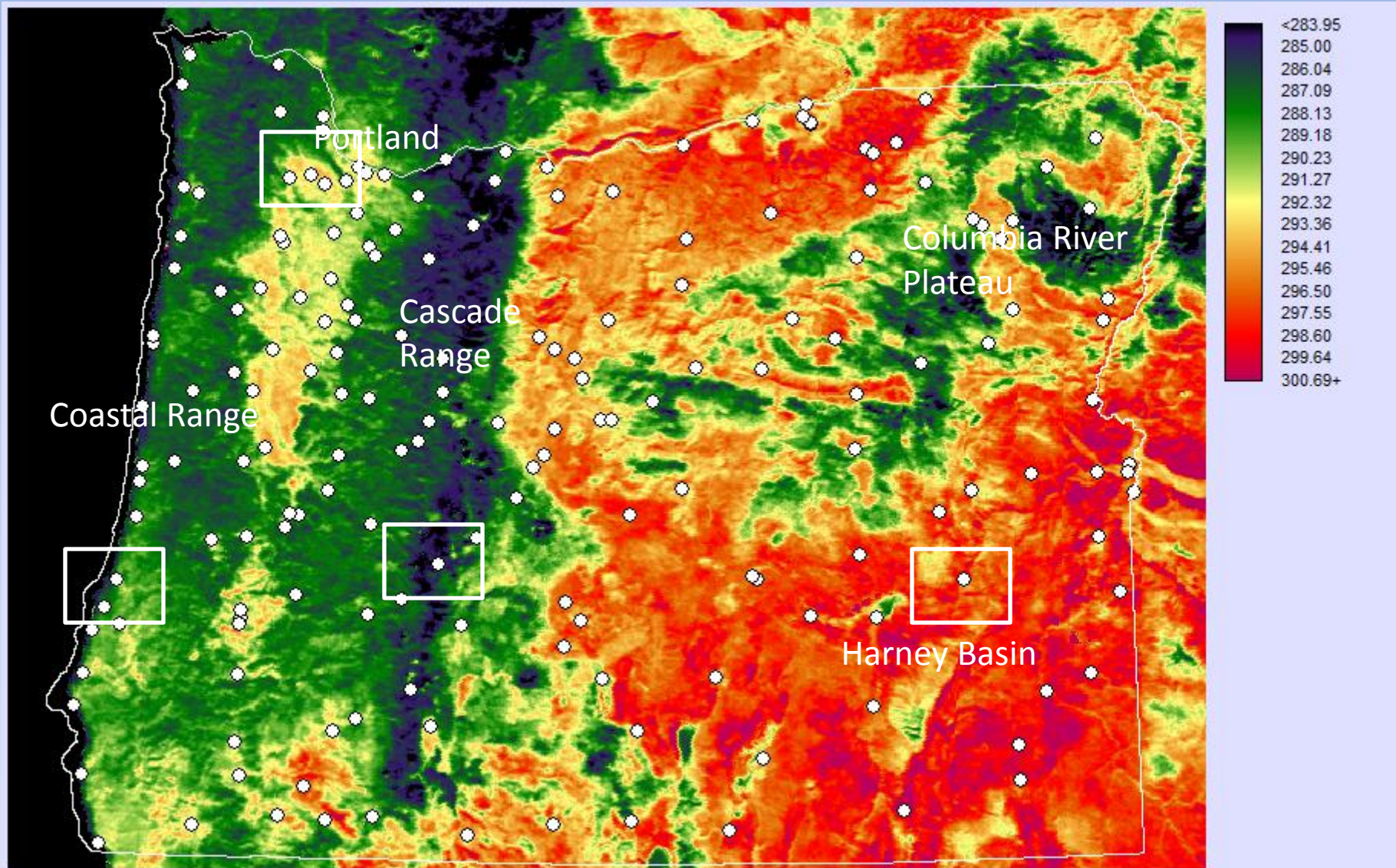
- Examining temperatures for a few “well” selected stations.*
- Looking at patterns in space and time by examining specific profiles for prediction and observed temperatures.*

PROCESS:

1. Select a few stations for the assessment.
2. Extract the predicted temperatures from time series predicted for Fusion and CAI.
3. Consolidate time series of observed daily temperature for the 186 unique stations
3. Calculate residuals based on all as well as validation stations.
4. Select, plot and compare predicted and observed temperatures in temporal profiles and transects
5. Compare residuals (to be included at a later stage).

STATIONS UPDATED FROM THE POSTGRES DATABASE

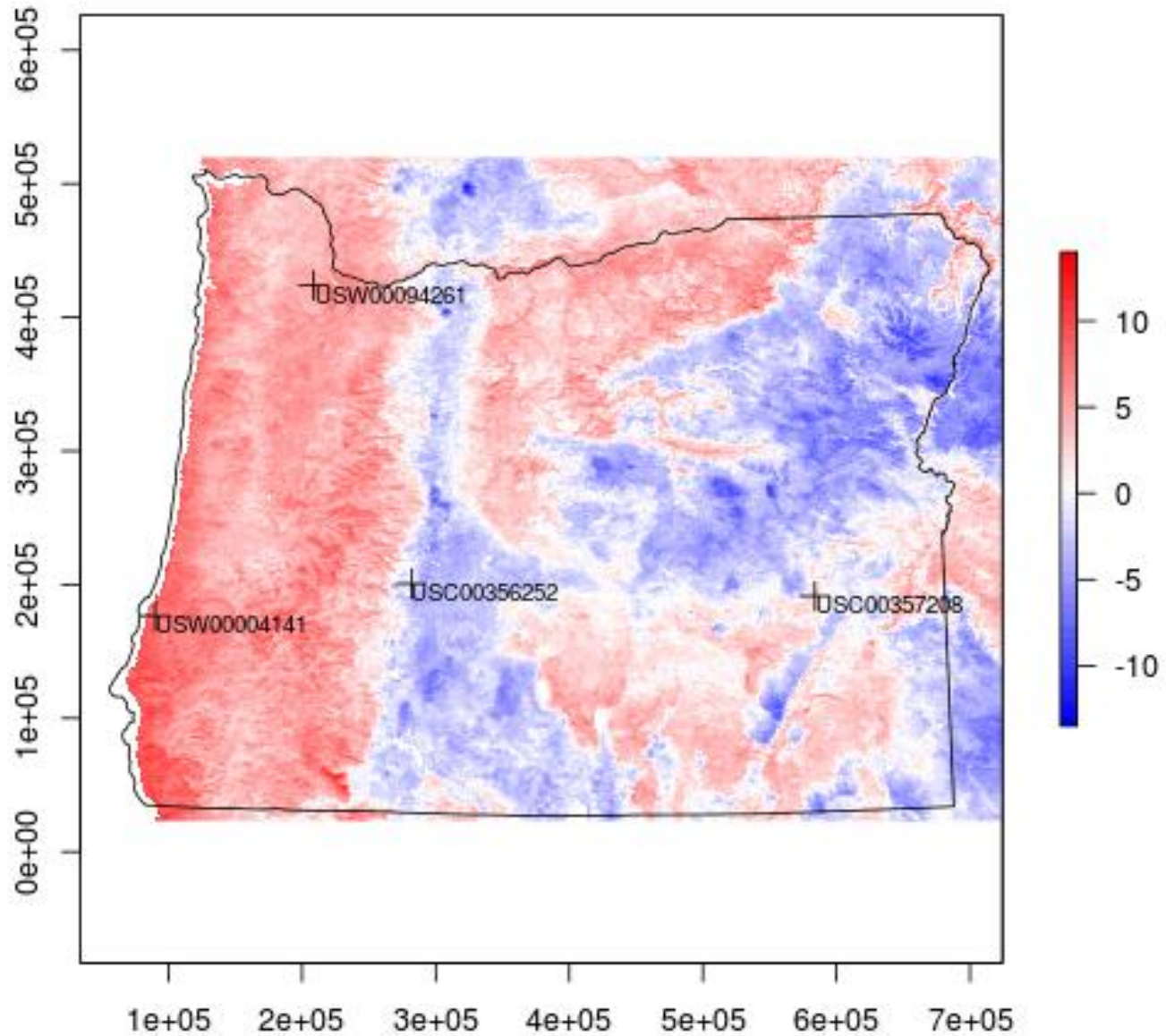
Codes were updated to allow the use of the new POSTGRES database...



mean_month10_rescaled.rst

By examining the landscape we selected four areas of interest: urban area near Portland,⁶⁵ a coastal region, a mountainous area from the Rockies and the a interior basin area.

Selected stations for comparison (Background: mean January LST)

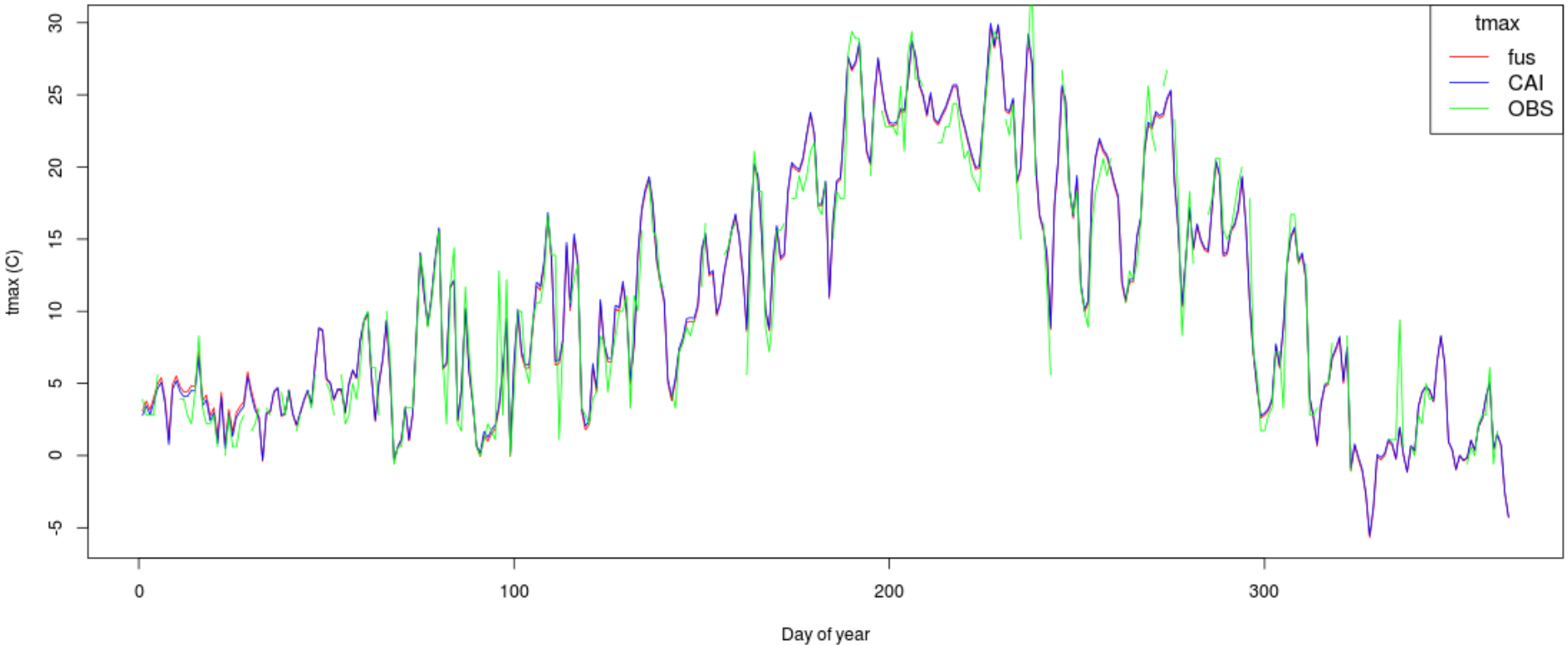


We selected stations in the specific areas of interest based on their GHCND code identifier.⁶⁶

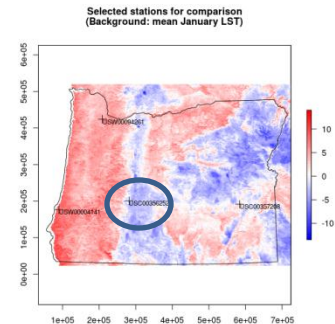
STATION 1: MOUNTAIN STATION

Elevation:

temporal profile for station USC00356252

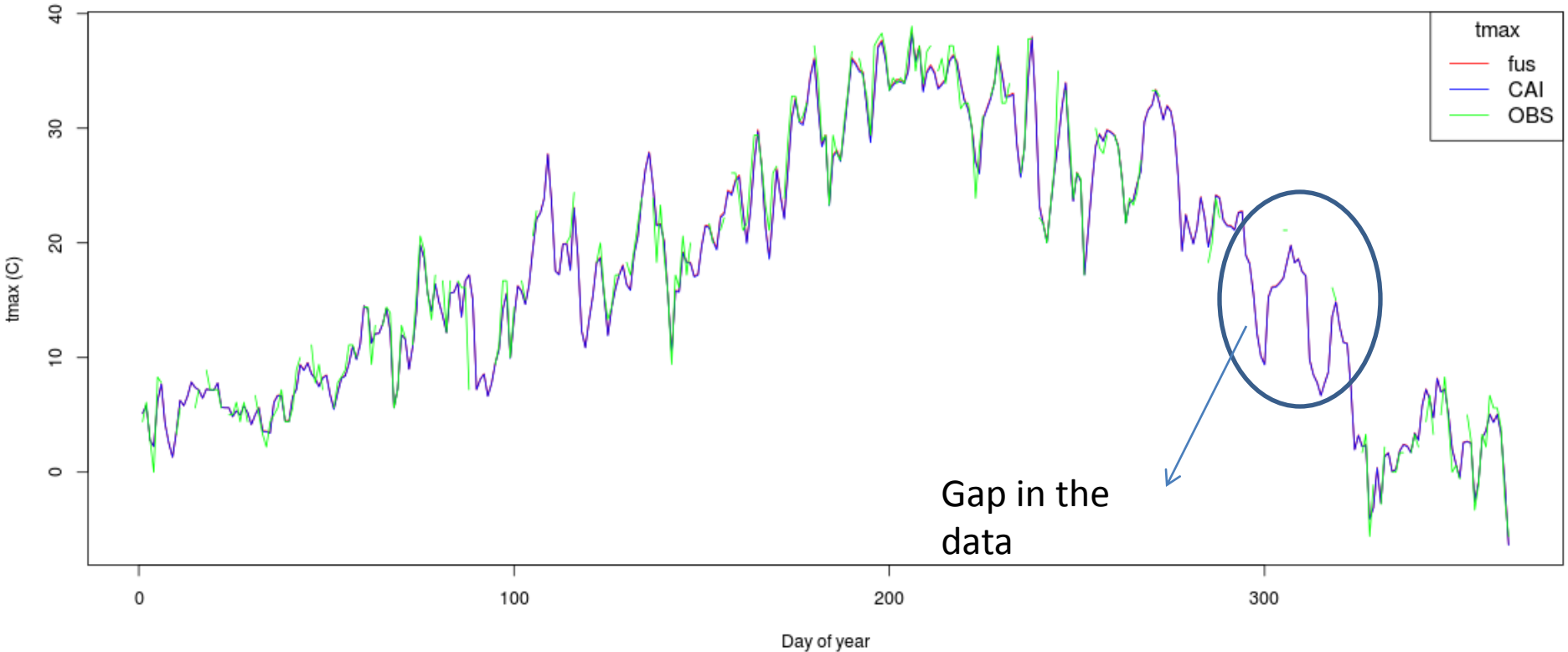


Temporal profiles are extracted for each station from the prediction stack (365 images) of maximum temperature for fusion, CAI. We used the observed time series from the GHCND database. The figure reveal a similar pattern of temperature for all three time series for this mountainous station.

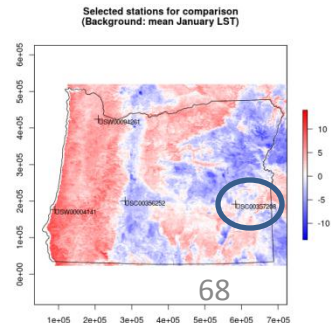


STATION 2: BASIN STATION

temporal profile for station USC00357208

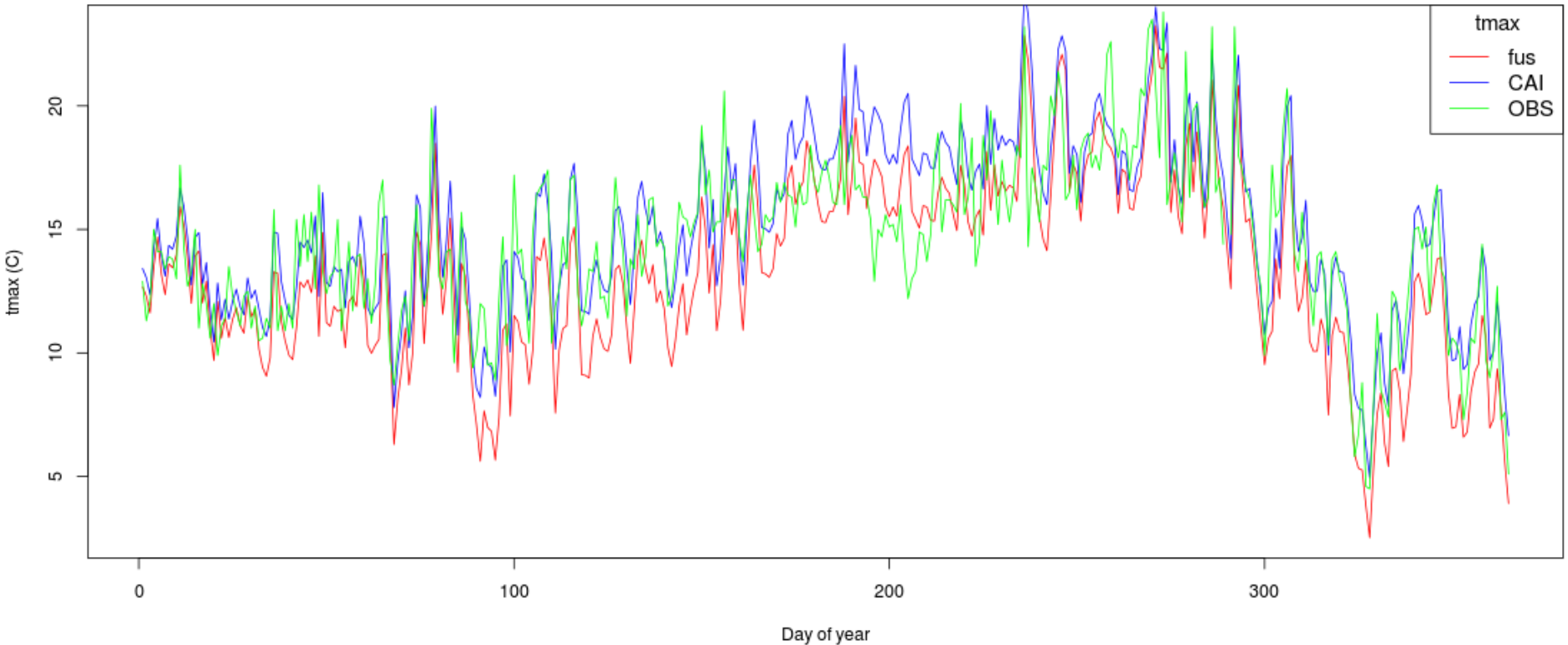


The selected basin station also shows similar pattern in the times series profile for fusion (fus), climatology aided interpolation (CAI) and the observed time series of tmax. We also note the gap in the data which represent missing values at specific dates.

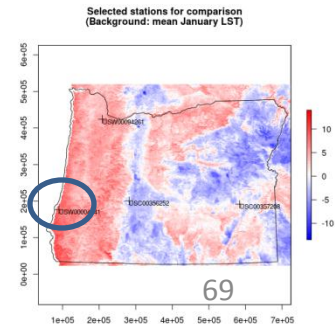


STATION 3: COASTAL STATION

temporal profile for station USW00004141

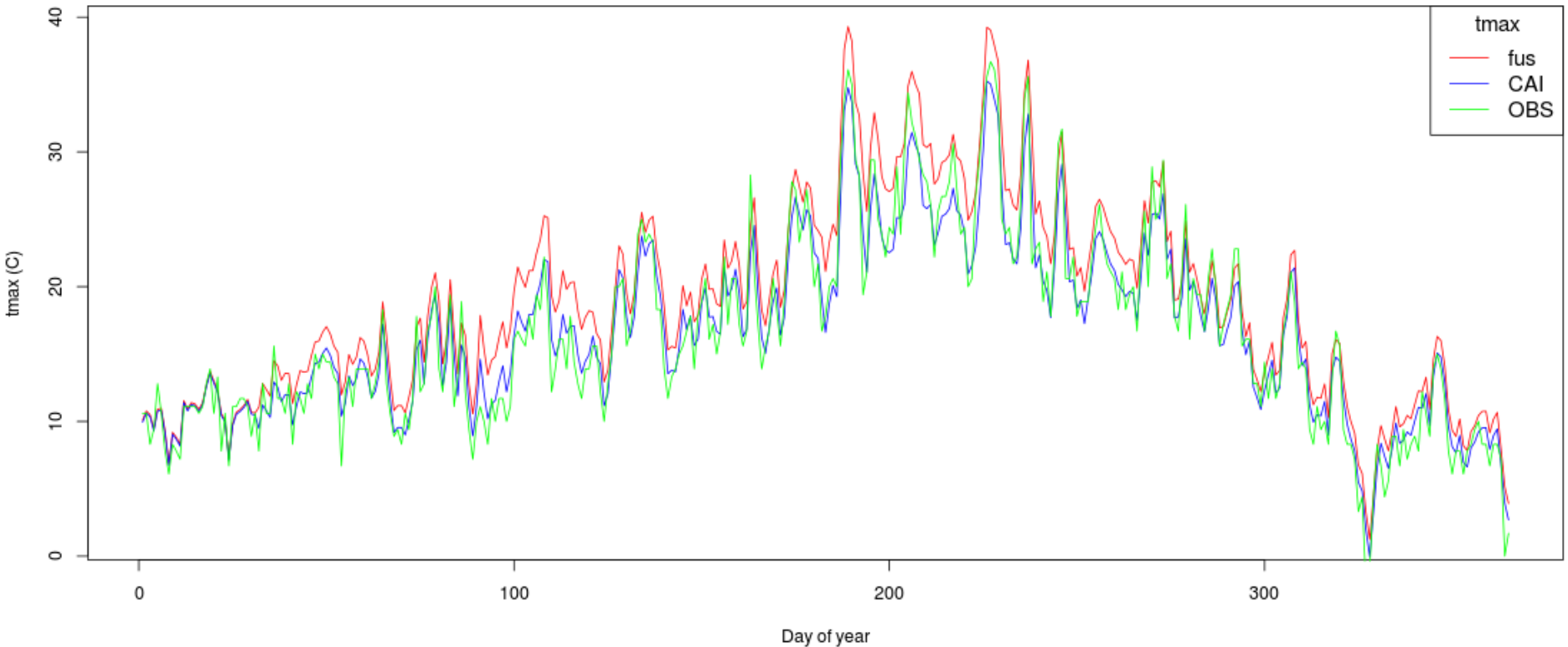


The selected coastal station shows more differences between the observed and predicted time series. The fusion time series (in red) appear to underestimate the maximum temperature (OBS in green) except during a short time period in summer (around DOY 200).

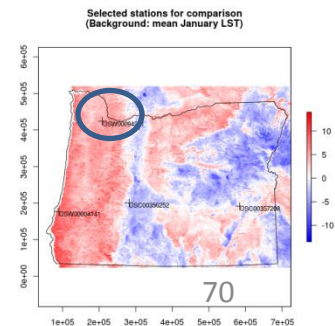


STATION 4: URBAN STATION

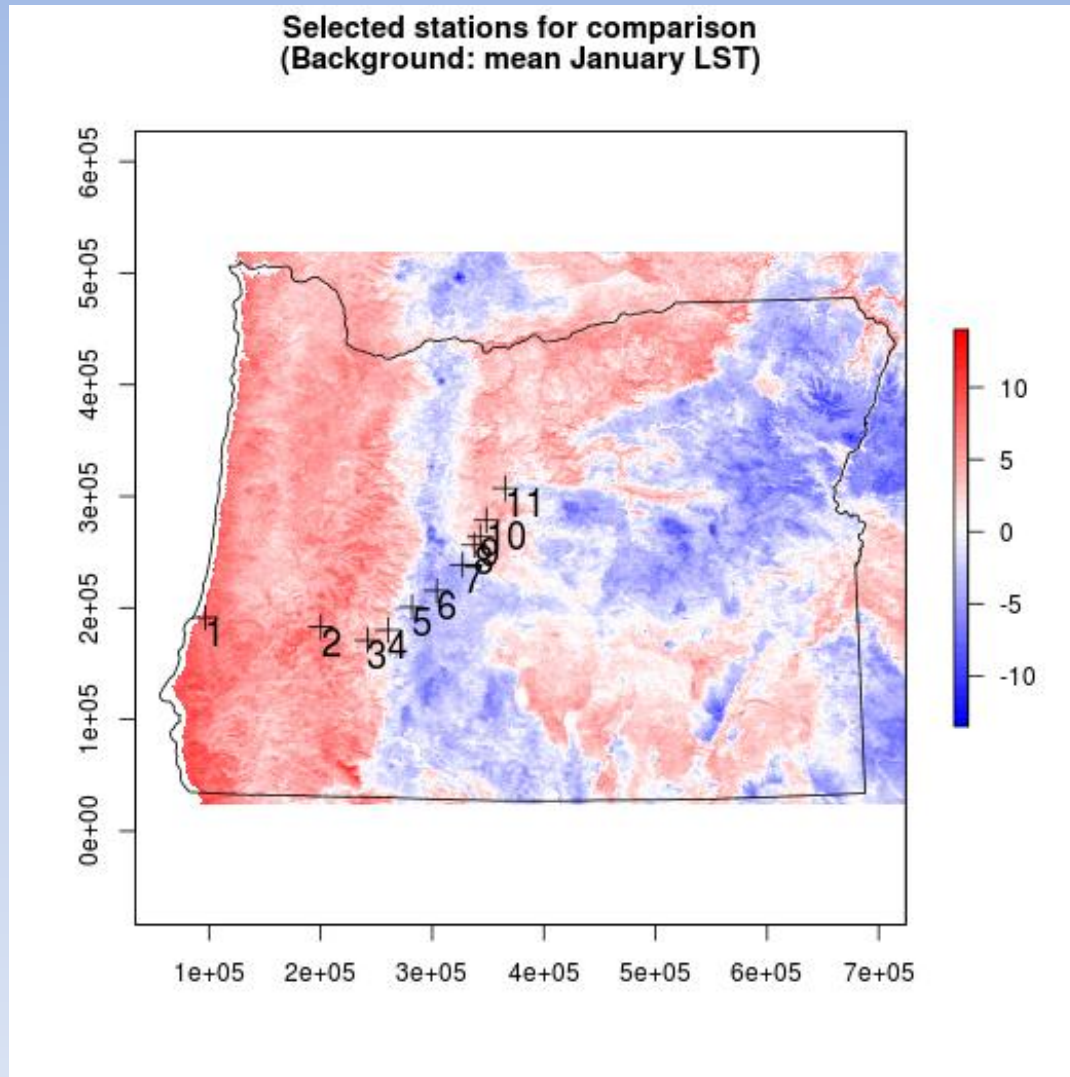
temporal profile for station USW00094261



This meteorological station is located in an urban area near Portland. The time series shows differences between predictions and observed values of tmax with fusion mostly overestimating the observed time series.



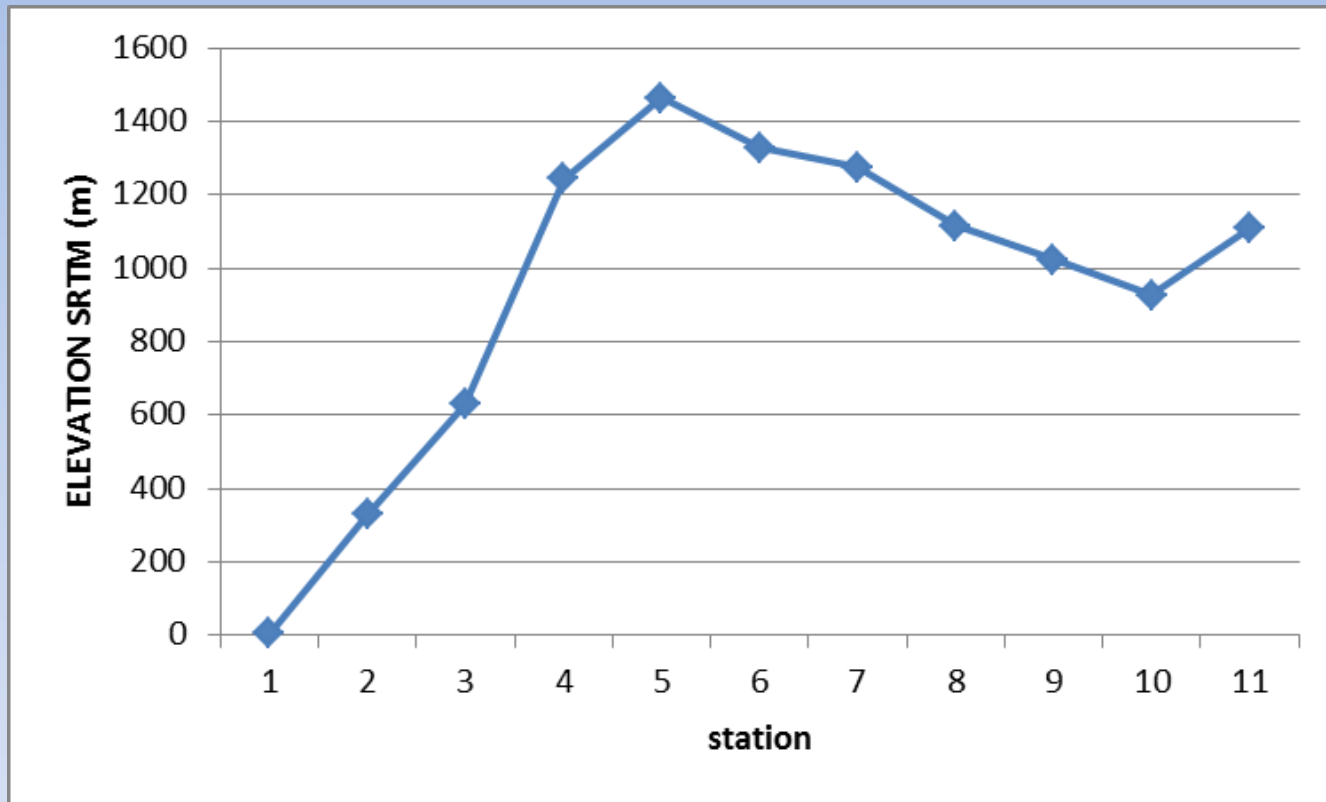
SPATIAL PROFILE: TRANSECT AND TMAX PREDICTION



We selected a sequence of 11 meteorological station to create a transect of maximum temperature across the landscape transitioning from coastal to mountainous areas in the interior.

SPATIAL PROFILE: TRANSECT AND TMAX PREDICTION

ELEVATION STATION 1 to 11

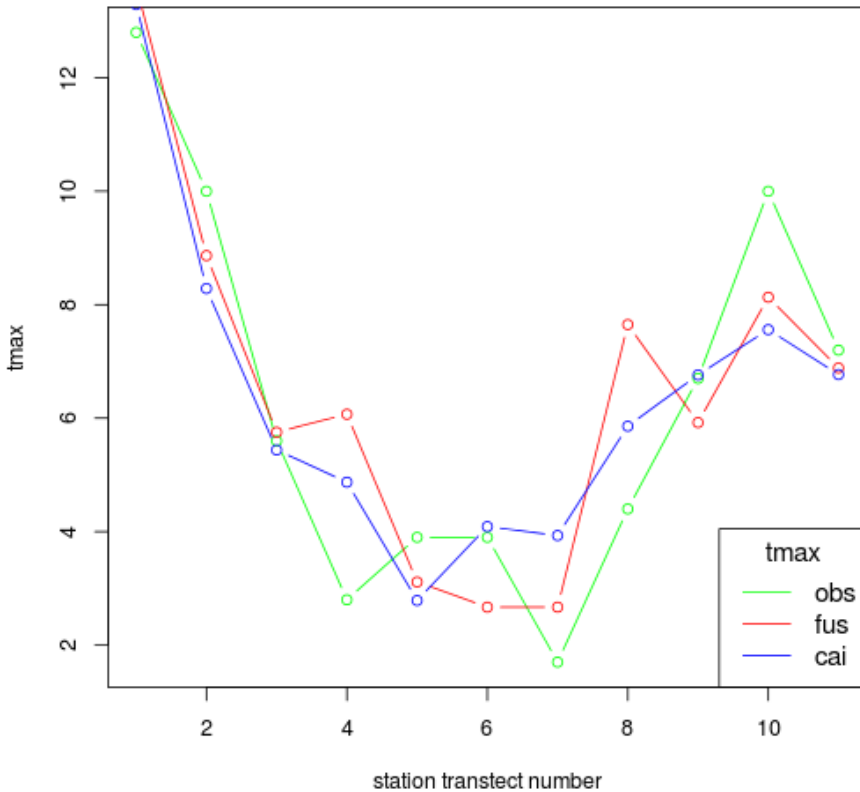


Add
more
info

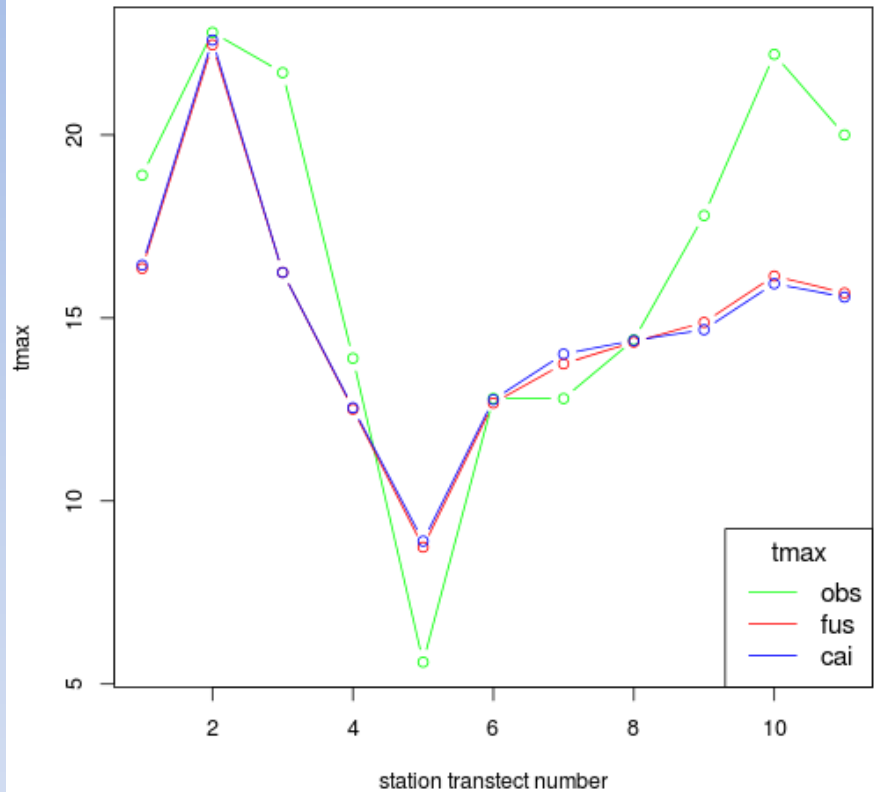
Elevation peaks at about 1450 meters station 5.

SPATIAL PROFILE: TRANSECT AND TMAX PREDICTION

Daily tmax prediction 01-01-2010



Daily tmax prediction 01-09-2010



The lowest temperatures are found between station 5 and station 7 (high elevation). Difference between predicted and observed temperatures (in green) appear to be more important on September 1 than January 1.

IV. PRELIMINARY CONCLUSIONS

- General conclusions
- Specific conclusions about CAI and Fusion comparison

PRELIMINARY CONCLUSIONS

→General conclusions about all five methods...

Given the current results, we can conclude at this stage...

1. Comparison over a full year show that on average methods give similar results in terms of RMSE and MAE. Results conform to conclusions found in the literature.
2. Indirect-multiple steps methods (CAI and Fusion) perform better with lower average MAE and RMSE. This is in line with the conclusions found in the literature.
3. MAE and RMSE metrics are not sufficient to evaluate the model outputs i.e. some predictions are overly smooth and do not include expected topographical features.
The inclusion of covariates such as elevation or LST add some of the missing spatial variability.

PRELIMINARY CONCLUSIONS

→ *Specific conclusions about CAI and fusion methods:*

Given the current results, we can conclude at this stage...

1. CAI and fusion with kriging are ranked as performing the best to interpolate values of daily tmax.
2. Prediction from Fusion with Kriging show more spatial variability than CAI with kriging.
3. Spatial pattern of fusion with kriging makes more sense but more analysis at station levels are needed to assess both methods' performance.

WHAT NEXT?

Given the current results, we can conclude at this stage...

1. Complete the Oregon case study by running remaining codes and examining in more details differences between CAI and fusion output.
2. Write report and paper draft on method comparison for the Oregon case study.
3. Complete review paper on interpolation methods.
4. Start building data for the next case study (Venezuela) and identify essential assessment components.
5. Start considering performance workflow and issues related to scaling up the interpolation techniques?

ADDITIONAL SLIDES

This information may be useful during the discussion about method comparison.

LAND COVER CONSENSUS CATEGORIES

Aggregated Classification class	Class No.	GLC2000 ¹	UMD	MODIS	GlobCover ²
Forest	1	1,2,3,4,5,6,7,8	1,2,3,4,5,6	1,2,3,4,5,8	40,50,60,70,90,100,160,170
Shrub	2	9,10,11,12,14	7,8,9	6,7,9	110,120,130,150
Grass	3	13	10	10	140
Crop	4	16	11	12	11,14
Mosaic ³	5	17,18		14	20,30
Urban	6	22	13	13	190
Barren	7	19	12	16	200
Snow	8	21		15	220
Wetland	9	15		11	180
Water body	10	20	0	17	210

Table 5. Legend for the 10 aggregated land cover classes and the corresponding classes from the six individual global land cover legends. Modified from (Nakaegawa 2011).

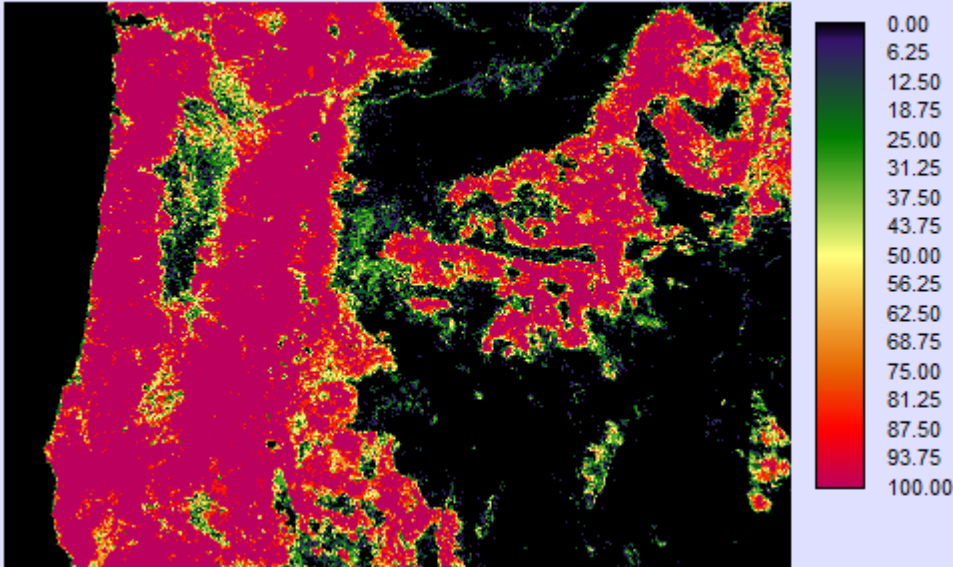
¹I added class 3 to 'forest' since it was missing in original table. The class 2 entry under 'shrub' is probably an error and so is removed.

²GlobCover class assignment needs to be finalized.

³Mosaic is composed of cropland and natural vegetation.

LAND COVER 1: FOREST

rojection from modis_sinusoidal to NAD_1983_Statewide_Lambert_Meter



- 34% of land has 100% forest/LC1
- 40.24% of land has between 0 and 10% forest
- 37.55% of land has 0% LC1

Graph Type: Bar Graph, Line Graph, Area Graph

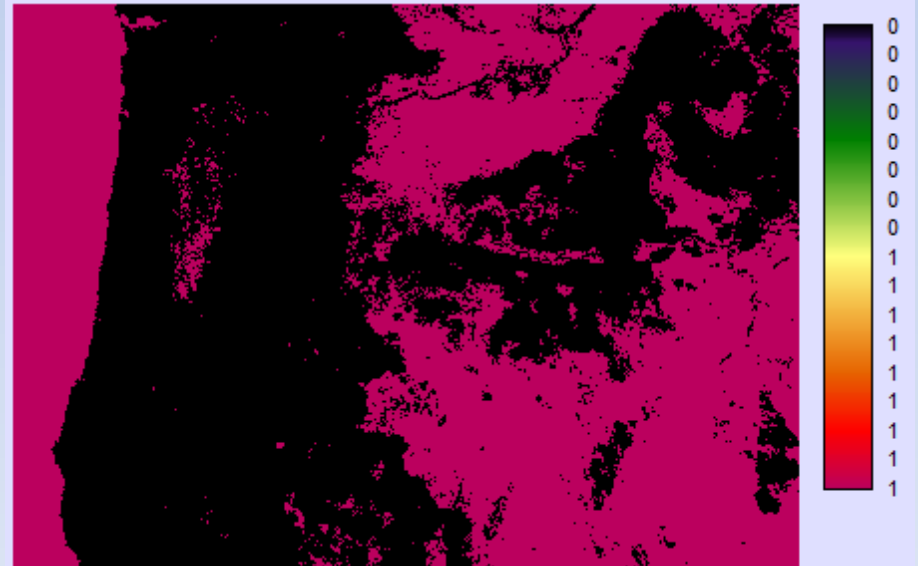
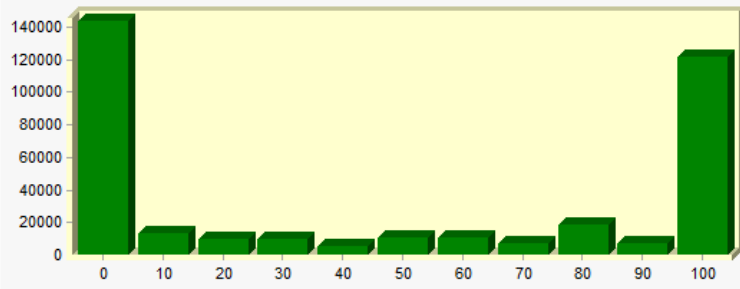
Mode: Frequency, Cumulative

Graphic View Settings: Display graph from 0 to 101, New width 10, New class number [] Update

Histogram of 'W_Layer1_ClipppedTo_OR83M' using 'mask_water_or83m' as mask

Summary Statistics

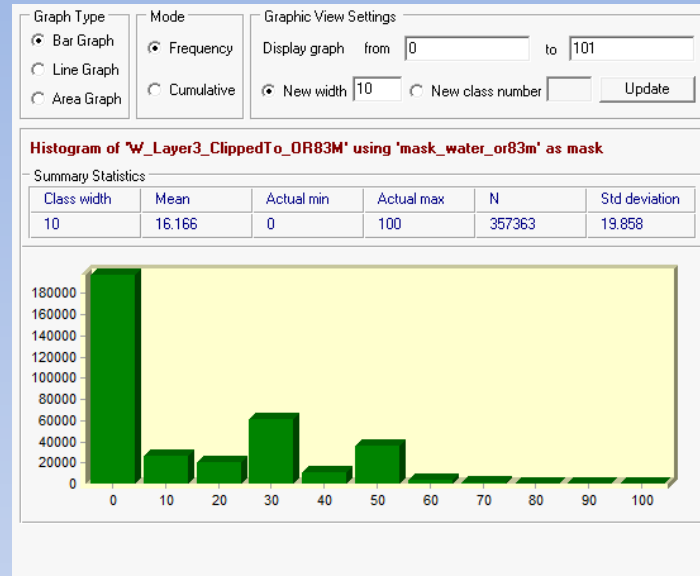
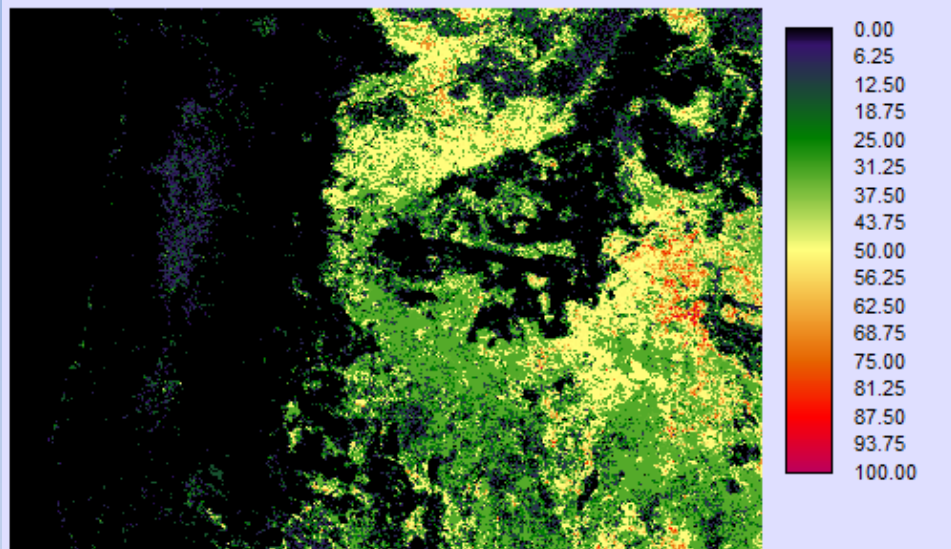
Class width	Mean	Actual min	Actual max	N	Std deviation
10	48.184	0	100	357363	45.503



LAND WITH 0% LC1

LAND COVER 3 AND ELEVATION

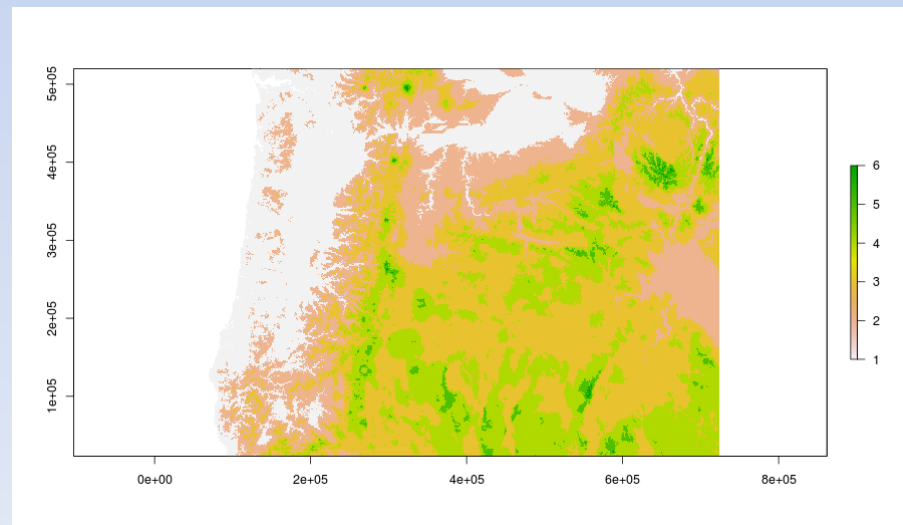
projection from modis_sinusoidal to NAD_1983_Statewide_Lambert_Meter



- This is the second most widespread land cover in OR.
- 49.84% of the study area has zero percent of LC3.
- LC3 is almost the negative of LC1 (forest).

ELEVATION CLASS

value	count	elev_class	percent
1	76550	0-500	19.17
2	75038	500-1000	18.79
3	129578	1000-1500	32.45
4	69178	1500-2000	17.32
5	6144	2000-2500	1.54
6	346	2500-4000	0.09
NA	42486	No Data	10.64



FUSION METHOD

Monthly tmax: TMax

- Derive monthly mean at every station based on a reference time period for every month.

Day LST averages and BIAS

- Calculate monthly averages from daily MOD11A1
- Difference between Day LST averages and monthly Tmax at stations: this is the “bias”.
- Produce a bias surface at every location using: Kriging, TPS/GAM.

Daily deviation: delta

- Difference between daily values and monthly TMax at stations: this is the “delta”.
- Produce a delta surface at every location using: Kriging, TPS or GAM.

RUN3 GAM METHOD

Additional run to take into account land cover...

Mod1: $t_{max} \sim s(\text{lat}, \text{lon}) + s(\text{ELEV_SRTM}) + s(\text{Northness}, \text{Eastness}) + s(\text{DISTOC}) + s(\text{LST}) + s(\text{LC4})$

Mod2: $t_{max} \sim s(\text{lat}, \text{lon}) + s(\text{ELEV_SRTM}) + s(\text{Northness}, \text{Eastness}) + s(\text{DISTOC}) + s(\text{LST}) + s(\text{LC6})$

Mod3: $t_{max} \sim s(\text{lat}, \text{lon}) + s(\text{ELEV_SRTM}) + s(\text{Northness}, \text{Eastness}) + s(\text{DISTOC}) + \text{LST} * \text{LC4}$

Mod4: $t_{max} \sim s(\text{lat}, \text{lon}) + s(\text{ELEV_SRTM}) + s(\text{Northness}, \text{Eastness}) + s(\text{DISTOC}) + s(\text{LST}, \text{LC6})$

Mod5: $t_{max} \sim s(\text{lat}, \text{lon}) + s(\text{ELEV_SRTM}) + s(\text{Northness}, \text{Eastness}) + s(\text{DISTOC}) + s(\text{LST}, \text{LC4})$

Mod6: $t_{max} \sim s(\text{lat}, \text{lon}) + s(\text{ELEV_SRTM}) + s(\text{Northness}, \text{Eastness}) + s(\text{DISTOC}) + s(\text{LST}) + s(\text{LC6})$

Mod7: $t_{max} \sim s(\text{lat}, \text{lon}) + s(\text{ELEV_SRTM}) + s(\text{Northness}, \text{Eastness}) + s(\text{DISTOC}) + \text{LST} * \text{LC4} + \text{LST} * \text{LC3} + \text{LST} * \text{LC1}$

Mod8: $t_{max} \sim s(\text{lat}, \text{lon}) + s(\text{ELEV_SRTM}) + s(\text{Northness}, \text{Eastness}) + s(\text{DISTOC}) + \text{LST} * \text{LC1} + \text{LST} * \text{LC3}$

Number of predictions over a full year:

Mod1:

Mod2: To be added...

Mod3:

Mod4:

Mod5:

Mod6:

Mod7:

Mod8:

→ Problem given the prevalence of low percentages and the configuration of land covers⁸³